CRACK GROWTH IN HARDENED CEMENT PASTE

by KEITH DAVID BALDIE

A thesis submitted for the degree of Doctor of Philosophy of the University of London, and for Diplomate of Imperial College

Department of Metallurgy and Materials Science
Imperial College of Science and Technology
University of London

September 1985

ABSTRACT

This thesis describes the examination of the microstructure of hardened cement paste [HCP], in particular, cracking in HCP, and the measurement of subcritical crack growth in HCP.

A scanning electron microscope has been used to examine, fracture surfaces, complementary fracture surfaces, polished surfaces, and polished surfaces containing introduced cracks. This examination has provided information about fracture paths in HCP, which shows that the main hydration products [C-S-H gel and calcium hydroxide] form the majority of crack path elements. The interpenetration of these products during hydration, and the expected variations in strength of these hydration products suggest that both must be recognised as significant contributors to the mechanical properties of HCP. The examination of cracks in polished surfaces appears to be a very useful way of determining the microstructural aspects of cracking, and its possible future applications are discussed.

Two methods of determining the subcritical crack growth parameter [n] were performed, the first, load-relaxation in double torsion plates yielded a value of 64, while the second, the variation in the critical stress intensity of single edge notched beams with loading rate yielded a value of 27. The much higher value determined by load relaxation is thought to be due to both, the effect of crack resistant inhomogeneities in the microstructure which have a more marked effect on load relaxation measurements, and a susceptibility to creep in the double torsion plates which reduced the amount of crack growth. The susceptibility to creep was identified by a shift of the crack velocity-stress intensity [V-K] curves to higher stress intensities with repeated loading. The value of subcritical crack growth parameter of 27, determined by the variation of critical stress intensity with loading rate, is therefore regarded as the more valid.

ACKNOWLEDGEMENTS

I wish to thank Professor P.L. Pratt, Doctor H.M. Jennings, the Department of Metallurgy and Materials Science of Imperial College, and the Science and Engineering Research Council for the opportunity to undertake the present research.

I would also like to thank all the members of the Cement research group, past and present, for their comradeship, in particular: Mr L. Dutton for technical assistance; Dr. C.J. Gillham for his introduction to computing; and Dr. K.L Scrivener for stimulating discussion. I am also grateful to Mr J. Turner of the Department of Civil Engineering of Imperial College for assistance with cement casting.

I would like to thank my wife, the afore mentioned Dr. K.L. Scrivener, for her support, and finally, my parents, Mr D. and Mrs A.A. Baldie for their long term support and assistance with my education.

CONTENTS

ABSTRACT			2
ACKNOWLEDGEMENT			3
CONTENTS			4
LIST OF FIGURES			8
LIST OF TABLES			10
LIST OF PLATES			11
GLOSSARY			14
CHAPTER 1		INTRODUCTION	17
CHAPTER 2		STRUCTURE, STRENGTH AND SLOW CRACK GROWTH OF HARDENED CEMENT PASTE	19
	2A	STRUCTURE OF HARDENED CEMENT PASTE	19
	2A.I	Cement Manufacture	19
	2A.II	Cement Hydration	19
		.i Individual Components	19
		.ii Cement	22
	2B	STRENGTH OF HARDENED CEMENT PASTE	24
	2B.I	Strength of Materials	24
		.i Griffith theory	24
		.ii Applicability of the Griffith theory	25
	2B.II	Applicability of Fracture mechanics to HCP, mortar and concrete	26
	2B.III	Crack propagation patterns	28
		.i Single crack	29
		.ii Microcracking and Crack Branching	29
		.iii Multiple Crack Initiation	31
	2B.IV	Strength of HCP	32
	2B.V	Strength of porous materials	34

	2C	SUBCRITICAL CRACK GROWTH IN HARDENED CEMENT PASTE	36
	2C.I	Crack Velocity-Stress Intensity [V-K] Plots	36
	2C.II	Indirect methods of Obtaining Subcritical crack growth data	39
		.i Time to Failure tests	39
		.ii Strain rate dependance of strength	40
	2C.III	The effect of microstructure and test technique on the subcritical crack growth parameter	40
	2C.IV	Stress Corrosion	43
	2D	SUMMARY OF MECHANICAL FAILURE AND STRESS CORROSION IN HARDENED CEMENT PASTE	45
CHAPTER	3	EXPERIMENTAL TECHNIQUES	46
	3A	SPECIMEN PREPARATION	46
	3A.I	Casting	46
	3B	MICROSTRUCTURAL EXAMINATION	48
	3B.I	Scanning Electron Microscope [SEM] Imaging methods	48
		.i Specimen Preparation	50
	3C	MECHANICAL TESTING	54
	3C.I	Specimen preparation	54
		.i Double Torsion	54
		.ii Single Edge Notched Beams	54
	3C.II	Measurement of the Subcritical Crack growth parameter-n	56
		.i Double Torsion load-relaxation	56
		.ii Single edge notched beams-Variation in Critical stress intensity with loading rate	60
CHAPTER	4	COMPUTERS AND COMPUTING	63

4A	COMPUTERS	63
4A.I	Computers used in this research	64
	.i Apple IIe	64
4B	COMPUTING	65
4B.I	Programming	65
	.i Programming speed	65
	.ii Program efficiency	67
	.iii User friendliness	69
4C	COMPUTER MONITORING AND DATA PROCESSING	71
4C.I	Subcritical Crack growth measurement	71
	.i Data logging	71
	.ii Data Processing	71
CHAPTER 5	SCANNINIG ELECTRON MICROSCOPY OF HARDENED CEMENT PASTE	73
5A.I	Microstructure of HCP	73
	.i Unhydrated cement	73
	.ii C-S-H	74
	.iii Calcium Hydroxide	77
	.iv AFt	77
	.v AFm	81
	.vi Porosity	81
5A.II	Prehydrated microstructure	81
5B	CRACK PATHS IN HCP	83
5B.I	Complementary fracture surfaces	83
5B.II	Introduced cracks in polished surfaces	88
	.i Drying shrinkage cracking	89
	.ii Introduced cracking	89
5B.III	In-situ drying shrinkage cracking	94
5C	SUBCRITICAL CRACK GROWTH	97
5C.I	Double Torsion load-relaxation	97
	i. Crack length measurements	97
	ii. Load-relaxation measurements	99
5C.II	Variation in K_{1c} with loading rate	118

CHAPTER 6		DISCUSSION	121
	6A	CRACK PATHS IN HCP	121
	6A.I	.i The role of unhydrated cement cores	121
		.ii The role of hydration products	122
		.iii The role of porosity	125
		.iv Summary	127
	6A.II	The effect of prehydrated cement	128
	6B	SUBCRITICAL CRACK GROWTH	129
	6B.I	Load-relaxation	129
		.i V-K curves	129
		.ii Applicability of load-relaxation test	131
	6B.II	Variation in K_{ic} with loading rate	139
	6B.III	Effects of microstructure and test method	141
	6B.IV	Lifetime predictions	142
	6B.V	Stress corrosion	144
CHAPTER 7		CONCLUSIONS AND SUGGESTIONS FOR FURTHER WORK	145
APPENDIX 1		Characterisation of the cement used	150
APPENDIX 2		Computer program listings and flow charts	153
APPENDIX 3		Strength of calcium hydroxide crystals	166
APPENDIX 4		Specimen lifetime prediction	170
REFERENCES			172

LIST OF FIGURES

Figure 2.01	Feldman & Sereda model of C-S-H gel.	21
Figure 2.02	Dugdale-Barenblatt tied-crack model.	27
Figure 2.03	Crack propogation patterns.	30
Figure 2.04	Theoretical V-K curve of chemically enhanced subcritical crack growth.	37
Figure 2.05	The effect of inhomogeneities on subcitical crack growth.	42
Figure 3.01	Double torsion plate moulds.	47
Figure 3.02	Emission from specimens in the scanning electron microscope.	49
Figure 3.03	Cutting procedure for preparation of specimens containing cracks grown from a notch.	53
Figure 3.04	Introduction of curved initial notch in DT plates.	55
Figure 3.05	Double torsion plate, and testing arrangement.	57
Figure 3.06	SENB test arrangement.	61
Figure 5.01	Compliance-notch length measurements.	98
Figure 5.02	Load-relaxation curves.	103
Figure 5.03	Background relaxation curves.	108
Figure 5.04	V-K curves.	110
Figure 5.05	Variation in Critical stress intensity with loading rate.	120
Figure 6.01	Schematic representation of DT plate showing	137

region of contact.

Figure 6.02 Predicted specimen lifetime determined from subcritical crack growth data. 143

Figure A1.1 Isothermal calorimeter output for hydrating cement. 152

Figure A3.1 Loading apparatus for strength measurements of calcium hydroxide. 167

LIST OF TABLES

Table 5.01	Cumulative lengths of crack path elements observed on polished surfaces of HCP.	95
Table 5.02	Subcritical crack growth parameter and V-K intercept determined by load relaxation in DT plates.	101
Table 5.03	Average values of subcritical crack growth parameter and V-K intercepts, and Student t-test results.	102
Table 5.04	Median K_{1c} values for 3 point bend SENBs at different loading rates.	118
Table 6.01	Values of subcritical crack growth parameter determined for HCP.	130
Table A3.1	Values of strength of calcium hydroxide single crystals.	169
Table A3.2	Values of critical stress intensity of calcium hydroxide single crystals.	169

LIST OF PLATES

Plate 5.01	Large anhydrous core. BEI polished surface.	75
Plate 5.02	C_3S, C_2S and interstitial anhydrous cores. Upper Upper boxed section, small rings of C-S-H. Lower boxed section, AFt. BEI polished surface.	75
Plate 5.03	Anhydrous core in inner product C-S-H shell. SEI fracture surface.	76
Plate 5.04	Inner product C-S-H shell, SEI fracture surface.	76
Plate 5.05	Planar fracture through inner product C-S-H. SEI fracture surface.	76
Plate 5.06	"Grain" of inner product C-S-H, partly covered by outer product C-S-H. SEI fracture surface.	78
Plate 5.07	Higher magnification view of the outer product C-S-H covering in plate 5.06. SEI fracture surface.	78
Plate 5.08	Acicular outer product C-S-H. SEI fracture surface.	78
Plate 5.09	Interpenetrating calcium hydroxide and C-S-H. SEI fracture surface.	79
Plate 5.10	Small hexagonal crystals of calcium hydroxide. SEI fracture surface.	79
Plate 5.11	Massive calcium hydroxide. SEI fracture surface.	79
Plate 5.12	AFt rods in pore. SEI fracture surface.	80
Plate 5.13	AFm platelets embedded in inner product C-S-H. SEI fracture surface.	80
Plate 5.14	AFm platelets inside shell of inner product C-S-H.	80

SEI fracture surface.

Plate 5.15 Clusters containing a large number of anhydrous particles in prehydrated cement. BEI polished surface. 82

Plate 5.16 Cluster boundary in prehydrated cement, showing a surrounding layer of calcium hydroxide. BEI polished surface. 82

Plate 5.17 HCP fracture surface showing typical fracture elements; B & B′, inner product C-S-H, C & C′, calcium hydroxide; D & D′, outer product C-S-H; E & E′, pore containing AFt. SEI complementary fracture surfaces. 84

Plate 5.18 Fracture through a mass of calcium hydroxide showing two distinct crystallographic orientations. SEI complementary fracture surfaces. 85

Plate 5.19 Fracture through an extensive mass of inner product C-S-H, which includes an anhydrous core [H]. SEI complementary fracture surfaces. 86

Plate 5.20 Fracture around a "grain" of inner product C-S-H [F & F′], and through a shell of inner product C-S-H to reveal an anhydrous core [G′] and an empty shell [G]. SEI complementary fracture surfaces. 87

Plate 5.21 Introduced crack dividing and running through an anhydrous core, and between inner and outer product C-S-H. BEI polished surface. 90

Plate 5.22 Introduced crack running through large mass of inner product C-S-H. BEI polished surface. 90

Plate 5.23 Typical features of an introduced crack. BEI polished surface. 90

Plate 5.24 Introduced crack running through a large region of calcium hydroxide. BEI polished surface. 91

Plate 5.25 Drying shrinkage cracking in calcium hydroxide. BEI polished surface. 91

Plate 5.26 Introduced crack tortuosity caused by anhydrous cores. BEI polished surface. 92

Plate 5.27 Introduced crack entering and passing around an anhydrous core. BEI polished surface. 92

Plate 5.28 Introduced crack passing through an anhydrous core. BEI polished surface. 92

Plate 5.29 Crack growth due to specimen drying shrinkage in the SEM specimen chamber. BEI polished surface. 96

GLOSSARY

The oxides present in cement are abbreviated according to standard cement chemistry notation, i.e.;

$C = CaO$,	$S = SiO_2$,	$A = Al_2O_3$,
$F = Fe_2O_3$,	$H = H_2O$,	$\bar{S} = SO_3$.

Thus tricalcium silicate, $3CaO.SiO_2 = C_3S$; tricalcium aluminoferrite, $4CaO.Al_2O_3.Fe_2O_3 = C_4AF$; AFm, $3CaO.Al_2O_3.CaSO_4.12H_2O = C_3A.C\bar{S}.H_{12}$

A	The V-K intercept, a parameter describing subcritical crack growth.
AFm	Tetracalcium monosulpho-aluminoferrite hydrate, in cement typically $C_3A.C\bar{S}.H_{12}$.
AFm	Tetracalcium trisulpho-aluminoferrite hydrate, in cement typically $C_3A.[C\bar{S}]_3.H_{32}$.
BEI	Backscattered electron image.
C_3S	The major phase of HCP, $3CaO.SiO_2$, also known as Alite. As in the other phases of cement [see below] the anhydrous phases contain significant impurities, but for simplicity these phases will be represented by the oxide abbreviation of the pure phase.
C_2S	$3CaO.SiO_2$, a.k.a. Belite
C_3A	$3CaO.Al_2O_3$, generally present as an intimate mixture with.....
C_4AF	$4CaO.Al_2O_3.Fe_2O_3$ in a component referred to as interstitial phase.
C-S-H	Calcium silicate hydrate, a variable composition gel which is the major product of cement hydration.

Cement	Ground cement clinker.
Cement clinker	Nodular product of cement manufacturing kiln.
Cement paste	Mixture of cement and water (see HCP).
Concrete	Mixture of cement paste, sand and coarse aggregate.
DT	Double Torsion.
HCP	Hardened cement paste. Cement paste which has hydrated to form a rigid mass.
Interstitial phase	C_3A and C_4AF
K	Stress Intensity
K_c, $[K_{1c}]$	Critical Stress Intensity [for Mode 1 opening]
n	The subcritical crack growth parameter
OPC	Ordinary Portland Cement.
SEI	Secondary electron image.
SEM	Scanning microscope.
SENB	Single Edge Notched Beam.
V	Crack Velocity/Subcritical crack growth velocity.
w/c	Water/cement ratio of cement paste.

COMPUTING GLOSSARY

Command	An instruction in a program.
Computer	A machine which can process data.

Computing	Using a computer to process data
CPU	Central processing unit.
Data	A piece or pieces of information.
Datafile	Data stored on magnetic disc.
Disk/disc	A magnetic data storage disc.
Filename	A label for data on a disc.
Input	Any data enterred into the computer for processing.
Interface	A connection between a computer and another device.
Memory	Storage devices, e.g. electronic memory in the computer or external memory such as nmagnetic discs.
Output	Any data output from the computer after processing.
Program	A list of commands, interpreted by the computer, which result in specific data processing.
Programming	Compiling a list of commands to perform a data processing task.

CHAPTER 1 - INTRODUCTION

Concrete has been used in modern times since 1843, yet the amount of scientific research which was conducted on cement and concrete upto the 1960s was minimal. Since the 1960s interest in cement research has increased considerably, but in comparison to other materials such as steel, aluminium and silicon the amount of research work performed is still small. The major reasons for this is that cement is relatively cheap, and has been used in excess to provide the required properties. However, in a number of instances, e.g. the corrosive effects of $CaCl_2$ in concrete and the instability of high alumina cement, some catastrophic and extremely expensive failures have occured. The reason for these failures is the application of empirically determined relationships in inapplicable situations.

Research into cement is the logical starting point for research into concrete, because cement is the component of concrete responsible for the setting and development of strength of concrete. A materials science approach, which examines the relationship between structure and properties, is necessary to provide an understanding of cement and concrete at their most basic. From this basis, improvements in cement and concrete will be less likely to fail in an unexpected manner, and the long term improvements will be greater as they will be based on firmer scientific foundations.

The present work concerns cement, specifically 28 day old hardened cement paste [HCP] of original water/cement ratio 0.4. This work should form a basis for further research into other cements, and ultimately concrete.

The literature on the structure, strength and subcritical crack growth of HCP is reviewed in chapter 2.

Chapter 3 outlines the experimental techniques which were developed and used in this project, for microstructural examination, and subcritical crack growth measurement. Chapter 4 describes the use of micro computers as an aid to experimental work.

The microstructure of HCP, as observed by scanning electron microscopy is described in the first part of chapter 5, including examination of fracture surfaces and polished surfaces. The microstructure of cracks in polished surfaces is discussed.

In the second part of chapter 5 the results of subcritical crack growth measurements are presented. Two different test methods were used to determine the subcritical crack growth parameter, load

relaxation in double torsion plates and the variation in critical stress intensity with loading rate.

Chapter 6 is a discussion of the results from both microscopy and subcritical crack growth measurements, and chapter 7 contains conclusions and suggestions for further work.

CHAPTER 2 - STRUCTURE, STRENGTH AND SUBCRITICAL CRACK GROWTH OF HARDENED CEMENT PASTE

2A STRUCTURE OF HARDENED CEMENT PASTE

2A.I CEMENT MANUFACTURE (Bye, 1983)

The raw materials for cement manufacture are a mixture of calcareous minerals e.g. chalk or limestone, and siliceous minerals e.g. clay or shale. Chalk and limestone are almost pure calcium carbonate, while clay and shale are hydrous aluminium silicates, containing significant amounts of iron and magnesium and lesser amounts of several other compounds. Appropriate amounts of these minerals are mixed to produce a raw mix with the required overall chemical composition, which then enters a rotary kiln. As the mix passes along the length of the kiln the temperature increases to a maximum of $\sim 1500^{o}C$ during which time several processes take place, the end product of which is nodules of clinker containing impure C_3S, C_2S, C_3A, C_4AF, and some other minor constituents e.g. magnesia [MgO] and free lime [CaO]. C_3S and C_2S form as discrete crystals in a matrix of C_3A and C_4AF. A typical cement would contain 45-75% C_3S, 12-35% C_2S, 5-10% C_3A and 5-10% C_4AF. The clinker nodules are interground with 3-4% of gypsum, which is added to control the setting behaviour, resulting in a fine grey powder [typically $300-400 m^2 kg^{-1}$], which consists of grains which usually contain more than one phase. On addition of water the cement reacts to form a rigid solid, hardened cement paste [HCP].

2A.II CEMENT HYDRATION (Lea, 1970)

2A.II.i Individual Components

When Portland cement is mixed with water, several reactions occur, and the final microstructure of HCP obviously is a combination of the products of these reactions. Cement consists of four main compounds, C_3S, C_2S, C_3A and C_4AF, which are present as an intimate mixture in individual cement grains (Scrivener & Pratt, 1984) and consequently there is considerable interaction between these compounds during hydration. To understand these reactions better it is useful to know how individual compounds hydrate in isolation, then to examine hydrating cement in terms of these individual reactions

and any possible interaction between compounds.

2A.II.i.a C_3S and C_2S

The silicates, C_3S and C_2S react similarly with water to form Calcium-silicate-hydrate, C-S-H, and calcium hydroxide. C-S-H is a gel with a variable composition (Parrott, 1985), approximately $C_{1.7}SH_2$, whereas calcium hydroxide is a highly stoichiometric crystalline material (Moore, 1980).

$$C_3S + 3H \rightarrow C\text{-}S\text{-}H + 1.3CH$$
$$C_2S + 2H \rightarrow C\text{-}S\text{-}H + 0.3CH$$

Direct observation of C-S-H particles is not possible, but the high surface area [~$400m^2g^{-1}$], and the observation of weak broad peaks in X-ray diffractometry (Grudemo, 1977), suggest that it consists of sheets 30-40Å thick and extending ~500Å in the other dimensions.

The fine structure of C-S-H gel has been envisaged in a number of models, of which that of Feldman & Sereda (Feldman & Serada, 1970; Sereda et al, 1980) is the best developed. This model (see figure 2.01) describes the gel as consisting of a number of sheets of C-S-H, 2-4 molecules thick, with chemically bonded interlayer water and physically adsorbed water. It can be seen from figure 2.01 that the gel has a disordered structure which includes both inter- and intra-crystallite porosity.

On a coarser scale the structure of C-S-H has been widely examined by electron microscopy. In particular several workers have examined hardened cement paste [HCP] using scanning electron microscopy [SEM] (Diamond, 1976; Marchese, 1977; Dalgleish et al, 1980) which has shown C-S-H with a number of morphologies, variously descibed as spherulitic, fibrillar, honeycomb etc., unfortunately this technique requires the drying of the specimen which may disrupt or distort the structures present in the wet state. On the other hand a number of workers (Double et al, 1978; Jennings & Pratt, 1980; Scrivener, 1984) have examined HCP in "environmental cells" of high voltage transmission electron microscopes in which a moist atmosphere can be established, making it unnecessary to dry the specimen; and they observed C-S-H forming as exfoliating foils.

Calcium hydroxide is the most crystalline of the hydration products, its hexagonal structure produces strong X-ray diffraction peaks (Grudemo, 1977). In HCP it is observed as massive regions

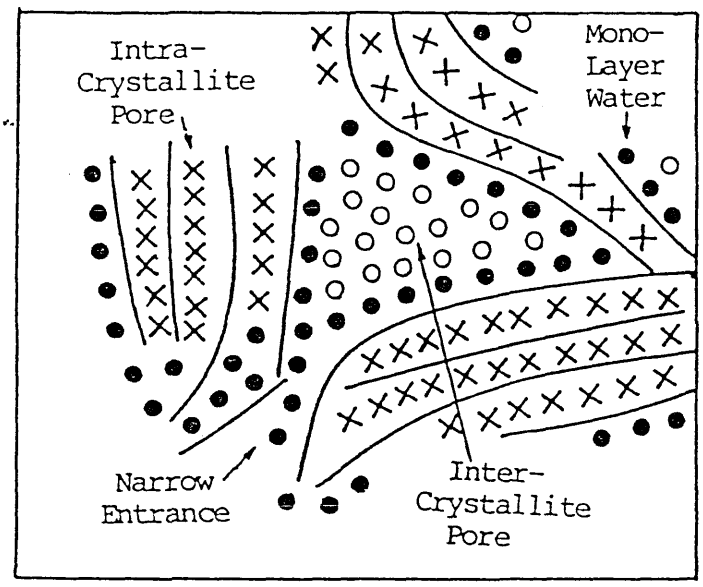


Figure 2.01 Feldman & Sereda model of C-S-H gel (after Sereda et al, 1980)

which are intergrown between C-S-H and the other components of HCP. On fracture surfaces it is seen as flat expanses, interrupted by other components and cleavage steps.

2A.II.i.b C_3A and C_4AF

In cement the aluminate compounds, C_3A and C_4AF, react in the presence of calcium sulphate to form either a trisulphate or a monosulphate iron substituted aluminate hydrate, depending on the amount of sulphate available. The trisulphate, $C_3(A,F).(C\bar{S})_3.H_{32}$, known as AFt forms in the erly stages of hydration when the sulphate concentration is high.

$$C_3A + 3C\bar{S}H_2 + 26H \rightarrow C_3A.(C\bar{S}).H_{32}$$

The monosulphate, $C_3(A,F).C\bar{S}.H_{12}$, AFt can also form directly from C_3A where the sulphate concentration is low [A], or by reaction of AFt with C_3A [B] as sulphate concentration falls.

[A] $C_3A + C\bar{S}H_2 + 10H \rightarrow C_3A.C\bar{S}.H_{12}$

[B] $2C_3A + C_3A.(C\bar{S})_3.H_{32} + 4H \rightarrow 3C_3A.C\bar{S}.H_{12}$

C_4AF hydrates in much the same way as C_3A, the products being AFt and AFm in which iron replaces some aluminium.

AFt and AFm both have hexagonal crystal structures, the morphology of the former being rods and the latter plates.

2A.II.ii Cement

When discussing cement, as well as knowing the reaction products, it is also important to realise that the anhydrous compounds hydrate at different rates, and that the hydrating phases may interact. It is generally found (Lea, 1970) that the rate of reaction of $C_3A > C_3S > C_4AF > C_2S$ when hydrated individually, however, in cement gypsum [$C\bar{S}H_2$] is added specifically to retard C_3A and C_4AF hydration (Bye, 1983). The hydration products of the anhydrous phases in HCP often include significant contamination.

A 28 day old hydrated cement paste therefore typically consists of C-S-H, calcium hydroxide, AFt, AFm, unhydrated C_3S, C_2S, C_3A and C_4AF, some remaining water and significant porosity. A basic model which reasonably well describes the overall structure of HCP is

presented by Granju & Maso (1984). The model proposes that a dense C-S-H gel binds unhydrated cement cores. Unfortunately this model oversimplifies the structure, it assumes that the grains are monomineralic C_3S, which hydrates to form C-S-H which is of constant density except for a thin outer layer of acicular C-S-H at the interface with pore water. The model obviously does not include the AFt and AFm, or, more significantly, calcium hydroxide. Microscopy (Dalgleish et al, 1980) shows calcium hydroxide present as extensive masses, which in C_3S pastes (Marchese, 1977) intergrows with C-S-H. The amount of product produced by the hydration of C_2S, C_3A and C_4AF is small, either because they are present in small amounts or because they react slowly, but this does not permit the exclusion of these phases from the description of HCP. These phases are particularly relevant in the model of HCP proposed by Scrivener (1984), who suggests that in the earliest stages of cement hydration a shell of aluminate hydrates forms a boundary layer around the cement grains, and that C_3S hydration takes places inside this shell to form a layer of dense inner product, and outside this shell to form an outer product whose density is dependent on the space available between the grains. This model also explicitly assumes that cement which is predominantly C_3S is made up of grains which are generally polymineralic, and that as there are differences between the hydration rates and mechanisms of the anhydrous phases it is unreasonable to assume that C-S-H is present as an enveloping mass around each cement grain.

The model of 28 day old HCP that is the basis for the following text is, unhydrated cores of various anhydrous phases, of which the C_3S is surrounded by a layer of dense C-S-H [inner product C-S-H] which is in turn surrounded by a layer of C-S-H [outer product C-S-H] whose density is variable and generally less than that of inner C-S-H. There are discontinuities in the C-S-H where the underlying anhydrous material was not C_3S, which may be filled with the hydration products of these other phases, or by calcium hydroxide. Calcium hydroxide is also present in a number of originally water filled spaces, though a number of spaces do remain [capillary porosity].

2B STRENGTH OF HARDENED CEMENT PASTE

2B.I STRENGTH OF MATERIALS

2B.I.i Griffith Theory

It is commonly found that the observed strength of a material is much less than the strength determined by theory. This was explained by Griffth (1920) as being due to cracks and other flaws in the material.

Griffith suggested that a crack would grow rapidly and cause fracture when the strain energy release rate [G] was equal to the rate of increase in the energy required to form new surfaces. Griffith considered an elliptical crack of length 2c in an infinite plate, and the strain energy [U] was shown to be;

$$U = \frac{\pi c^2 \sigma^2}{E}$$

where σ is the applied tensile stress and E is the elastic modulus. The energy to create new surfaces W is simply;

$$W = 4cT$$

where T is the specific surface energy. Thus the criterion for fracture is;

$$\frac{d}{dc}\frac{\pi c^2 \sigma^2}{E} = \frac{d[4cT]}{dc}$$

i.e.

$$\frac{2\pi c \sigma_f^2}{E} = 4T = G_c$$

where G_c is the critical strain energy release rate, and σ_f is the failure strength. This relation is more familiarly expressed as,

$$\sigma_f = \sqrt{\frac{2ET}{\pi c}}$$

The stress intensity, K, relates the stress at the crack tip to the applied load and specimen geometry, and in plane stress is simply related to the strain energy release rate;

$K^2 = EG$, and hence $K_c^2 = EG_c$

where K_c is the critical stress intensity. By comparison with the above equation for critical strain energy release rate, G_c, the critical stress intensity, K_c, can be simply expressed as;

$$K_c = \sigma_f\sqrt{\pi c}$$

where σ_f is the load required for failure, given a crack length, c. Although strain energy release rate [G] and stress intensity [K] are very closely related, a situation has arisen in which the former is used by mechanical and civil engineers, to the exclusion of the latter, which is the preferred measurement of metallurgists and materials scientists.

2B.I.ii The Applicability of the Griffith criterion for failure

Materials which obey the above failure criteria must be brittle, their fracture must consist solely of elastic deformation until the energy available in this elastic deformation [U] is sufficient to cause cracking. These materials behave in a linear elastic manner upto the point of failure, and the failure criteria are collectively known as linear elastic fracture mechanics [LEFM].

In materials where plastic deformation occurs [the vast majority] fracture mechanics must be used which take into account the energy required for plastic deformation. In a number of materials this has been overcome by simply assuming that the region of plastic deformation is very small, and including a specific surface energy term for plastic deformation [T_p] in the Griffith expression for failure,

$$\sigma_f = \sqrt{\frac{2E[T+T_p]}{\pi c}} \text{ , or where } T_p >> T \quad \sigma_f = \sqrt{\frac{2ET_p}{\pi c}}$$

The relationship assumes that the bulk of the material behaves in a linear elastic manner, and results in the same inverse square root relationship between failure strength and crack length.

More complicated descriptions of crack tips in materials which contain a region of plastic deformation have been suggested by Dugdale (1960) and Barenblatt (1962). In these models the crack tip is tied by

closing forces acting across it (see figure 2.03). The relationship between failure strength and the crack length depends on these closing forces.

In the Dugdale model, which was conceived to describe the behaviour of steel, a constant closing stress [σ_y] acts across the crack tip. The relationship between crack length [c] and failure load is usually expressed as a critical crack opening [δ_c], at which the closing stress falls to zero, and the crack propogates.

$$\delta_c = \frac{8\sigma_y c}{\pi E} \ln \sec \left[\frac{\pi\sigma}{2\sigma_y}\right]$$

In the Barenblatt analysis the closing stress is not constant, but varies with crack opening (see figure 2.02), resulting in a more complex relationship between crack opening, crack length and failure load, which depends on the particular variation in closing stress.

2B.II THE APPLICABILITY OF FRACTURE MECHANICS TO HCP, MORTAR AND CONCRETE

A large number of researchers have performed a very large number of tests on HCP, mortar and concrete to determine whether linear elastic fracture mechanics can be applied.

The investigations performed on HCP (Higgins & Bailey, 1976; Gjorv et al, 1977) have shown it to be highly notch sensitive, whereas mortar and concrete are much less so (Gjorv et al, 1977). However, in HCP, mortar and concrete the specimen dimensions appear to alter the measured values of critical stress intensity (Higgins & Bailey, 1976; Mindess, 1984), and in the case of mortar and concrete it has been shown that K_c decreases with increasing relative notch depth (Gjorv et al, 1977).

It had previously been observed that the stress-strain behaviour of concrete and mortar were non-linear (Moavenzadeh & Kuguel, 1969; Hillmeier & Hilsdorf, 1977), implying that a significant amount of inelastic deformation is occuring, and suggesting that linear elastic fracture mechanics were not directly applicable. There is considerable evidence [from fracture properties (Brown, 1972); from acoustic emission (Evans et al, 1976); and from direct observation (Hsu et al, 1963)] that the fracture of mortar and concrete occurs by the coalescence of microcracks to form a macrocrack. The microcracks

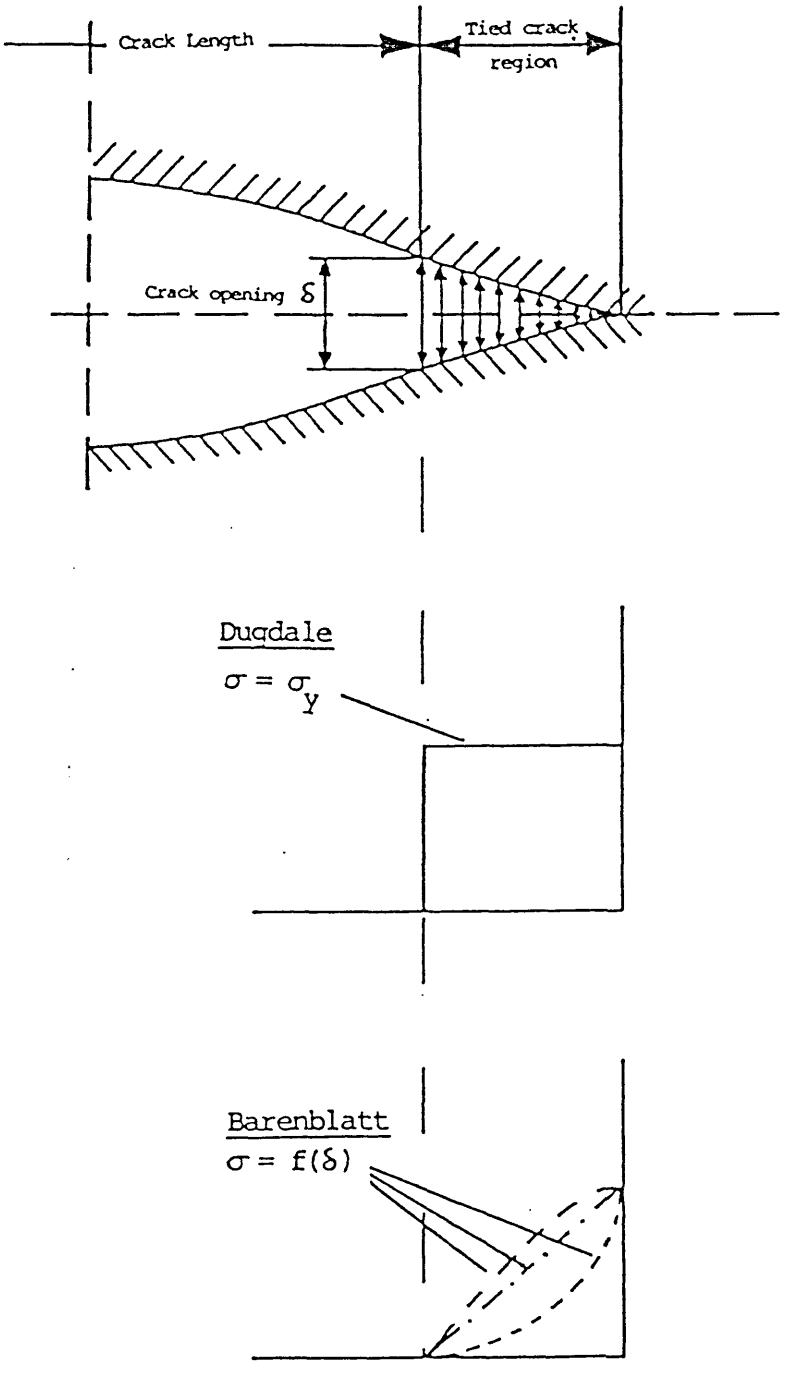


Figure 2.02 Dugdale-Barenblatt tied-crack model

are generally nucleated at the aggregate/matrix bond in a zone ahead of the crack, which increases in size to a limiting value with increasing crack extension (see section 2B.III.ii).

On the other hand the HCP behaves in a much more brittle manner, although there is still a significant region of non-linear behaviour at high stresses.

Many workers have assumed that HCP behaves in a similar manner to concrete and mortar, regarding the unhydrated cores as micro-aggregate. This assumption does not appear to be valid when the differences in stress-strain behaviour and the appearance of fracture surfaces are considered. Microscopic examination of HCP fracture surfaces (Walsh et al, 1974) shows that they consist predominantly of C-S-H and calcium hydroxide, rather than pull-out of unhydrated cement cores. This is unlike concrete and mortar, in which aggregate pull-out forms a significant part of the fracture surface. The implication is that the anhydrous core/hydrate bond is relatively strong, and is therefore less likely to act as a site for microcracking.

It is still unclear whether linear elastic fracture mechanics can be applied to HCP. However before continuing to discuss its applicability it is necessary to examine the implications of the complex crack patterns which can occur on a macro-scale in HCP.

2B.III CRACK PROPAGATION PATTERNS

When a crack propagates through a material, the idealised process of a Griffith crack propagating in a straight line through a continuum is very seldom the case. More often inhomogeneities, e.g. grain boundaries and second phases, in the material cause a crack to deviate from a straight line, e.g. along the grain boundaries, or by coalescence of microcracks formed in weaker phases; the crack pattern is determined by the material. To gain a representative measurement the test circumstances must be such that the pattern of crack propagation is consistent, and in order to do this the nature of the crack pattern must be known.

In the case of HCP, the microstructure is highly inhomogeneous, and three possible crack patterns have been proposed in the literature: a single crack (Moavenzadeh & Kuguel, 1969); micro-cracking and crack branching (Grudemo, 1979); and multiple crack initiation and subsequent growth of a single crack (Hillerborg & Hilsdorf, 1977).

2B.III.i Single crack (see figure 2.03.i)

In the simplest case of a single crack running from a notch in a homogeneous material, the critical stress intensity is a material constant, i.e. it is independant of the length of cracking in the specimen, and also the type of specimen. Complications can arise; for example if a sharp crack has not been initiated at the notch root, the measured stress intensity may include a component necessary to initiate a crack;in the case of inhomogeneous materials the specimen dimensions must be sufficiently large so that the measurements made are performed on a representative mass of the sample.

The evidence of a simple single crack process occurring in cement is limited to direct observation of fracture surfaces (Moavenzadeh & Kuguel, 1969), which were regarded as flat, which is obviously not the case. Brown (1972) did not find any variation with crack length in the measured value of critical stress intensity in HCP cement which may imply a single crack fracture process, but as this behaviour can also occur under particular circumstances with other crack patterns (see below), it seems that the single crack model should only be regarded as a first approximation for HCP.

2B.III.ii Microcracking and Crack Branching (see figure 2.03.ii)

In a material which contains a number of particles susceptible to cracking, either because they are weaker or under increased local stress fields, microcracks in these particles may form adjacent to the major crack. The formation of a process zone ahead of a crack tip, will result in a process zone wake as the crack grows. Evans & Faber (1984) have shown that such a process zone wake, consisting of microcracks [or extensive crack branching] will shield the main crack tip from the full effects of the applied load by decreasing the local elastic modulus, and by dilation occuring as a result of microcracking or branching. This results in an increasing resistance to cracking [R] as the crack grows, which reaches a maximum at a crack extension of approximately 5 times the wake width, or in the case of a wake whose width continues to increase the resistance will continue to rise. This so called rising R-curve has been observed in notched beam alumina specimens (Hubner & Jillek, 1977; Knehans & Steinbrech, 1982), and was shown by optical microscopy (Hubner & Jillek) to be due to extensive crack branching. In the case of concrete and mortar, a rising R-curve has been observed (Brown, 1972; Naus et al, 1974; Wecharatana & Shah, 1980), due to extensive microcracking (Hsu et al,

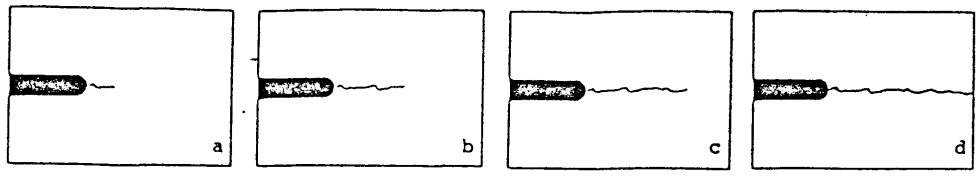


Figure 2.03.i Single crack.
A single crack propogates through a material with small deviations caused by inhomogeneities.

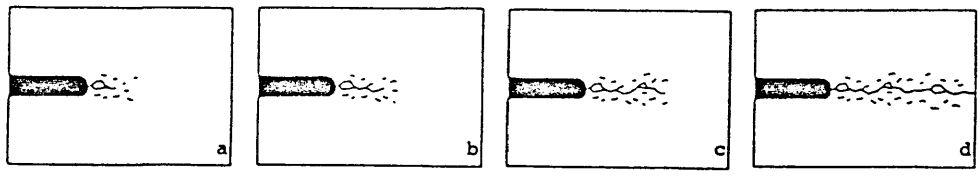


Figure 2.03.ii Microcracking.
In a material susceptible to microcracking a process zone of microcracks forms ahead of the crack tip, which becomes a wake as the crack grows.

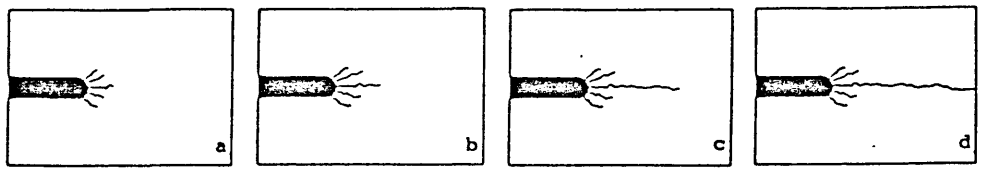


Figure 2.03.iii Multiple crack initiation.
In a material where a number of cracks are initiated the effective stress intensity at each crack tip will vary. As the cracks grow, local inhomogeheities result in a single crack becoming the only one in a stress field sufficient to cause crack growth.

Figure 2.03 CRACK PROPAGATION PATTERNS

1963). In HCP the presence of an increased resistance to crack growth due to a zone of microcracking has only been proposed (Grudemo, 1979; Davidge, 1983).

There is evidence (Higgins & Bailey, 1976) that one of the processes of crack growth in HCP is the coalition of microcracks ahead of the crack tip, and although a zone of microcracking around the crack tip could not be seen there are several factors which suggest that microcracking is likely to occur in HCP. These are: residual stresses in the material, caused by local expansion which accompanies the formation of hydration products; the relative weakness of some of the hydration products [outer product C-S-H and suitably oriented calcium hydroxide]; the presence of irregularly shaped features likely to act as stress concentrators, capillary pores, unhydrated interstitial material; the widely varying elastic modulii of adjacent components, which may also act as stress concentrators. These factors make it almost inevitable that some microcracking does occur in HCP.

It is important to remember that the constant value of K_c for HCP measured by Brown (1972) does not preclude a microcracked region, it may merely imply that it is of limited and constant extent. The initial crack advance of 1.5mm, which occurs at the constant value of K_c (Brown) implies (Evans & Faber, 1984) that a microcracked region would have a maximum extent of 300μm.

2B.III.iii Multiple crack initiation (see figure 2.03.iii)

Examining the fracture mechanics of the constituents of conrete, Hillerborg & Hilsdorf (1977) found that the critical stress intensity measured on compact tension specimens of HCP decreased with increasing crack growth to a minimum value at a crack length of 20mm, and so proposed a mechanism of multiple crack initiation at the notch root. The effective stress intensity on any particular crack is decreased by the presence of the others, as in the case of crack branching. As crack growth continues local inhomogeneities in the structure and stress field arrest the growth of individual cracks until a single crack remains which is under the influence of all the applied load, and results in the base line value of the critical stress intensity.

This behaviour is difficult to reconcile with the microscopical evidence (Higgins and Bailey, 1976), who observed only a single crack propagating from the notch root in a wedge loaded pseudo compact

tension specimen. A possible explanation is that the specimens were tested at the comparatively early age of 7 days [w/c=0.4]. At this age the hydration products will be much less compact than at the more normal testing age of at least 28 days. This may alter the mechanical properties [strength, modulus of elasticity, specific creep] sufficiently to promote a different fracture mechanism.

2B.IV STRENGTH OF HCP

Having examined the possible complications due to crack propagation patterns on a macro-scale, the atomistic model for HCP fracture can be considered further. Relatively recently a series of papers have been published on a novel form of HCP known as macro-defect free [MDF] cement which have specifically adressed the question of the applicability of the Griffith criterion to HCP. MDF cement was developed by the ICI New Science group (Birchall et al, 1981) following their supposition that normal HCP obeyed the Griffith criterion for failure, i.e. that its failure was due to inherent flaws [air voids] introduced during mixing. MDF cement, which is made with the addition of a rheological modifier which allows the material to be lightly rolled, also appears to obey the Griffith criterion. However in this case the processing methods have reduced the inherent flaw size to ~100um, and produced a resulting bend strength of upto $150MNm^{-2}$. The strength for a given flaw size is also increased, due to the increased elastic modulus and fracture surface energy of MDF, ascribed to the lower porosity hydration products.

That the MDF cement behaves as a Griffith type material is of limited relevance to conventional HCP. Further details of the processing (Birchall, 1983), microstructure (Sinclair & Groves, 1985) and reaction mechanisms (Rodgers et al, 1985) have revealed that MDF consists of well packed anhydrous grains bonded together by a complicated hydrate/polymer. Nevertheless the proposition that normal HCP is obeying the Griffith criterion is of great interest; unfortunately the results presented by Birchall et al (1981) showed considerable scatter, thus it is difficult to assign a specific flexural strength-notch length relationship. This scatter is also seen in the results of Alford (1981).

The earlier strength determinations in specimens of various sizes by Higgins & Bailey (1976) also showed some scatter but a trend could be identified, leading to a relationship between strength and slit length in an infinitely large body. These workers suggested that a

Dugdale tied-crack relationship (Dugdale, 1960) was a better representation of their results than a Griffith relationship. The Dugdale model (see section 2B.I.ii) proposes that a zone of plastic deformation can be represented by a crack tip which is "tied" over a finite length by a closing stress [σ_y]. This closing stress falls to zero when a critical crack opening [δ_c] is reached, allowing the crack to propagate. In this case the strength [σ] for a given crack length [c] is (Lawn & Wilshaw, 1975),

$$\sigma = \frac{2\sigma_y}{\pi} \operatorname{arcsec}\left[\exp\left[\frac{\delta_c \pi E}{8\sigma_y c}\right]\right]$$

This proposition of a zone near the crack tip, in which cohesive forces act seems reasonable, particularly as it has been suggested that significant bonding in C-S-H results from interlayer and adsorbed water. The values of yield stress and critical crack opening displacement proposed by Higgins and Bailey of $12MNm^{-2}$ and 1μm appear reasonable, but obviously preclude a simple tying mechanism of a single interlayer of water [<<1μm]. Higgins & Bailey propose that C-S-H platelets, or interlocking C-S-H fibres act to tie the crack. However, environmental cell transmission electron microscopy (Scrivener, 1984) has shown that C-S-H has a sheet, or foil, structure when wet. It is possible that it is these foils which tie the crack in this model, which yield by sliding relative to one another. This sliding prcess would involve interlayer water molecules, in a process similar to that proposed by Bentur et al (1979) for creep, but on a much larger scale and involving contact areas with relatively few bonds.

While a tied crack model appears to adequately explain the notch sensitivity of HCP, it does not explain the reasons for variation in K_c with beam depth.

A number of minimum values of specimen depth have been derived, generally for concrete, for the testing of beams (Walsh, 1973 & 1976; Hillerborg et al, 1976; Carpinteri, 1981). When applied to HCP these give values of limiting depth for SENBs of between 20mm (Walsh, Carpinteri) and 50mm (Hillerborg). Higgins & Bailey (1976) observed that the critical stress intensity was still increasing for beams of up to 110mm depth, which suggests that the minimum values above, underestimate the necessary specimen size for HCP. If beams with a

depth larger than 110mm are necessary for representative measurements of K_c, this implies that the determinations of inherent flaw size will require the use of equally large specimens, particularly as the fracture toughness appears to decrease at low notch length/crack length ratios (Higgins & Bailey, 1976).

To summarise the arguments on the applicability of linear elastic elastic fracture mechanics to HCP. Firstly, it has undoubtedly been shown that HCP is notch sensitive. Secondly, although the behaviour of HCP is in some ways similar to that of mortar and concrete it cannot be assumed that models developed for concrete and mortar can be directly applied to HCP,and vice versa. In particular there is considerable circumstantial evidence that a microcracked region forms in cement but no evidence that it is of significant extent or increasing extent as appears to be the case in concrete and mortar. Thirdly, the size of specimen required for valid determinations of fracture parameters is larger than those which have generally been used so far. Fourthly, although the Griffith criterion for failure gives a reasonable fit to the most extensive measurement program so far performed (Higgins & Bailey, 1976), a better fit is provided by a Dugdale type tied-crack, i.e. a quasi-linear fracture mechanics analysis.

2B.V STRENGTH OF POROUS MATERIALS

Porosity can have a significant effect on the strength of a material by, reducing the effective cross-sectional area, and concentrating stresses at contact points. A number of relationships have been determined which relate the strength [o] of a material to its porosity [p];

$$\text{Balshin (1949)},\ \sigma = \sigma_o\,[1-p]^Y$$
$$\text{Ryskewitch (1953)},\ \sigma = \sigma_o\,\exp[-Zp]$$
$$\text{Schiller (1971)},\ \sigma = \sigma_{cr}\,\ln[p_{cr}/p]$$

where σ_o is the zero porosity strength, p_{cr} is the zero strength, σ_{cr} is a critical strength, and Y and Z are constants.

HCP contains a significant amount of porosity [~30%], which varies significantly with w/c ratio and age. There is a definite increase in the strength of HCP with a reduced porosity (Roy & Gouda, 1973), and all three of the above relationships can, by variation of constants be

adapted to fit HCP strength-porosity measurements (Roy & Gouda; Schiller). This is not suprising, because the relationships can be made to overlap in places, and the measurements of strength and porosity of HCP both show considerable variation.

Roy and Gouda (1973) prepared low porosity pastes, by hot pressing, and suggested that the increase in strength of cement was due to the decrease in overall porosity, which increased the effective cross-sectional area, and reduced the stress concentration at contact points. More recently Alford (1981) has suggested that the behaviour can be explained in terms of the Griffith criterion for failure, and that the increase in strength which occurs at low porosity is a result of the coincidental decrease in the size of the largest flaw. This is a difficult point to argue, because the identification of the largest flaw in HCP is very difficult (Alford, 1981) as it may not necessarily be the largest single pore, but may be a number of smaller features.

2C SUBCRITICAL CRACK GROWTH IN HARDENED CEMENT PASTE

The stress concentrating effect of a pre-existing crack in a brittle material under load may result in a stress at the crack tip approaching the critical stress intensity of the material. Under such circumstances crack growth can occur if the effective surface energy of the material (see section 2B.I) is decreased by thermally activated or by chemically enhanced bond rupture (Lawn & Wilshaw, 1975). Under these circumstances failure by the rapid crack propagation will be preceeded by subcritical crack growth, i.e. crack growth taking place at a stress intensity below the critical stress intensity. This process, by increasing the length of existing flaws, decreases the load bearing capacity of the component. It is therefore of importance to characterize this phenomenon in order to determine its significance in specific applications.

2C.I CRACK VELOCITY-STRESS INTENSITY [V-K] PLOTS

The most elegant method of characterising subcritical crack growth is to relate the velocity [V] of subcritical crack growth to the applied stress intensity [K]. A generalised V-K plot for chemically enhanced bond rupture, often refered to as stress corrosion, is shown in figure 2.05 (Evans, 1972) which shows that above a limiting stress intensity, which will depend on the degree of chemical enhancement to bond rupture, there are three regions of differing behaviour. In Region I crack growth is controlled by the rate of chemical reaction at the crack tip, and the crack velocity increases with increasing stress intensity. As more energy is provided by the increasing stress intensity, the crack tip effectively becomes more reactive. The velocity reaches a limiting value when the rate of crack growth is determined by the rate of diffusion of corrosive species to the crack tip [Region II]. In Region III where the crack velocity rapidly increases again there is a mixture of corrosive and mechanical failure. Most interest is centred around Region I where the crack velocity [V] is related to the stress intensity [K] thus (Evans, 1972),

$$V = AK^n$$

where A and n define the resistance of a material to subcritical crack growth. A is refered to as the V-K intercept, and n as the subcritical

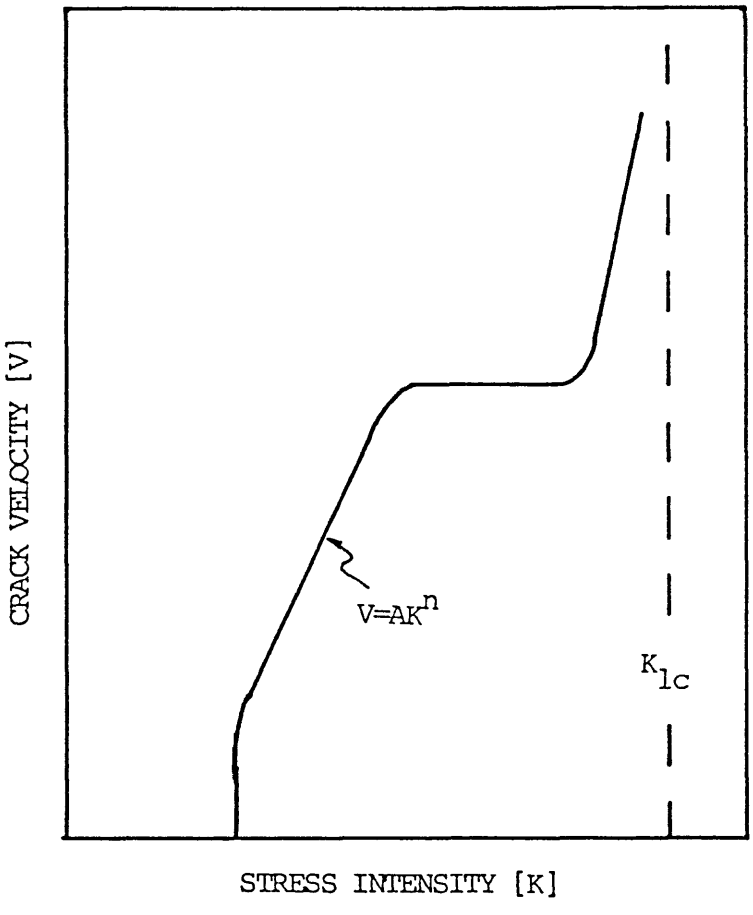


Figure 2.04 Theoretical V-K curve for chemically enhanced subcritical crack growth (after Evans, 1972)

crack growth parameter.

These parameters are of interest because Regions II and III of the V-K plots are very often small, in which case almost all the subcritical crack growth occurs in region I and the time [τ] required for a crack to grow to a size at which catastrophic failure will occur can be calculated relatively simply (Davidge et al, 1973).

$$\tau = \frac{2K_{1i}^{2-n}}{\sigma^2 Y^2 A[n-2]}$$

where K_{1i} is the initial stress intensity due to a constant load [σ], Y is the stress concentrating shape factor of the specimen, and n and A are as defined above. High n and high A values lead to longer lifetimes under a given applied load.

There are a number of possible methods of determining V and K, using a number of specimen geometries. The most common types of specimen are the double cantilever beam [DCB], and more recently the double torsion [DT] plate. Fixed loading is usually used in crack velocity studies using DCBs, where the crack growth is monitored optically and the stress intensity calculated from the load, specimen dimensions and measured value of crack length.

DT specimens have rapidly gained in popularity as for the majority of the length of the specimen, the stress intensity is independant of crack length (Trantina, 1977). The crack length can be measured using compliance techniques, and the crack velocity can be determined from the slope of a load relaxation plot. This precludes the necessity of optical monitoring of the DT specimen, allowing it to be used for materials where the crack is difficult to identify [e.g. cement], and in inaccessible conditions [e.g. vacuum chamber, furnace or cryo chamber]. There are possible complications with DT plates, the crack front is not straight, but extended along the tension face, although this does not appear to affect the V-K curve (Evans, 1972). Trantina (1977) also showed that the maximum stress intensity at a crack front varied with crack angle, making it important to make the starting notch of similar shape to the expected crack front shape.

The V-K curves for several brittle ceramic materials have been determined (Glass - Wiederhorn, 1967; Glass ceramics - Pletka & Wiederhorn, 1974; Alumina - Evans, 1972; Vitreous carbon - Nadeau, 1974) which in all cases showed a Region I, and in the cases of glass

and alumina also included Regions II and III. V-K curves have also been determined for HCP (Nadeau et al, 1974; Mindess et al, 1974; Beaudoin, 1985a&b) which have generally been confined to Region I, occasionally with a hint of Region II (Mindess et al), and Region III only observed when specific w/c ratios and testing humidities were used (Beaudoin). As in other measurements of HCP properties there is considerable variation in the values of subcritical crack growth parameter. Values of n for HCP cited by Nadeau, Mindess and Hay (see refs. above) in separate papers are 36 (Nadeau et al, 1974) and 76 (Mindess et al, 1974). With this degree of uncertainty it is not possible to predict component lifetimes reliably.

The observation of Regions II and III of the V-K plot by Beaudoin (1985a&b) only occured at a relative humidity of 32% in low w/c ratio [<0.35] specimens. More interestingly the V-K curves moved towards higher stress intensities at higher temperatures. The position of the V-K curves also changed with humidity in a complicated manner which was similar to the variation in other measurements of fracture properties by this worker (Beaudoin, 1982). The suggested significance of these variations will be described in section 2C.IV.

2C.II INDIRECT METHODS OF OBTAINING SUBCRITICAL CRACK GROWTH DATA

There are two other methods of determining subcritical crack growth data, the time to failure under constant load and the variation in strength with strain rate.

2C.II.i Time to failure tests

Often referred to as static fatigue tests, the time to failure under a fixed load is measured, and as stress intensity is a function of the applied load, the time to failure will be linked to the applied load by the relationship shown in figure 2.04. This testing method is time consuming and susceptible to errors caused by variations in the strength of specific specimens in a group, consequently it does not appear to have been used for HCP where strength distributions are particularly wide. However a very extensive, and systematically analysed, static fatigue program has been performed on mortar (Barrick & Krokosky, 1976) at various temperatures and relative humidities, in an attempt to determine the processes of stress corrosion, which will be discussed in section 2C.IV.

2C.II.ii Strain rate dependance of strength

The load, and hence the stress intensity applied to the specimen are related to the strain rate via Youngs modulus. As the rate of applied load increases, so too does the increase in stress intensity, i.e. at low strain rates the specimen will be under a stress intensity which induces subcritical crack growth for a longer time than a specimen loaded at a high strain rate. The result of this is that at the lower strain rates a crack will extend further, and reach a length at which catastrophic failure will occur, at a lower load than a similar crack which is loaded more rapidly. Evans (1974) has shown that the slope of a log[strength] vs. log[strain rate] will be 1/[1+n] and that the value of A can be determined from the intercept of this plot. This technique has been used for cement by Mindess & Nadeau (1977), Mindess (1984). Once again the values of n showed significant variation, from 18 to 37, and interestingly the material used by Mindess & Nadeau to obtain the value of 18 for n, using this method, was the same as that used to obtain a value of 36 for n by a V-K plot determination. This difference in values determined by different methods has been observed for a number of materials, and will be discussed below.

2C.III THE EFFECT OF MICROSTRUCTURE AND TEST TECHNIQUE ON THE SUBCRITICAL CRACK GROWTH PARAMETER

Disparity between the values of n determined by load relaxation in DT plates, and by the strain rate dependance of the critical stress intensity has been observed for a number of ceramics; 25μm Al_2O_3 (Davidge et al, 1973); glass ceramic, 9 & 18μm Al_2O_3 (Pletka & Wiederhorn, 1982); glass ceramic (Baskaran et al, 1985). This suggests that the subcritical crack growth parameter is not necessarily a material constant, and is influenced by test method. In all cases the value of n determined from load relaxation in DT plates was greater, and in all cases the materials include inhomogeneities, grain boundaries or second phases, which are likely to have different resistances to crack growth. Thus disparity appears to be a result of discontinuous crack growth in inhomogenoeus materials.

Several observers have noted that the velocity of a subcritical crack growth is not continuous: Freiman et al (1974) observed discontinuous crack growth in DT specimens of polycrystalline aluminas; in constant displacement measurements on glass ceramic DT specimens Pletka et al (1979) noticed fluctuations in the load,

implying that particular areas of the specimen were more or less resistant to crack growth than others; and in beams of silicon nitride Mendiratta & Petrovic (1978) found considerable variation in the extent of crack growth for the same applied load. These observations suggest that a heterogeneous material cannot be regarded as being homogeneous, even in the case of relatively large specimens, as the influence of the heterogeneities may be different in different test procedures.

It has been suggested (Pletka & Wiederhorn, 1982) that load relaxation in DT plates is strongly influenced by particles resistant to crack growth, resulting in values of n which are unrepresentive.

Figure 2.05 shows schematically the effect of the different test procedures over a small region containing a resistant particle [R]. In both cases the change in stress, and crack velocity which occurs is the same, suggesting that the same amount of subcritical crack growth has occured.

In a beam tested to determine the strain rate dependance of critical stress intensity the stress intensity rises from an initial value equal to the lower limit for crack growth through a typical component. The crack velocity increases with increasing stress intensity until a tougher particle is encountered, at which point the crack velocity drops. By a combination of crack bowing (Faber & Evans, 1983) and increased applied load the resistant particle is passed. After passing the tough particle the increased local strain due to bowing is redistributed to the bulk, while the increased applied load causes the crack to grow relatively rapidly.

In the relaxation test the example shows the load starting from the final load of the above example, and as the crack grows through the typical material the load, stress intensity and velocity decrease. On encountering a more resistant particle the crack velocity is further reduced until crack bowing in the adjacent material increases the local stress intensity sufficiently for the crack to pass the particle. After passing the particle the increased local strain due to bowing is again redistributed throughout the material, and as this is the only component making up the increase, the stress intensity and crack velocity revert to typical values. There is no relatively rapid region of crack growth, and as such the resistant particle more strongly affects the overall velocity.

The result of the different behaviour in the two tests is that the values of n determined by the strain rate dependance of critical

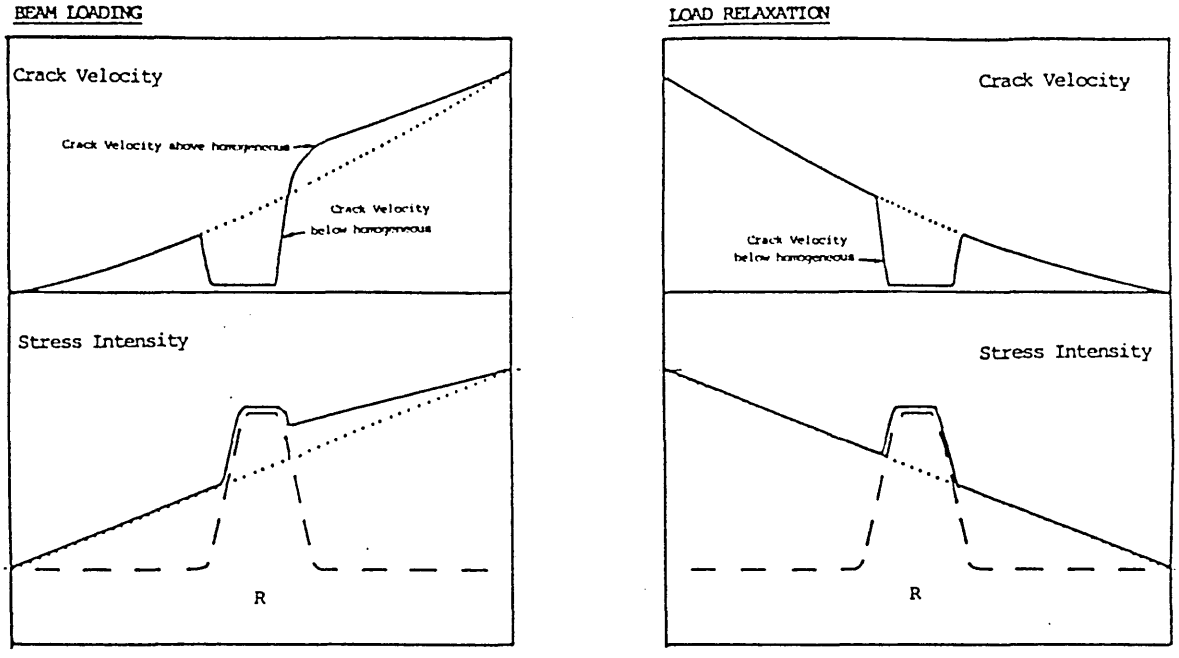


Figure 2.05 The effect of inhomogeneities on subcritical crack growth measurements.

stress intensity is representative of HCP as a whole, whereas the value determined by load relaxation will be more representative of the resistant particles, i.e. high.

2C.IV STRESS CORROSION

A possible reason for subcritical crack growth is stress corrosion. The corrosive species responsible can often be determined by varying the medium in which the tests are performed. For silica glass Wiederhorn (1967) found that the transition from Region I to Region II of the V-K curve occurred at lower crack velocities when the relative humidity was reduced, suggesting that water was active in the corrosion process; changes in pH of the testing medium (Wiederhorn & Johnson, 1973) showed that silica glass was more resistant to cracking in acidic solutions, suggesting that OH^- ions were active in bond rupture. Variation in V-K plots with temperature have been used to determine the activation energies of subcritical crack growth (Wiederhorn et al, 1974; Evans & Wiederhorn, 1974).

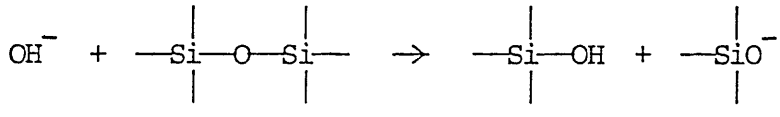
Very few studies have been made of the stress corrosion behaviour of HCP (Beaudoin, 1985a&b) and mortar (Krokosky, 1973; Barrick & Krokosky, 1976) under different testing environments. Barrick and Krokosky (1976) found, in static fatigue tests, that the probability of failure of notched beams decreased with decreasing humidity and with increasing temperature. The decrease with increasing temperature is unusual, because for many processes [including bond rupture] the rate increases with increasing temperature, according to the Arrhenius equation, hence the probability of failure would increase with increasing temperature. The solubility of $Ca[OH]_2$, is unusual in that it decreases with increasing temperature (Weast, 1974), and this could be the rate determining process in the stress corrosion of HCP. In the case of silica glass the concentration of OH^- appears to be particularly significant (Wiederhorn & Johnson, 1973).

Similar conclusions may be drawn from the work of Beaudoin (1985a&b), who determined V-K plots for HCP at different humidities, temperatures and in decanol. The variation of V-K plots [and other mechanical properties (Beaudoin, 1982)] with humidity [100-0%] was complex, but showed an overall shift towards lower contributions by chemical enhancement with decreasing humidity. The effect of increased temperature, between the extremes of 5 and 70°C shifted the V-K curves to higher K values, however included in this overall shift was an opposite shift to lower K values between 22 and 40°C. The tests

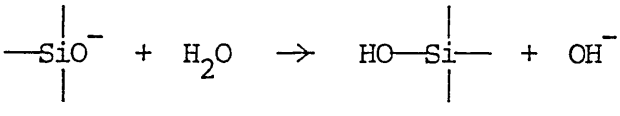
in decanol [lime insoluble], resulted in an Arrhenius type temperature dependance, i.e. the V-K plots shifted to lower K values with increasing temperature.

These observations are consistent with the supposition that OH^- ions are responsible for the corrosion process, except the inversion in the K shift between 22 and 40°C. This inversion may be because a significant contribution to the rate of the corrosion process is determined by an Arrhenius type dependancy, as observed in the V-K plots determined in an OH^- free environmrent.

The suggested corrosion mechanism is as follows;



then;



The higher crack velocity behaviour of Region III, where stress corrosion is not rate determining, has only recently been observed (Beaudoin, 1985a&b) under very specific conditions of humidity, and it may be that under the more normal testing conditions of specimen saturation the pore solution contains an effectively limitless supply of hydroxyl ions.

2D SUMMARY OF MECHANICAL FAILURE AND STRESS CORROSION IN HCP

The conclusions drawn from measurements of strength were that HCP was a notch sensitive material, whose behaviour could be better described as that of a Dugdale [tied-crack] rather than a Griffith material. The nature of these ties were the foils which make up C-S-H, which yielded by sliding over one another. Subcritical crack growth measurements, showed that the determination of probable lifetimes for components is limited by the variation in the measured values of the subcritical crack growth parameters. The proposed mechanism of subcritical crack growth is based on hydroxyl ion attack, presumably of the silicate networks in C-S-H.

In both cases the presence of water appears to be necessary, in mechanical failure the sliding of C-S-H foils is expected to occur across interlayer water, and in subcritical crack growth the presence of hydroxl ions appear to be necessary. This is confirmed by the overall increase in critical stress intensity [K_c] and decrease in susceptibility to subcritical crack growth at lower humidities (Beaudoin, 1982, 1985a&b), although it is not possible to extrapolate directly the effects of humidity when there is not an accepted model for HCP at different humidities.

CHAPTER 3 - EXPERIMENTAL TECHNIQUES

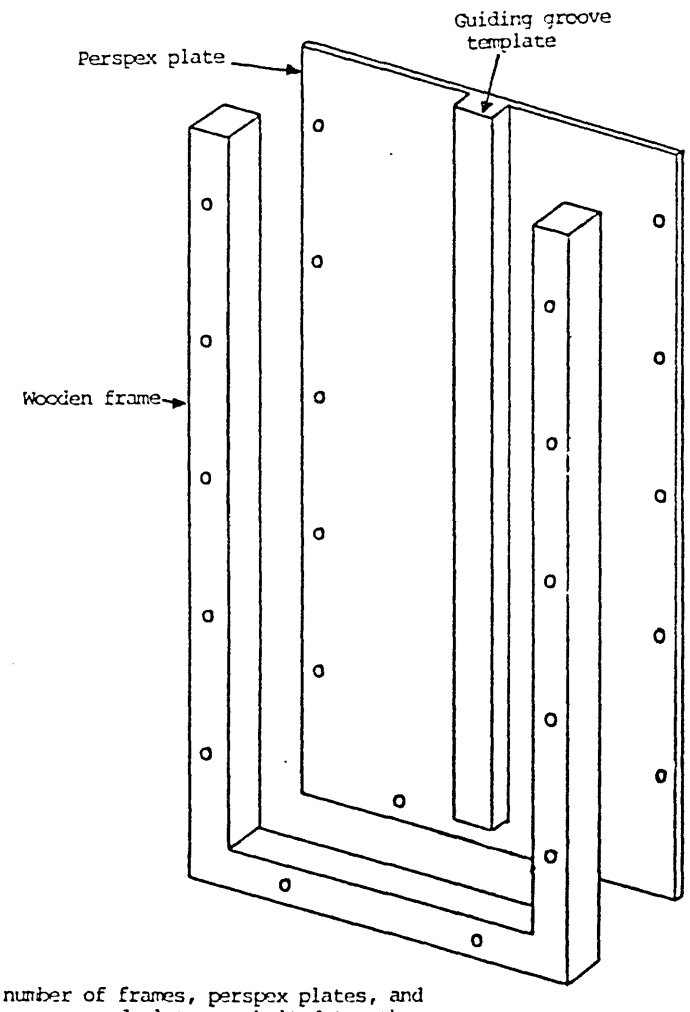
3A SPECIMEN PREPARATION

3A.I Casting

In all experimental work the same cement, a commercial Ordinary Portland Cement [OPC], and a fixed water to cement [w/c] ratio of 0.4 were used. The cement used was supplied to Imperial College Department of Civil Engineering in 6 tonne bulk loads. The cement was chosen because it was readily available in large amounts [over 3 years 500kg of cement were used], and the w/c ratio was chosen because, it is a realistic value compared to concrete, and which produced a mix of a consistency which allowed easy mould filling, but which does not segregate significantly during vibration.

3 types of specimen were cast: 2 different sizes of double torsion [DT] test plates; Type I - 22 x 190 x 450mm, Type II - 24 x 170 x 300mm; and small samples 15mm in diameter by 25mm tall, cast in polythene tubs. The moulds for DT plates were made from Perspex and wood (fig. 3.01), and contained 3 type I or 5 type II plates. A 10mm guiding groove was a cast in feature of both types of DT plate. The cement was mixed for 5 minutes in a large food-mixer [8kg of cement was added to 3.2kg of water] the moulds were then filled, and lightly vibrated for 5 minutes to remove entrained air. Vibration was kept as gentle as possible to minimise segregation, as the moulds were filled with the long dimension [the direction of crack growth] vertical. After 4 hours these moulds were covered with wet hessian and polythene to prevent water loss during early hydration when significant heat is evolved. 24 hours after casting the DT plates were removed from the moulds and stored vertically in a tank of saturated lime water at 20^{o}C until testing. Two sizes of DT plate were used because after constructing the first moulds [type II] it was thought desirable to have available longer plates, as this would allow a greater number of tests to be performed on a single plate.

The tub specimens for microstructural examination were made from batches of approximately 150g of cement mixed by hand, again for 5 minutes, using a metal spatula in a polythene beaker. The tubs were filled and consolidated, by tapping the mould on a bench. Again the specimens were removed from the moulds after 24 hours, and stored in saturated lime water until testing or preparation for microstructural examination.



A number of frames, perspex plates, and a perspex end plate are bolted together to form either 3 or 5 moulds.

Figure 3.01 Double Torsion plate moulds.

3B MICROSTRUCTURAL EXAMINATION

3B.I Scanning Electron Microscope [SEM] Imaging Methods

In a scanning electron microscope [SEM] several interactions occur between the incident electron beam and the specimen which result in the emission of several "types" of electrons and electromagnetic radiation (figure 3.02). The particular SEM [JEOL JSM 35CF] used during this work was equipped for detection of secondary electrons, back-scattered electrons and X-rays.

The surface structure of the specimen can be imaged using secondary electrons [SEI], as the intensity of secondary electron emission depends on the atomic number of the specimen, and more importantly the angle between the incident electron beam and the specimen. High resolution [50nm] images can be obtained, because the secondary electrons detected are produced in a thin layer near the surface of the specimen, and the image is shadowless because the secondary electron detector is biased and so collects electrons emitted from all parts of the surface. For these reasons the SEI mode is used to examine fracture surfaces of HCP, where the structure of the various hydration products, and anhydrous particles can be observed.

Back-scattered electrons as the name implies are incident electrons which have undergone a number of elastic collisions within the specimen resulting in the electron being re-emitted from the surface of the specimen. The intensity of back-scattered electrons is also to some extent dependant on orientation, but is most strongly determined by atomic number, the number of electrons backscattered increasing monotonically with atomic number. By using a pair of back-scattered electron detectors symmetrically placed either side of the incident beam, their signal may be combined to give images [BEI] which are either, atomic number, or, orientation dependant. The potential resolution of back-scattered images is slightly lower [200nm] than that of SEI because the back-scattering events occur within a greater volume of the specimen. To obtain the best resolution of differences in atomic number flat, polished surfaces must be used.

When an electron is incident on a particular atom within the specimen it may transfer some of its energy to that atom by increasing the energy of an individual electron, which subsequently loses that energy by emitting X-rays. The energy of the emitted

Figure 3.02.i -

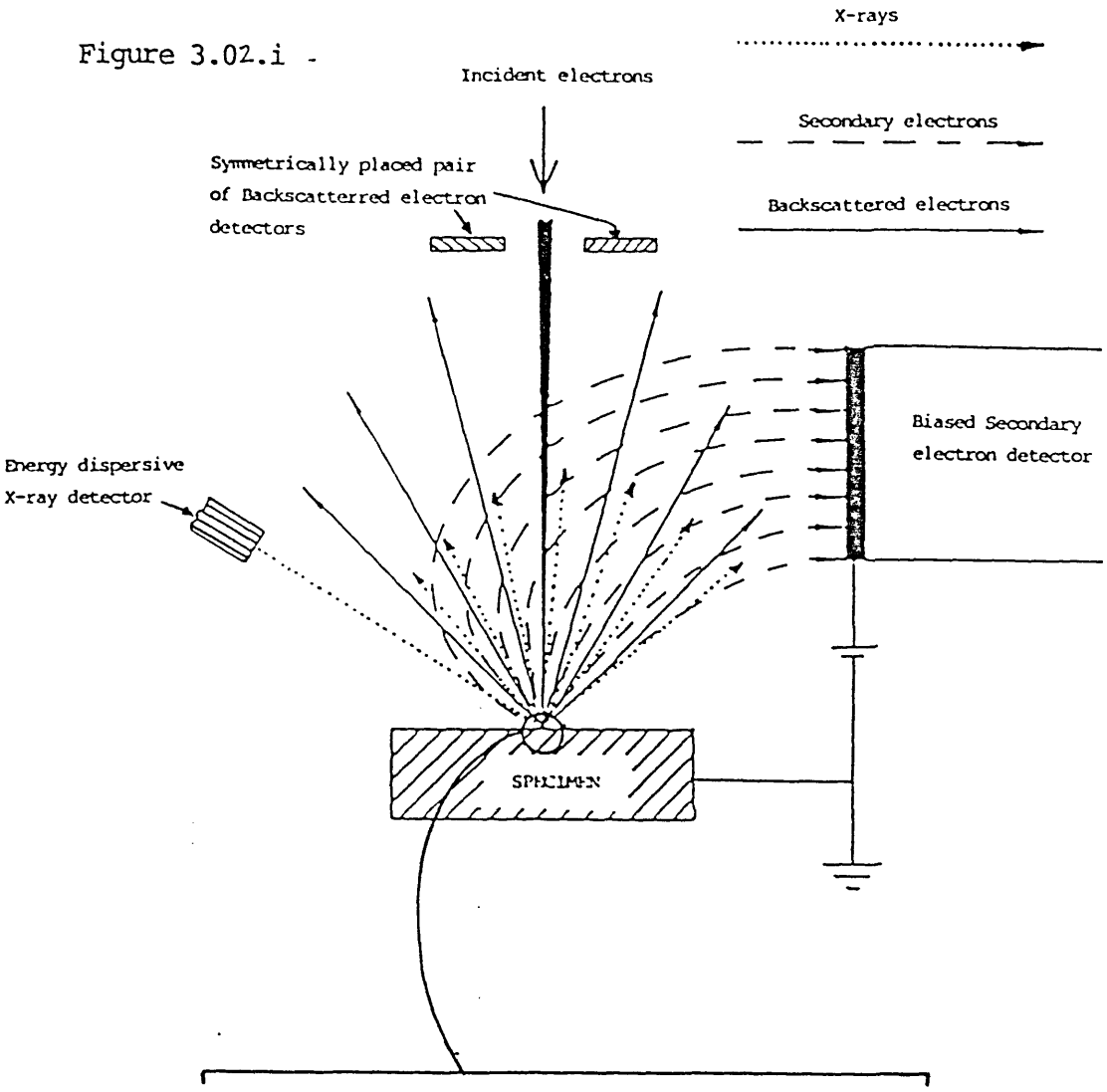


Figure 3.02.ii

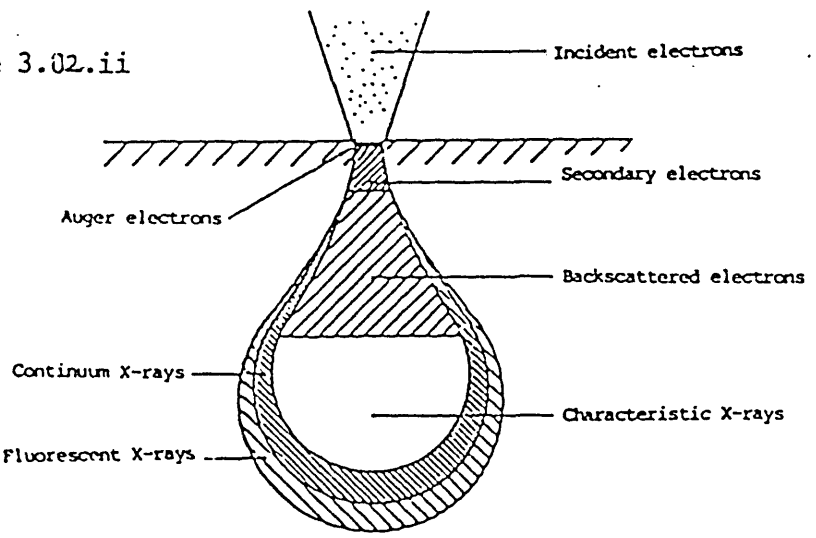


Figure 3.02 Emission of electrons and X-Rays, and arrangement of detectors in the SEM (i), and the characteristic "pear" of emission in the specimen (ii).

X-rays is a characteristic of the atomic number of the atom, therefore an image may be produced of areas emitting a characteristic X-ray energy, and hence containing atoms of a particular element. More commonly the complete X-ray spectrum is used to determine the elemental composition of a particular point on the specimen. Again X-ray analysis is only suitable for flat surfaces and the resolution is low [2-3μm] as the interaction volume in which X-rays are produced is large.

3B.I.i Specimen preparation

For examination in the SEM specimens must be dried [as the microscope column is under a high vacuum], and coated with a thin layer of conducting material [gold or carbon] to prevent the build up of surface charge during examination. The specimens were dried in one of three ways, by direct evacuation in a vacuum dessicator, by methanol exchange, or by freeze drying. The method chosen depended on the type of specimen, and the imaging technique used. For high resolution secondary electron images [SEI] of hydration products freeze drying was used as it minimised the disruption of the fine structure. For back-scattered electron images [BEI] of crack paths in HCP methanol exchange was used as it lessens cracking due to drying shrinkage. For examination of mechanical test piece fracture faces direct evacuation was used.

Freeze drying involved freezing the water present in a HCP specimen by placing it in a mixture of methanol and solid carbon dioxide at $-70^{\circ}C$, then transferring the specimen to a low temperature vacuum chamber where the water was sublimed off. The specimens which were freeze dried were generally those from the 15mm diameter by 25mm high tubs, small sections of which, 2-3 mm thick and up to 10 x 10 mm in area, were chipped from the inner part of the specimen. These sections, glued to 10mm diameter aluminium stubs with "silver dag", and coated with a 200Å thick layer of gold, were examined in the microscope. Gold was used in preference to carbon for the conductive coating on unpolished surfaces because it gives a more even coating. The specimens produced by this method were sometimes cracked due to thermal shock, but the fine structure of the hydration products is retained, and contamination is prevented as the bulk of the specimen is isolated, firstly with frozen water, and later by vacuum. Freeze drying was not regarded as a suitable drying method for mechanical test piece fracture surfaces because it was assumed that

some damage to the specimen surface would occur during freezing, either by thermal shock or chemical contamination. For this reason direct evacuation was used as the drying method for these specimens.

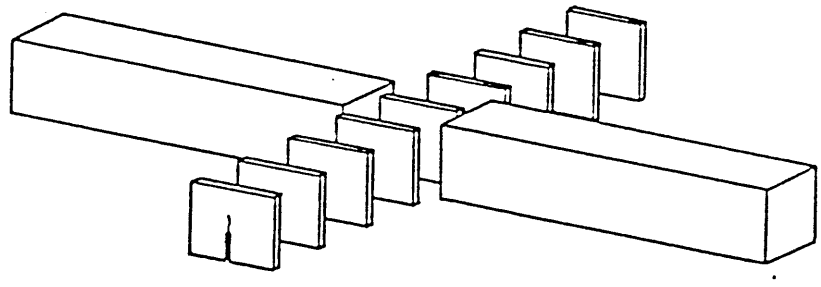
Specimens dried by direct evacuation must be less than 1 cm^3, to allow the water to be removed within a reasonable time, therefore small sections of DT plates and 3-point SENBs fracture faces were either cut from the test peice with a diamond cutting wheel, or chipped off with a razor blade. The specimens were dried for 24 hours over silica gel in a vacuum dessicator, and the whole specimen, or parts of it were then attached to aluminium stubs and coated with a layer of gold. Direct evacuation produced specimens suitable for SEI examination very easily, however there were some major drawbacks, drying shrinkage cracks were produced on a macro- and micro-structural level, and it must be assumed that a number of artefacts are produced by precipitation onto the surface from the pore water during drying. Surfaces are also particularly susceptible to carbonation, the formation of calcium carbonate from lime, or lime bearing compounds, and carbon dioxide. This is a particular problem as it is a fast reaction, which can only be minimised by evacuating the specimen as rapidly as possible.

For examination of introduced crack paths in polished surfaces direct evacuation and freeze drying were unsuitable drying methods due to the extraneous cracking they introduced, therefore the methanol exchange method of drying was used. In this technique the water within a HCP specimen is replaced by methanol, and the methanol is subsequently evaporated off. It is considered (Parrot, 1983) that this technique minimises the effects of drying shrinkage by avoiding the surface tension effects present when water is evaporated directly.

Two methods of introducing cracks were used, followed by the same preparation for microscopical examination. The first method used slices 1-2 mm thick, cut from the cylindrical tub specimens using a diamond cutting wheel. Cracking was induced with a Vickers diamond indentor at loads of between 5 and 20kg, and the slices were then immediately placed in a large volume of methanol [500 cm^3]. The second technique used notched beams, which were slowly loaded until the onset of failure, signified by the levelling off of the loading curve, at which point the specimen was immediately unloaded. Cracking was known to have occured at this stage, because it was possible to load and unload the beam by hand, and observe the crack frothing as air and water were sucked in and out of the crack. The section of HCP

adjacent to the notch was cut out using a diamond impregnated saw, and this cube of material was then cut into several slices (see figure 3.03) and as in the previous case placed in a large volume of methanol.

After three days, exchange of methanol for water was assumed to be complete (Patel, 1984). The specimens were then slowly evacuated to remove the methanol. In some cases this was done with the specimens submerged in a bath of epoxy resin, in an attempt to replace methanol with epoxy resin, which would form a physical support for the structure of the HCP and further prevent cracking. Resin curing took place at 60^{o}C, but impregnation was generally found to be ineffective as the resin penetration into the specimen was minimal. As these specimens were to be examined in back-scattered electron mode the surfaces were then polished for 4 hours each on 14, 6, 3, 1 and 0.25 μm diamond impregnated polishing laps. Finally the polished surfaces were coated with a layer of carbon. Carbon is used as the conducting surface coating on polished surfaces rather than gold because gold coating reduces contrast and resolution in BEI, and the energy of a characteristic X-ray emitted by gold overlaps with one from sulphur, which is often of interest to cement researchers. Although this drying method reduced cracking due to drying shrinkage, particularly in the the thinnest slices, it did not remove the problem completely. Carbonation of the surfaces of the slices did occur during the lengthy exchange procedure, although surface contamination was removed in the subsequent polishing.



A cuboid of material around a notch is removed, then sliced to reveal the crack.

Figure 3.03 Cutting procedure for preparation of sections containing cracks grown from a notch.

3C MECHANICAL TESTING

3C.I Mechanical Testing Specimen Preparation

3C.I.i Double Torsion Testing

The preparation of specimens for load relaxation measurements on Type I and II double torsion plates was relatively straightforward as the crack guiding groove was a cast in feature. The only preparation of the as cast plates was the introduction of an initial "crack", which was accomplished with a diamond cutting wheel, blade thickness 1mm. It was possible to adjust the height of the wheel so that the shape of the introduced crack was of a similar profile to that of a growing crack (see figure 3.04), and the length of the introduced crack was kept constant at a value of approximately 100mm.

3C.I.ii 3-Point Single Edge Notched Beam [SENB] Bend Testing

The specimens used for 3-point SENB testing were prepared from the plates used for double torsion testing. The beams were cut using a diamond cutting wheel to a length of 210 mm and a width of 22 mm, to give a square, or almost square section, for Type I and II plates respectively. The notch was introduced with the same saw [width 1mm] to a depth of 9.5 mm.

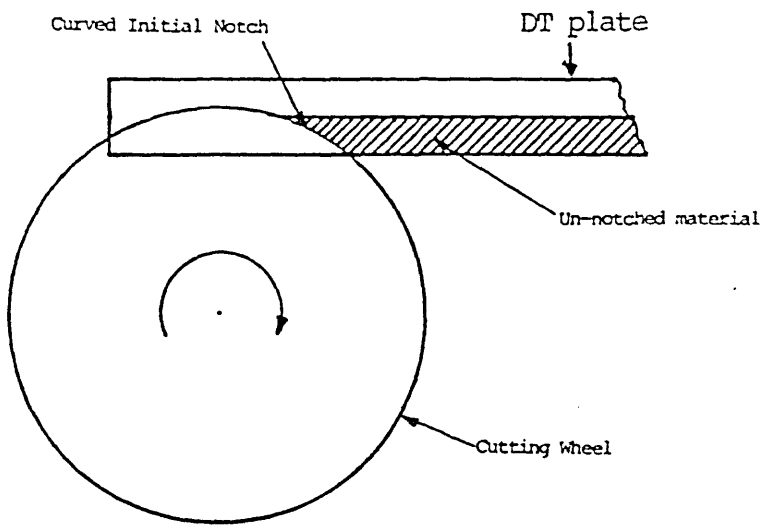


Figure 3.04 Introduction of an initial curved notch into a DT plate

3C.II MEASUREMENT OF SUBCRITICAL CRACK GROWTH PARAMETER - n

3C.II.i Double Torsion Load-Relaxation

From load-relaxation measurements performed on double torsion plates (figure 3.05), values of crack velocity [V] can be calculated at a variety of stress intensities [K]. The subcritical crack growth parameter, n can be determined from these V-K pairs using the relationship determined by Evans (1974);

$$V = AK^n$$

where A is the V-K intercept, and n is the subcritical crack growth parameter.

The calculations of V and K from double torsion load-relaxation measurements are intrinsically simple (Pletka et al, 1979);

$$V = \frac{P_i a_i}{P^2} \frac{\partial P}{\partial t}$$

$$K = Pw_m \sqrt{\frac{3}{wd^3 d_n (1-\nu)\zeta}}$$

where dimensions are those shown in figure 3.05, P is the load, ν is Poissons ratio and ζ is a specimen constant dependant on the thickness ratio ($\psi = 2d/w$), $\zeta = 1 - 0.632\psi + 1.20\psi\exp(-\pi/\psi)$. The subscript $_i$ refers to the initial load and initial crack length, i.e. immmediately after loading.

These calculations are laborious when performed directly from chart output of a mechanical testing machine, as they involve the measurement of load, and rate of change in the load. For this reason a simple interfacing system was used which linked the testing machine to a micro computer, which logged the load-relaxation data and calculated values of V and K. This system of measurement and calculation allowed much more rapid calculation of V-K pairs, because processes such as removal of background relaxation from actual load-relaxation due to crack growth, as well as the final calculations can be performed much more quickly by computer. It was therefore possible to perform a large number of tests, and there was flexibility in the system which allowed emphasis in the number of V-K

Figure 3.05.i

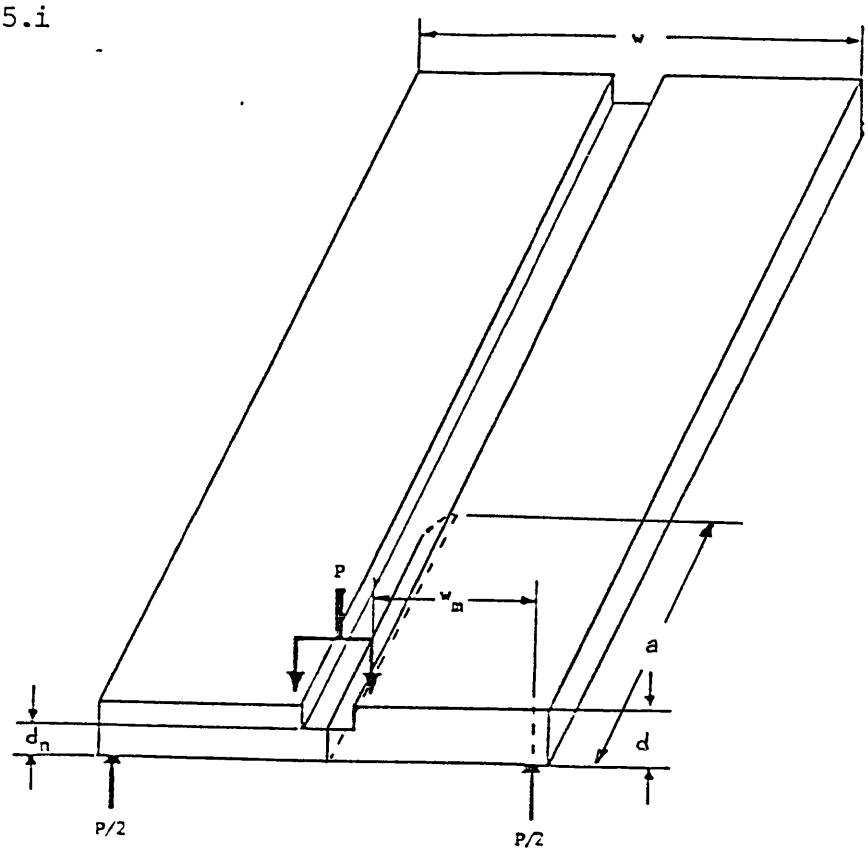


Figure 3.05.ii

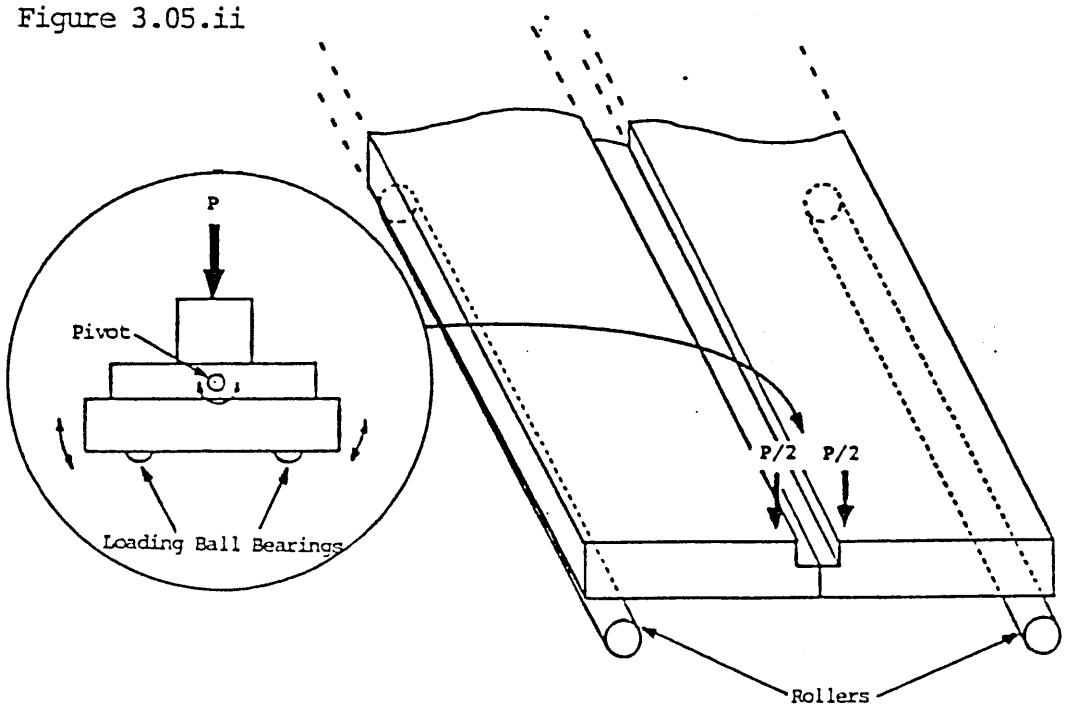


Figure 3.05 DT test specimen (i) and loading arrangement(ii).

pair calculations to be shifted to earlier, or later in the relaxation curve i.e. to higher or lower values of crack velocity and stress intensity.

Three separate measurements had to be performed on the specimen, these were Compliance, Background relaxation and Load-relaxation.

3D.II.i.a Measurement of DT plate compliance

The compliance of a DT plate was determined as the slope of the load-displacement curve, either, between 0.10 and 0.20kN during loading from 0.05-0.20kN, or, between 0.175 and 0.075 during unloading from 0.20-0.05kN. The crosshead speed for loading and unloading was 0.2 mm min^{-1}. While load-relaxation measurements were being made, the applied load was always kept above 0.05kN as this minimised the settling time which had to be allowed to reduce time dependant load changes. For consistency, 2 minutes settling time at a load of 0.05kN was allowed before commencing compliance tests whenever the specimen was being loaded from an initial load of zero during compliance-notch length calibration.

3D.II.i.b Measuremnt of DT plate relaxation

Relaxation measurements are the drop-off in load occurring in a loaded specimen. In practice this simply involves increasing the load on a specimen by raising the crosshead of the testing machine to a point which corresponds to a predetermined load, stopping the crosshead, and logging the value of load over a suitable time period. Unfortunately the simple test procedure is complicated by the fact that during load-relaxation measurements the measured drop in load consists of two components, the decrease due to crack extension and accompanying increase in compliance, and a background relaxation of the test apparatus [testing machine and specimen]. For the subsequent calculations of crack velocity and stress intensity it was necessary to correct for this background relaxation by measuring the relaxation of a specimen at a load below which crack growth would occur, and subtracting a scaled version of this background relaxation from the measured load-relaxation. The background relaxation was measured at approximately 50% of the load used for the load-relaxation test, i.e. the load-relaxation measurements were for loading from 0.10kN to between 0.40 and 0.50kN at a crosshead speed of 2 mm min^{-1}, and the background relaxation was measured between 0.05 and 0.20kN at a crosshead speed of 2 mm min^{-1}.

The background relaxation measurement was easily accomplished using the microcomputer logging system, and was easily subtracted from the load-relaxation measurement. However the values of subcritical crack growth parameter, n, calculated from these corrected curves were unusually large [>100]. This was found to be a result of wrongly assuming that the extent of background relaxation was merely a function of the maximum load. The background was measured after loading between values of load equal to one half of those values used in the load-relaxation measurment [i.e. background - 0.05 to 0.20kN, load-relaxation 0.10 to 0.40kN], and it was assumed that the background component of the load-relaxation would simply be approximately half [i.e 0.20kN/0.40kN] the measured background.

When the calculated values of n were found to be unexpectedly large, the effect of the full loading history on background relaxation was investigated. It was found that the extent of the background was a function of the base load as well as the maximum load, and that under the particular circumstances an extra empirical scaling factor of 0.8 due to the increased base load, as well as the ratio [~0.5] of the increased maximum loads, was necessary. The increased base load does not have as significant an effect as the increased maximum load, on the background relaxation, but as this small change significantly affected the values of subcritical crack growth parameter which were determined. This highlights the importance of good background determinations, and suggests that the reduction in background relaxation produced by maintaining a load of at least 0.05kN was worthwhile.

Testing was carried out on an Instron universal testing machine, linked via an Interactive Structures AI13 interface to an Apple IIe micro computer (see section 4C.I). For both background and load-relaxation measurements the load was logged at the rate of 10 readings per second, over a period of 5 minutes.

A consistent test procedure was used to ensure that the specimens were subjected to the same loading cycle, namely:

i. Measurement of compliance for a DT plate with sawn notches of increasing length (between 100 and 340mm), to determine a notch length-compliance calibration curve.

ii. Introduction of an initial sawn notch (~100mm) into a DT plate, and measurement of its compliance.

iii. Initiation of a sharp crack in this specimen by rapidly loading to 0.45kN, and unloading to 0.05kN after 10s.

iv. Measurement of the compliance of the DT plate with sawn notch and crack, and calculation of overall crack length from notch length-compliance curve.

v. Thorough wetting of the plate.

vi. Measurement of the background relaxation.

vii. Measurement of the load-relaxation.

viii. Steps iv.-vii. repeated until either, the specimen fails during testing, or, after upto 5 repetitions the specimen was rapidly loaded (20mm min^{-1}) to failure, as a measure of K_{1c}.

The specimens were kept wet by spraying with a household plant sprayer.

3D.II.ii 3-Point bend single edge-notch beam [SENB] - Variation in observed Critical Stress Intensity with Loading rate.

During 3-point bend SENB testing the observed critical stress intensity [K_{1c}] varies with loading rate because for the part of the loading cycle approaching the critical stress intensity the stress intensity is high enough to generate subcritical crack growth. The occurence of subcritical crack growth decreases the measured value of K_{1c} because the edge notch is increased in length by subcritical crack growth. The loading rate determines the extent of subcritical crack growth because it determines the time spent at loads above which subcritical crack growth can occur. Evans (1974) determined the relationship between critical stress intensity [K_{1c}] and loading rate [$\dot{x}$],

$$\log [K_{1c}] = \frac{1}{[1+n]} \log [\dot{x}] + B$$

where n is the subcritical crack growth parameter, and B is determined by n and the V-K intercept.

From this relationship, n could simply be deterined from the slope of a $\log K_{1c}$ - $\log \dot{x}$ plot.

The values of K_{1c} were determined for beams 22 x 22 x 220mm, with a 9mm notch, and a span of 190mm (see figure 3.05), the bottom support being a pair of fixed rollers, and the load applied via a freely rotating ball bearing to a third roller (see figure 3.05), where the value of K_{1c} is given by (Brown & Srawley, 1969),

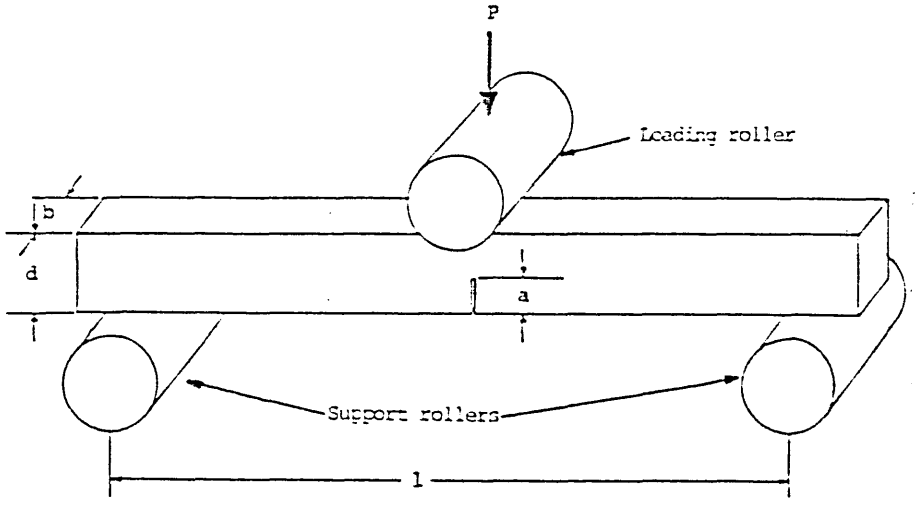


Figure 3.06 Single edge notched beam test arrangement.

$$K_{1c} = \frac{3YP1\sqrt{a}}{2bd^2}$$

Where a, b and d are the dimensions shown in figure 3.05, P is the applied load, and Y is the stress concentrating shape factor of the specimen, which for 3-point bend SENBs is given by,

$$Y = 1.93 - 3.07a/d + 14.53(a/d)^2 - 25.11(a/d)^3 + 25.8(a/d)^4.$$

9 crosshead speeds/loading rates were used, from 8.3×10^{-8} to $1.7 \times 10^{-2} ms^{-1}$, with 16 beams tested at each loading rate, the median value of K_{1c} at each loading rate being used to calculate the slope of the log $[K_{1c}]$ - log $[\dot{x}]$ plot and hence n.

Both an Instron universal testing machine and an ESH servo-hydraulic testing machine were used for measurements of critical stress intensity, the Instron being used for low rates of loading, and the ESH being used for the higher rates. Test times per specimen were of the order of a few seconds for loading rates down to $6.3 \times 10^{-5} ms^{-1}$, which presented no problems of the specimen drying out during testing. However, at lower loading rates the test time increased to a number of minutes, and it was necessary to test the specimens enclosed in fine gauge polythene bags to prevent the specimens drying out, and influencing results.

CHAPTER 4 - COMPUTERS AND COMPUTING

4A Computers

All computers work on the same basic principle of manipulating input data with a program, and more fundamentally by a Central Processing Unit (CPU). Data is entered - through a keyboard, from a magnetic disc, or from some other external device - it is then encoded into a series of binary numbers, as is the program, in which state the CPU can carry out manipulative processes on the data. The CPU is simply a large semiconductor device, and as the physical nature of the device determines the processes which it can carry out. The binary series representing the input data is processed, to produce another binary series representing the output of the computer, this output is decoded to a form which is intelligible either, to the computer operator e.g. a display on a screen, or to a storage device such as a magnetic disc. The differences between computers are primarily differences in the CPUs and the means of inputting and outputting from the CPU, this determines the amount of data that a computer can manipulate, and the speed at which it can be manipulated - the so called power of the computer. The amount of memory and the ability to interact with other equipment such as storage devices are ultimately determined by the CPU, but other factors such as price, physical size, ease of use, and market demand often mean that the full potential is not realised.

The concept of computer power [the speed at which the CPU operates, and the amount of data it operates on] leads to the division of computers into three categories; mainframe, mini and micro computers, although there is some overlap at the top and bottom of the particular ranges.

Mainframe computers are the most powerful, costing upwards of several £100 000, and are generally restricted to scientific research and large national or international organisations e.g. H.M Inspector of Taxes. They often occupy several rooms, can generally communicate to several other computers [mainframe, mini and micro] as well as a variety of other input and output devices.

Mini-computers, less powerful than mainframes are nevertheless extremely fast compared to human work rates, although they are often underused. A mini generally consists of a filing-cabinet size container which houses the computer along with some magnetic storage facility, linked to a keyboard, a Visual Display Unit (VDU), a

printer, and possibly other external links. They cost £10 000s and are typically used for wage control, stock keeping, financial planning etc. in commercial companies

Microcomputers are a much more recent introduction, and are rapidly increasing in power, so in the near future they will be able to perform the tasks of todays mini computers. Micro computers generally consist of three boxes; the computer and some magnetic memory; the VDU; and the keyboard, and generally cost £1000s.

To put things into some perspective, a slow micro-computer will count to 1 million in 16 minutes, whereas it would take a human being approximately 1 month, and at the other extreme the fastest mainframe computer could reach 1 million before you could say it.

4A.I Computers used in this research

Two types of computer were used for experimental work, an Apple IIe micro computer and a Data General Nova 4X mini computer. The reasons for using computers was twofold, first to improve "computer literacy", that is to be familiar with the ways computers work in both general and specific terms, and secondly because of their capacity to record and process large amounts of data rapidly, and accurately. The Data General computer was part of an image analysis system, and as such was used with software which was supplied with the system, therefore more general descriptions of computer handling techniques are included in the description of the Apple IIe.

4A.I.i Apple IIe

The Apple IIe was used as the "workhorse" of data acquisition and processing during this project. Its main task was to acquire data from load relaxation experiments and process this data into values of crack velocity and stress intensity, and ultimately the values of slow crack growth parameter, n. In addition, programs have been used for several other smaller tasks such as: fitting straight lines to data, graph plotting, simple conversions e.g. from chemical composition to Bogue composition, and not least as a word processor for writing this thesis.

First introduced in the early 1970s the Apple II system has been updated and improved to the present model the Apple IIe. Thus the Apple IIe has the major advantage of being a tried and tested product, with almost all of the bugs in the system removed. However, despite its updates, it is rapidly becoming out of date in terms of the tasks

it can perform and the speed at which it performs them.

4B COMPUTING

Computing is the manipulation of data, be it text or numerical, by the computer. The manipulations which the computer performs are determined by the program, or software which has been installed in the computer. For tasks such as word processing or data-base management there are numerous programs available from commercial programmers, but for a specialised application, such as a specific piece of scientific research it is necessary to write original software.

4B.I PROGRAMMING

The major consideration when using an Apple IIe, and any computer for that matter, is to employ the computers inherent quality of speed, to produce software which is as fast as possible. The methods used to make computers software fast can be split into three sections: first by increasing the ease of writing the software, which increases the probability of it working successfully; second by ensuring that the tasks performed within the program are performed as efficiently as possible; and third and most important, by making the program "user friendly", that is making any interactions with a user as simple as possible so that the response times of the user are minimised and the accuracy of response is increased, minimising errors and the need for repetition.

4B.I.i. Programming speed

As in the following sections on efficiency and user friendliness specific examples are used from the four major programs [RELMEAS, BACK, BACKOFF and ALL (see section 4C)] to illustrate the various methods of increasing speed.

The two most important techniques for making programming easier and faster are, using subroutines and abbreviating as much as possible. Taking abbreviations first, as they are used throughout all programs. It is easy to see that the following command for opening a datafile called "REL 1" is rather lengthy,

```
PRINT CHR$(4);"OPEN";"REL 1"
```

yet this command may be used several times throughout a program such as ALL, where it would have to be typed in every time. Any typing errors in this command will be reflected in a program which

does not work properly, and which has to be checked and editted. Therefore the command is abbreviated by defining a variable O$ [O for Open] at the start of the program thus

```
O$ = CHR$(4)+"OPEN"+"REL 1"
```

so that the command to open the datafile "REL 1" would simply be

```
PRINT O$
```

This is obviously a great deal easier to type, and also it is much easier to see any errors in such a short command. In RELMEAS, BACK and ALL variables such as these are defined for all tasks concerning datafiles;

O$ for Opening files
C$ for Closing files
W$ for Writing to files
R$ for Reading from files
A$ for Appending files

The other commonly used abbreviations are those for the keyboard reading routines. It is often required to know if a particular key has been pressed [e.g. in RELMEAS "S" is pressed to start data logging], and this is performed by "PEEKing" into the particular memory location [-16384] which contains a number equivalent to the last key pressed, and then "POKEing" another location [-16368] which clears this number from the memory, ready for another key depression. The whole routine would be as follows,

```
V=PEEK(-16384)
POKE -16368,0
```

if "S" were pressed this would result in a variable, V being equal to 211. This routine is used several times in a program, therefore the numbers are abbreviated, by defining two constants,

```
KB=-16384

KC=-16368
```

which are quicker to type, and easier to remember than their numerical equivalents, thus the abbreviated commands would be,

```
V=PEEK(KB)
POKE KC,0
```

One major "abbreviation" is the use of a core program which contains definitions of the most commonly used variables and commands.

As has already been mentioned, some processes are repeated several times throughout the course of a program. In this situation,

and in situations where a particular process may be selected as an option or, more significantly not selected; it is useful to have such processes as separate subroutines. The reasons for separating these is that in the case of the often repeated process the process may be accessed by a simple,

GOSUB xxxx [where xxxx is the program line on which the subroutine starts]

rather than typing out the same lines repeatedly, while in the case of an optional process, if the subroutine is placed near the end of a program it does not disrupt the continuity of the program with other than the GOSUB xxxx command. An example of the second case is the optional routine [lines 3000-3110] in ALL for editting the calculated values of stress intensity and crack velocity. A program which is made up of a series of subroutines is also easier to check for errors, because subroutines can easily be fed with test data, to check that they are producing the correct output.

Other common sense details which make programming easier are; numbering the lines in regular intervals, with enough room to enter additional lines if necessary; giving variables names which are easily remembered e.g. KB for KeyBoard; and testing newly written material as early as possible.

4B.I.ii Program efficiency

Programs are generally written at almost maximum efficiency because, unless an extremely circuitous method was used, the limmted number of commands generally make the most obvious methods the best. Unfortunately the programming techniques which can make a program more efficient i.e. work faster, also make the program more difficult to follow and therefore more difficult to write. The "fine tuning" of a program is generally performed on a program which is known to function properly, and involves a series of relatively insubstantial changes which can easily increase the speed of a program by over 100%.

The simplest example of this is a FOR...NEXT loop, which is a pair of commands which repeat any command or commands between them for as long as the loop defines e.g. the 5 times table could be printed as follows,

```
FOR I=1TO12
PRINT Ix5
NEXTI
```

which would substitute the values 1 to 12 into the PRINT statement,

and therefore print the values of 1x5, 2x5, ... upto 12x5. To print all the multiplication tables from 1x to 12x two "nested" FOR...NEXT loops could be used,

```
FOR I=1TO12
FOR J=1TO12
PRINT IxJ
NEXTI
NEXTJ
```

But the above process would be completed 50% faster by if the I and J were simply missed off the NEXT statements thus

```
FOR I=1TO12
FOR J=1TO12
PRINT IxJ
NEXT
NEXT
```

and slightly faster still if all the statements were written on a single line

```
FOR I=1TO12:FOR J=1TO12:PRINT IxJ:NEXT:NEXT
```

In this trivial example it is still obvious what will happen when the program encounters this particular line, but in more complicated situations where several lines contain a number of nested FOR...NEXT loops it may become difficult to follow the program, and, as a line can contain a number of statements [upto a total of 256 characters], editing becomes much more laborious. The routine [lines 240-250] in RELMEAS which inputs the load consists of three nested FOR...NEXT loops on I, J and K; the number of the data point governed by the I loop; the J loop sums 5 readings; and the K loop controls the interval between readings. In this instance it is not absolute speed which is essential, but the prerequisite that one cycle of the loop on I takes 0.1s, whereas in BACK and ALL, programs which are dealing with loops containing 3000 cycles of lengthy mathematical manipulation, it is imperative to minimise the length of time for each cycle.

In the section on abbreviations long numbers such as memory locations were given variable names [KB etc.], and as well as being easier to remember this also speeds up a program. Because the computer searches through a list of variable names in the order in which they were defined it is advantageous to define the most frequently used variables as early as possible e.g. in RELMEAS the variables A is used 30 000 times, so to ensure that the timing of the data logging remains constant it is necessary to ensure that any changes to the program do

not alter the position in which A is defined.

Brackets are another luxury which make program steps more obvious but decrease the speed at which a program runs, therefore brackets are deleted wherever possible e.g. lines 1000-1080 of ALL, which calculate crack velocity and stress intensity contain as few brackets as possible.

All of the above procedures tend to make the workings of a program less easily understood and it is generally useful to include some documentation within the program which describes the various parts of the program by using REM statements. REM statements allow the addition of "REMarks" to a program, and if placed outside large FOR...NEXT loops only slow a program down by a small amount. It should be remembered that the major savings in computing time, and, as such, the areas where improvement in efficiency should be concentrated, are within the large FOR...NEXT loops. In extremely complicated programs it is normal to have two versions of a program, the first is fully documented with REM statements, the second is the working version which does not include any REM statements.

4B.I.iii User Friendliness

After ensuring that a program works correctly and increasing its speed the final step, which makes it slower again, is to make those parts where user input is required as informative as possible. Programs which are unintelligible to their users are the least efficient, as the user is unable to respond correctly to the computer's requests for inputs. Being informative means displaying any information which is relevant to a requested input and as little as possible which is not.

There are two ways of displaying information on an Apple IIe, either with text or with graphics. Graphics are indispensable for such tasks as displaying load relaxation curves and V-K curves, but in the Apple IIe use of graphics limits text to the bottom three lines of the screen, so any other information or requests for input must fit into this space. In these situations the previously mentioned routine for checking that a particular key has been pressed is useful, because questions which can be answered by a single key code do not require a separate line on which to enter an input. The subroutine [lines 3000-3110] which edits V-K data obviously requires a plot of the V-K points. The routine therefore uses three key codes for input of editing instructions; the left and right arrow keys to select points

for deletion, and the "D" key to delete them.

The input of names and numbers is generally confined to complete screens of text, where the 24 lines available not only allows the display of as much information as necessary, but also allows these displays to be well spread out and so clearer e.g. in RELMEAS the input of specimen dimensions is done on a screen which only contains the general request for specimen dimensions, and the specific dimensions which are required. This request for input also indicates the units in which the input should be made [in this case kiloNewtons and millimetres], which the program, rather than the user, converts to SI units. The general request, "ENTER SPECIMEN PARAMETERS" is displayed in inverse mode [i.e. white on black] which has been used as a standard method of signifying an input request. The use of conventions such as inverse printing for input requests and standardisation of units makes using a group of programs much easier to use.

Datafiles are invaluable for storing any more than one or two pieces of data, a user soon becomes frustrated when he has to retype the same data, and errors can easily occur. There are several simple ways of making datafiles easier to use, e.g. displaying a catalog of the data disc when any request for a datafile name is made. This is particularily important when using an Apple IIe because a datafile will be overwritten without any warning if another datafile with the same name is dumped to disc. In all cases relaxation files were prefixed by "REL ", and this prefix was always included in any request for a filename and prefixed to the input answer [e.g. line 90 in RELMEAS]. In the case of the program BACK "REL B" must be a prefix to all datafile names, ensuring that only background files can be converted into background correction files.

When the computer is performing any relatively lengthy operation the user should be kept informed of what the computer is doing by short statements, e.g. a relaxation curve may take a number of minutes to go through a smoothing routine; unless a statement telling the user that smoothing is taking place is shown on the screen, the user may believe that the computer has crashed, and so interrupt a working program and start again. On the subject of errors, a simple error handling routine, which identifies the location and type of error which has occured, was included [line 0 and 60000- in all programs]

4C COMPUTER MONITORING AND DATA PROCESSING

Computers have been used extensively during the course of experimental work on subcritical crack growth for data logging and data processing, as well as for several other smaller data processing tasks.

4C.I Subcritical Crack Growth

Subcritical crack growth analysis required the acquisition of load-relaxation data from a mechanical testing machine and its subsequent processing; all of which was performed by a series of computer programs, the basis of which are outlined below. Flow diagrams and program listings are given in Appendix 2 for the four programs mentioned below, RELMEAS, BACK, BACKOFF and ALL.

4C.I.i Data Logging

The tests were performed on an Instron Universal testing machine to which an Apple IIe microcomputer was interfaced via an Interactive Structures AI13 analog to digital converter. The duration of each test was 5 minutes with 3000 readings per test [i.e. 10 readings per second], this was regarded as being a suitable compromise between accuracy and obtaining unnecessarily large amounts of data.

The load, measured by a load cell, was output as a linear voltage of 0-10V, equivalent to 0-full scale deflection [0-1kN in this case]. The interface converted signals of 0-5V into a 12-bit number [0-4096] which was input to the computer memory, i.e. the computer contained a series of numbers whose range of 0-4096 was equivalent to a load range of 0-0.5kN. As the computer and interface had the ability to input at a rate of over 200 readings per second there was sufficient time to perform and sum 5 inputs per load measurement, i.e. 5 x 0-4096 = 0-20480 was equivalent to 0-0.5kN. This number was stored in an integer array (see Appendix 2) and after the test was completed this array was dumped to magnetic disc. This process was performed by a program called RELMEAS.

4C.I.ii Data Processing

Data processing was done in two main parts, relaxation curves were corrected for background relaxation, and values of stress intensity and crack velocity were calculated.

The background relaxation was measured using the same program [RELMEAS] as the load relaxation, thus two files were obtained per

test run, which were called REL Bnn and REL nn, where B denotes background, and nn identifies a particular test. The correction for background relaxation is a proportional decrease from a maximum load, and other than the maximum load, specific loads are not required. A program called BACK therefore converted background files [REL Bnn] from a series of numbers equivalent load [10000] into a series of numbers equivalent to load decreases [100], which took up much less space on data discs and in computer memory. The original background file is deleted and replaced with the converted file which was also called REL Bnn. This inverted background [REL Bnn] was then added to the load relaxation [REL nn] by a third program BACKOFF, to create a corrected load relaxatation file REL nnX. The final program ALL calculates crack velocity [V] and stress intensity [K] from the corrected relaxation curve, plotted the values of V and K, and worked out the slope [n] and intercept [A] of this V-K plot.

CHAPTER 5 - SCANNING ELECTRON MICROSCOPY OF HARDENED CEMENT PASTE

The scanning electron microscope [SEM] used for microscopical examination was fitted with both secondary electron and back-scattered electron detectors. The secondary electron images [SEI] show the 3-dimensional structure of HCP fracture surfaces with good resolution whereas the back-scattered electron images [BEI] show the 2-dimensional arrangement of the various components of HCP with rather lower resolution.

5A.I MICROSTRUCTURE OF HCP

HCP with an original water/cement ratio of 0.4 hydrated for 28 days, and prepared for examination as outlined in section 3B.I.i, was examined in both SEI and BEI modes. This combination of modes in the SEM with observations made by other workers using other microscopical techniques, e.g. environmental cell transmission electron microscopy (Jennings & Pratt, 1979; Scrivener, 1984), ion-beam thinned sections (Dalgleish et al, 1980) can be used to interpret more fully the microstructure of HCP in terms of the expected hydration reactions. To simplify the complex microstructure of HCP the individual components [unhydrated cement, C-S-H, calcium hydroxide, AFt, AFm and porosity] are described separately.

The age of 28 days was chosen because it is significant both from a scientist's and an engineer's viewpoint. The 28 day cube strength is the standard measure of concrete quality used by civil engineers. More important, from a materials science viewpoint, is that at an age of 28 days, HCP has developed a mature structure. During the early stages of hydration [<7 days] significant changes in properties occur, caused by the increasing amount of hydration product. Beyond the age of 28 days, although hydration continues, it does so at a greatly reduced rate, and the structure and properties of HCP are not significantly altered.

5A.I.i Unhydrated cement - C_3S, C_2S, C_3A, C_4AF

There is still a significant amount of unhydrated cement [20-30%] after 28 days hydration which appears bright in BEI because of its relatively high average atomic number; the slight variation in average atomic number between the phases allows them to be identified. Anhydrous cement consists of particles over a wide size range [<1 to >100μm] and as would be expected it is generally the

larger particles [>20μm] which have not hydrated completely. Plate 5.01 shows a large unhydrated core [~75μm], and several smaller ones and various hydration products. The large core is typical in that it contains more than one phase, in this case it is predominantly C_3S, which appears pale grey and is surrounded by a darker layer of C-S-H [see below]. There is also a significant amount of interstitial material [C_3A and C_4AF] which generally appears as interpenetrating darker and lighter grey regions, but in some regions it can be seen that the C_3A has reacted to leave a skeleton of C_4AF. In the case of the C_3A reaction there is not an obvious layer of hydration products attached to the unhydrated material.

3 large cores are shown in plate 5.02; the leftmost is almost completely C_3S and is again surrounded by inner product C-S-H; the lower right is a large mass of interstitial material; and the upper right consists of a pair of C_2S grains, showing characteristic twinning, and some C_4AF. The C_2S grains show little sign of hydration, there is no layer of inner product C-S-H as in the case of C_3S.

Unhydrated cement is rarely seen on fracture surfaces which predominantly show the weaker regions of HCP, the hydration products. Where unhydrated cement can be identified on fracture surfaces it is generally inside a shell of inner product C-S-H (plate 5.03).

5A.I.ii Calcium-silicate-hydrate C-S-H

C-S-H is a gel produced from the hydration of the silicate phases, C_3S and C_2S. It has been observed with a number of different morphologies, the most clear distinction being between the so called inner and outer product. The inner product, C-S-H formed within the confines of the original cement grain, appears dark grey in BEI. Depending on the phase distribution within the original grain, the degree of hydration of the C_3S and the sectioning of the specimen, this inner product is seen as a layer, either isolated, where local C_3S hydration is complete, or surrounding a core of unhydrated C_3S (plate 5.02). Inner product has also been identified on fracture surfaces, and may be seen as; a dense shell, either empty (plate 5.04),or surrounding an unhydrated core (plate 5.03); or because at 28 days the shell is relatively thick, sections through shells of inner product are more commonly seen (plate 5.05); or where fracture has occured around the shell of inner product, a complete "grain" of inner product may be seen (plate 5.06).

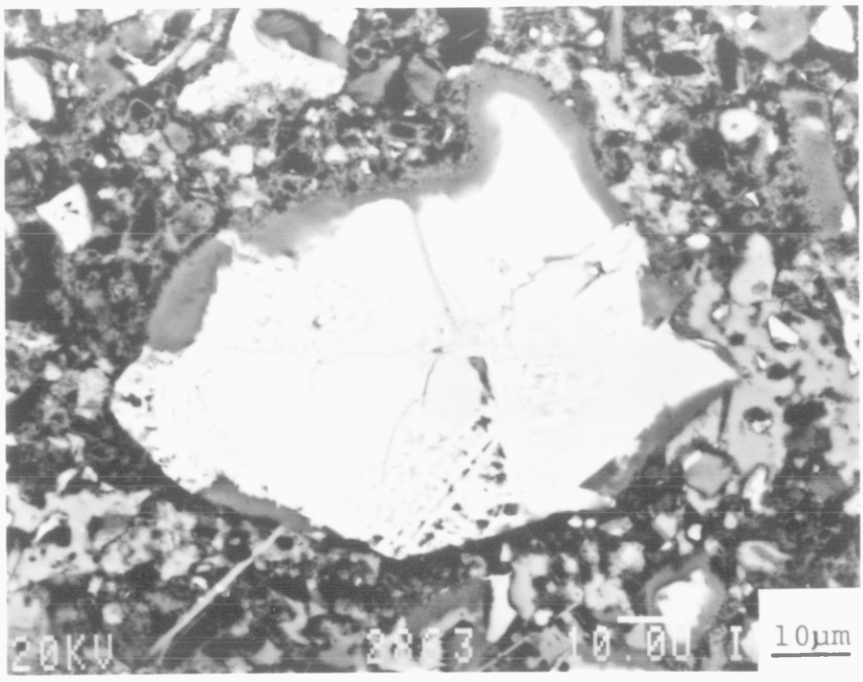


Plate 5.01 Large anhydrous core. BEI polished surface.

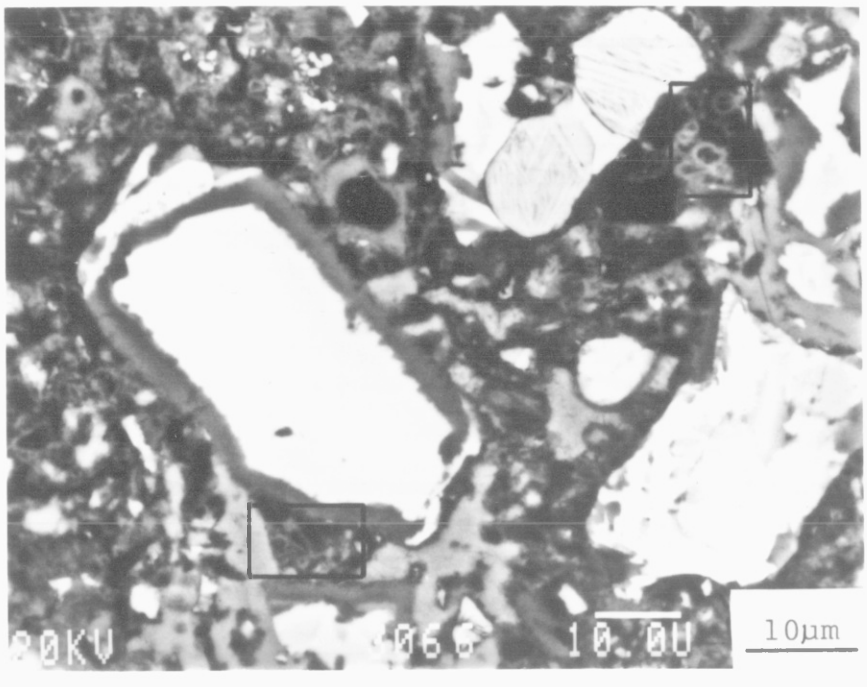


Plate 5.02 C_3S, C_2S and interstitial anhydrous cores. Upper boxed section, small rings of C-S-H. Lower boxed section, AFt. BEI polished surface.

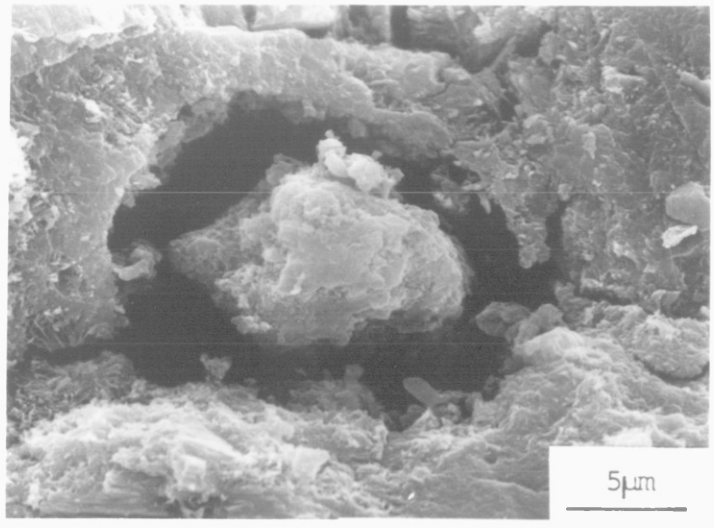


Plate 5.03 Anhydrous core in inner product C-S-H shell.
SEI fracture surface.

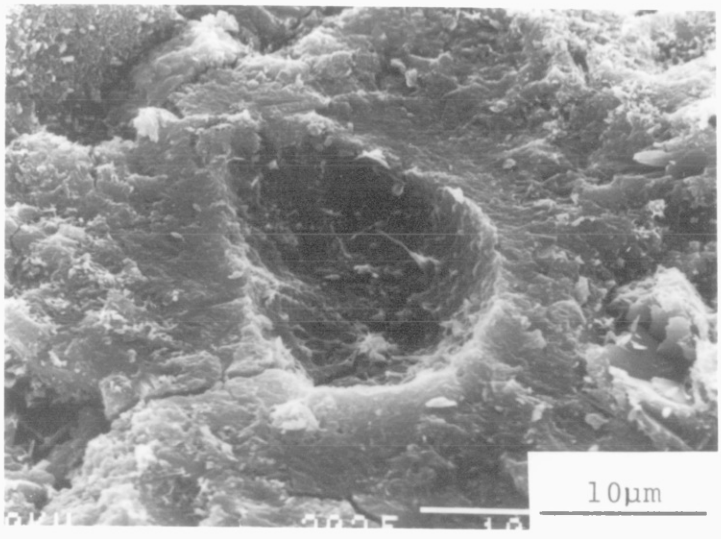


Plate 5.04 Inner product C-S-H shell.
SEI fracture surface.

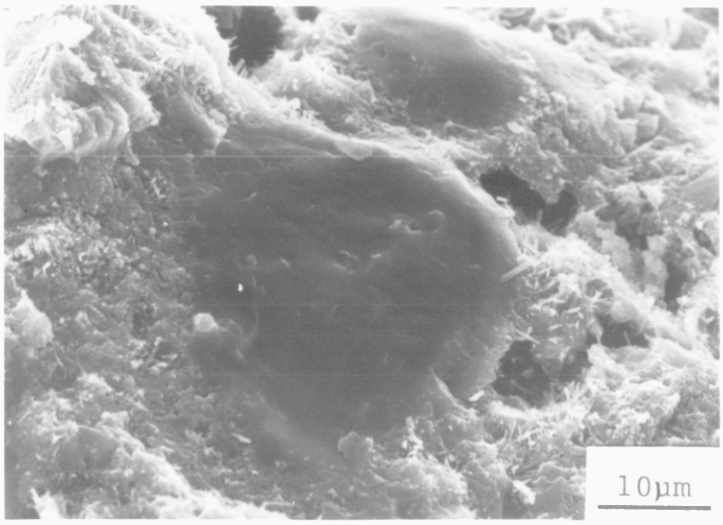


Plate 5.05 Planar fracture through inner product C-S-H.
SEI fracture surface.

Outer product C-S-H grows in the space between hydrating cement grains, which is of varying dimensions, and which possibly contains a variety of other products and solutions, consequently outer product assumes a variety of morphologies. Outer product which was formed in regions where the spacing between the grains was originally large appears on fracture surfaces as a radiating layer of short needles (plate 5.08), although environmental cell work (Scrivener, 1984; Jennings & Pratt, 1980) suggests that outer C-S-H forms as exfoliating sheets, which transform into needles on drying. More commonly outer product is observed as a mixture of C-S-H with other hydration products, plate 5.07 [a higher magnification view of plate 5.06] shows outer product C-S-H intermixed with AFt and possibly calcium hydroxide surrounding a grain of inner product.

On polished surfaces viewed in BEI, outer product can only be discerned as a less compact layer outside the shell of inner product, as around the large anhydrous core in plate 5.01. It should also be noted that in polished surfaces several small shells of inner product C-S-H, presumably from the hydration of small cement grains, are present (upper boxed section of plate 5.02) which may not be distinguishable as such on fracture surfaces.

5A.I.iii Calcium hydroxide - CH

Calcium hydroxide is the other product of the hydration of the calcium silicates, and has a hexagonal crystal structure which is susceptible to cleavage along the basal plane. Observed in polished surfaces calcium hydroxide appears as mid-grey, somewhere between C-S-H and the anhydrous phases, and is seen as extensive masses [up to 100μm] which are often seen intergrown with regions of C-S-H and anhydrous material (plate 5.02). This contact is also observed on fracture surfaces (plate 5.09), where calcium hydroxide C-S-H boundaries are indistinct. On fracture surfaces the crystalline nature of calcium hydroxide can be seen, with the hexagonal habit more obvious in small growths of calcium hydroxide (plate 5.10), and in larger masses the cleavage steps are observed (plate 5.11).

5A.I.iv AFt - $C_3(A,F)(C\bar{S})_3H_{32}$

AFt is the product of the hydration of C_3A, and to a much lesser extent C_4AF, in the presence of high sulphate concentrations, which forms in HCP as high aspect ratio rods. At 28 days AFt is generally observed on fracture surfaces within pores, and more open spaces

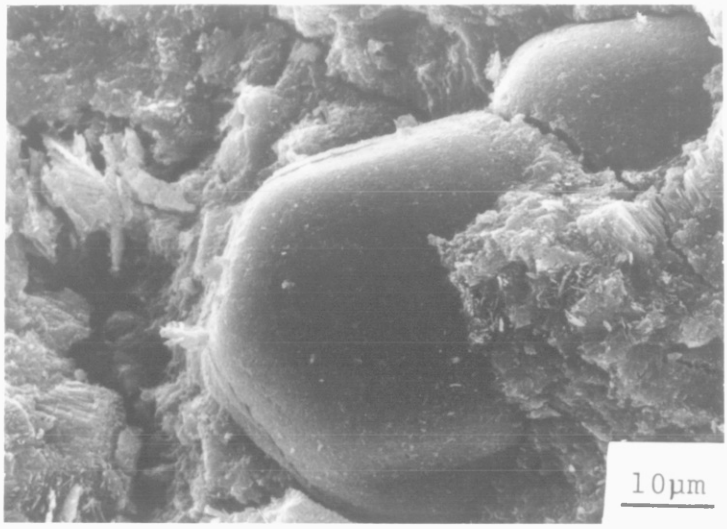


Plate 5.06 "Grain" of inner product C-S-H, partly covered by outer product C-S-H. SEI fracture surface.

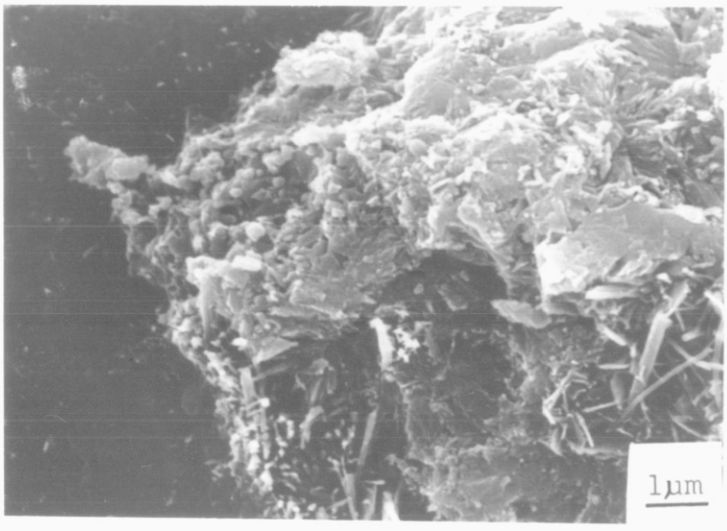


Plate 5.07 Higher magnification view of the outer product C-S-H covering in plate 5.06. SEI fracture surface.

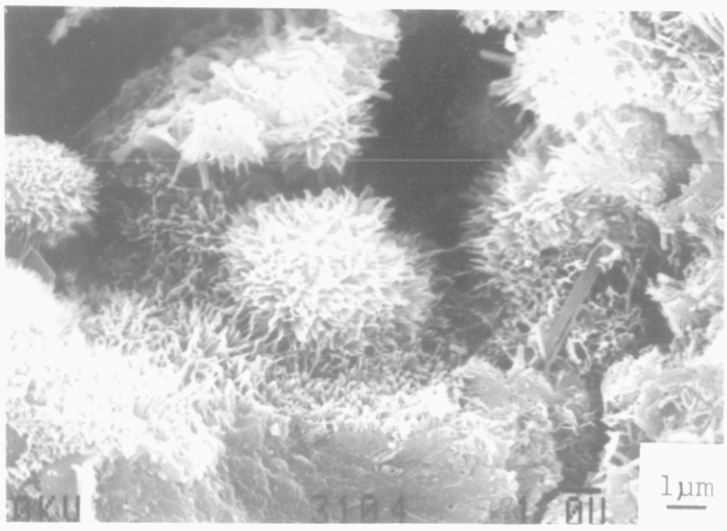


Plate 5.08 Acicular outer product C-S-H. SEI fracture surface.

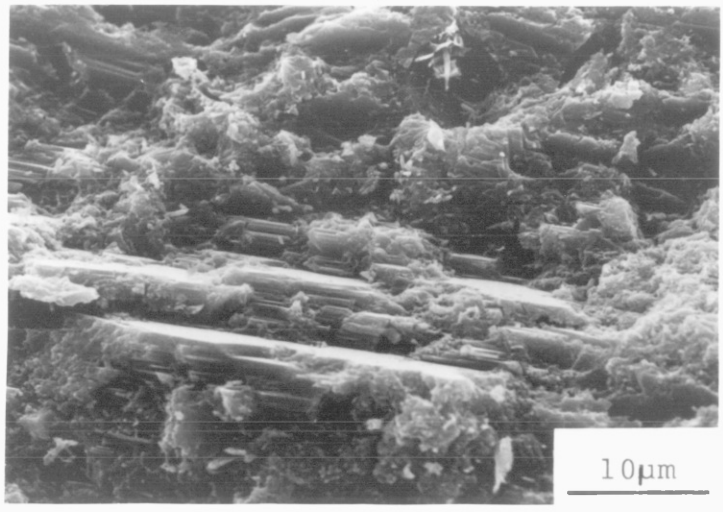


Plate 5.09 Inter-penetrating calcium hydroxide and C-S-H. SEI fracture surface.



Plate 5.10 Small hexagonal crystals of calcium hydroxide. SEI fracture surface.

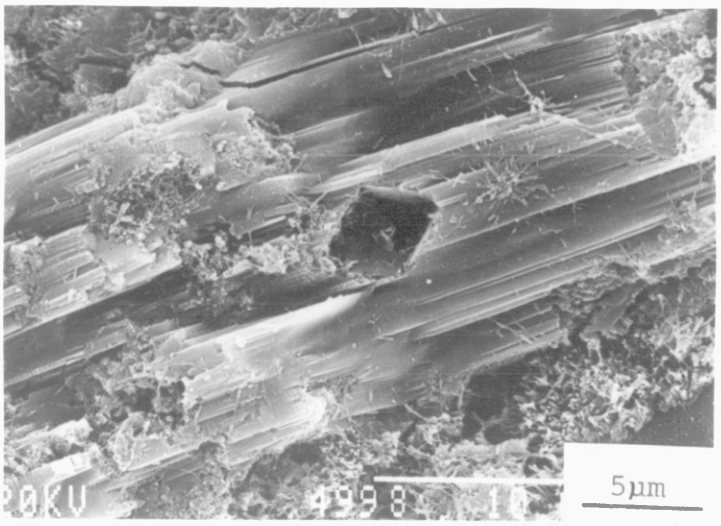


Plate 5.11 Massive calcium hydroxide. SEI fracture surface.

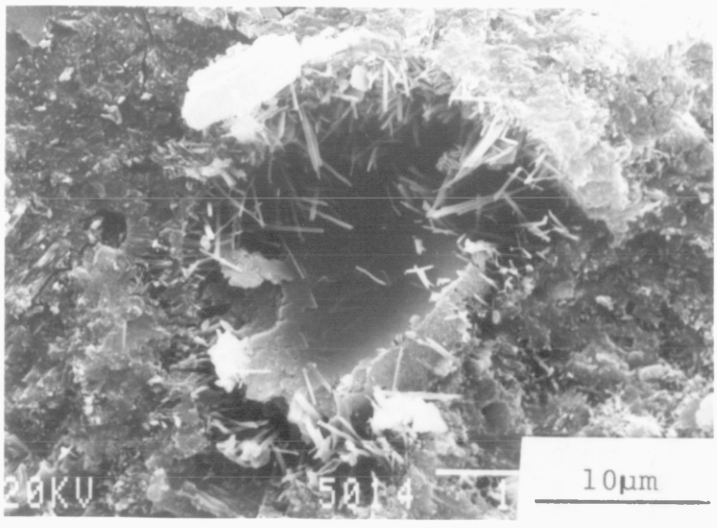


Plate 5.12 AFt rods in pore.
SEI fracture surface.

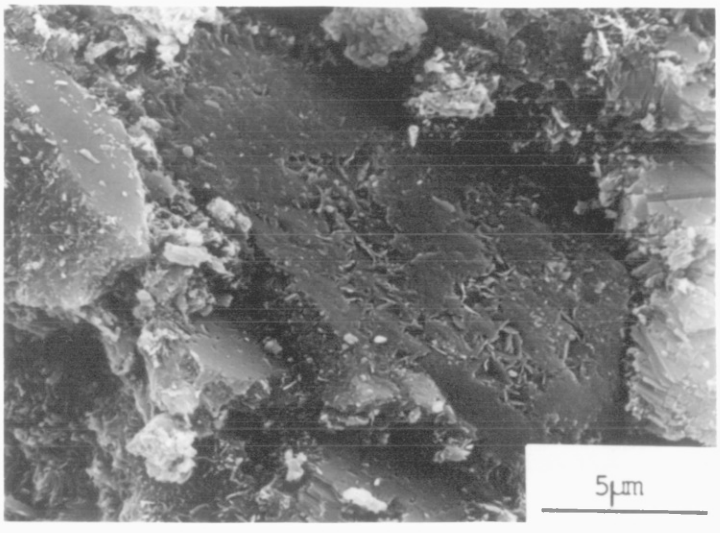


Plate 5.13 AFm platelets embedded in inner product C-S-H.
SEI fracture surface.

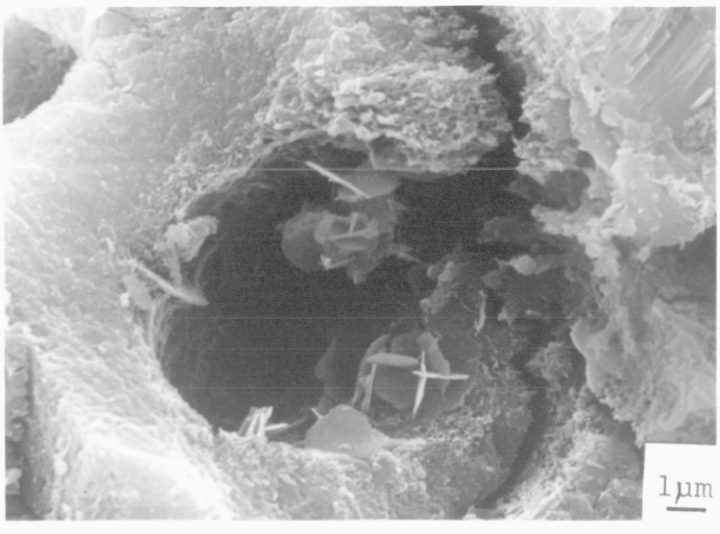


Plate 5.14 AFm platelets inside shell of inner product C-S-H.
SEI fracture surface.

(plate 5.12), though it may also be intermixed with outer C-S-H (plate 5.07). Both AFt and AFm [see below] are minor components of HCP, in terms of volume, which form as discrete networks, and AFt has been possibly been identified on polished surfaces as a interlocking rods (lower boxed section of plate 5.02).

5A.I.v AFm - $C_3(A,F)(C\bar{S})H_{12}$

AFm is a also product of the hydration of interstitial material, which on fracture surfaces is observed as small plates, which are usually associated with inner C-S-H; either embedded in a shell of inner product (plate 5.13); or growing insides a shell (plate 5.14).

5A.I.vi Porosity

There is considerable porosity in HCP [~30%] from large pores [~1mm] caused by entrained air down to porosity within the hydration products of a few Angstroms. Polished surfaces shows the distribution of the large scale porosity as black regions (plate 5.01), which often appear to be an intimate mixture with the hydrates. Fracture surfaces can show the fine scale porosity of the hydrates (plate 5.07), in particular plate 5.08 shows the variation in micro porosity of C-S-H, which is reflected in the compactness of the C-S-H observed in the dry condition in the SEM. At the bottom of the micrograph the C-S-H appears relatively compact, while that in the middle of the field appears highly porous. It is important to remember that apart from air pores the porosity in HCP will be filled with water, and the porous C-S-H will exist as foils rather than fibres.

5A.II Prehydrated microstructure

The preceding microstructural examinations were performed on HCP which was regarded as having a "normal" microstructure, whereas the cement used to make batches 2, 3 and 4 of double torsion specimens was observed to produce a less wet mix; and when examined after 28 days hydration, fracture surfaces were seen to contain darker regions up to 3mm in diameter, which although visible in optical examination were not observed to be different when examined in the SEM. On the other hand polished sections of this material showed these regions both in optical observation, and BEI examination in the SEM, where these areas were seen to be regions of more densely packed unhydrated cores (plate 5.15) surrounded by a layer of calcium hydroxide (plate 5.16). This microstructure suggested that these areas

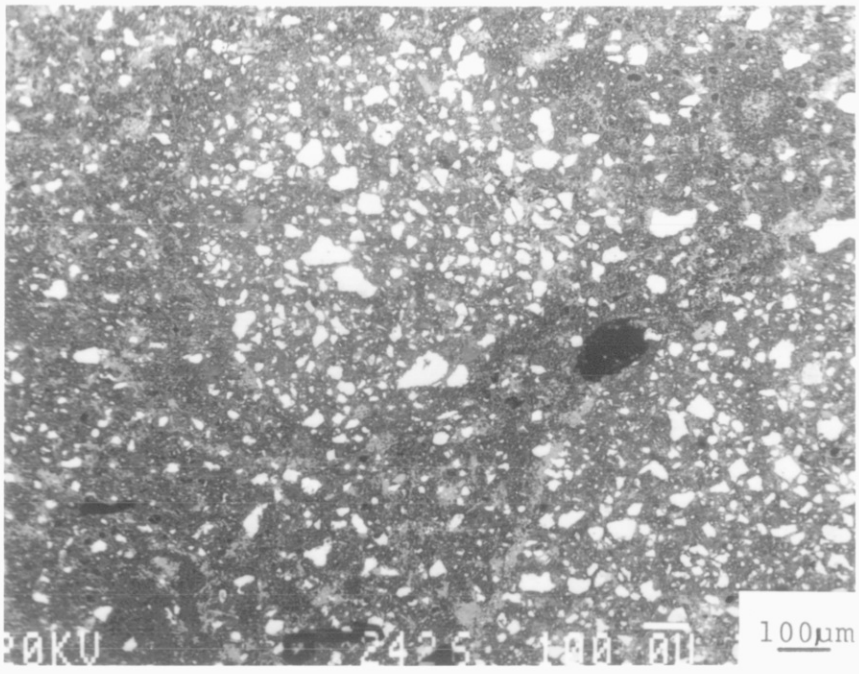


Plate 5.15 Clusters containing a large number of anhydrous particles in prehydrated cement. BEI polished surface.

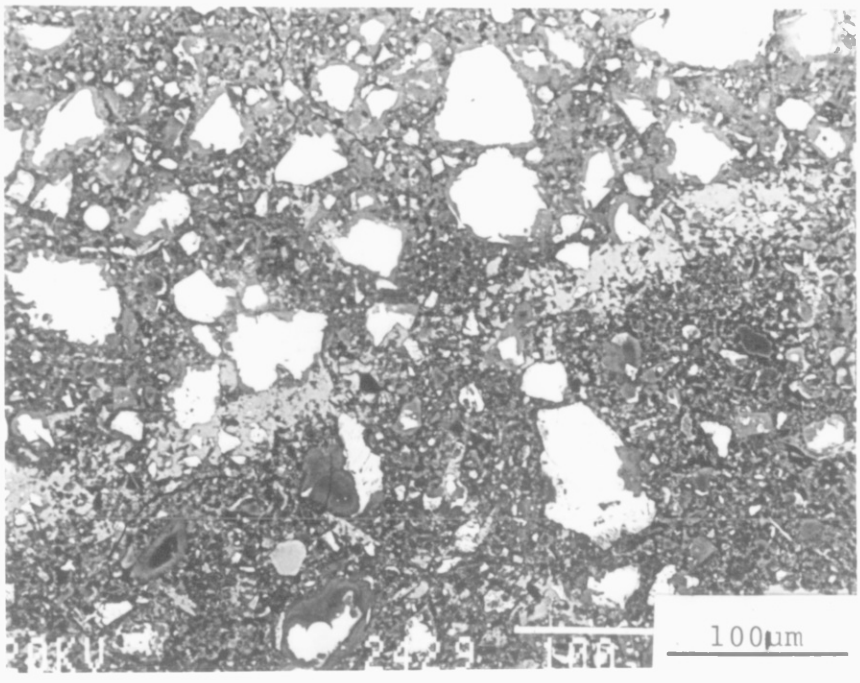


Plate 5.16 Cluster boundary in prehydrated cement, showing a surrounding layer of calcium hydroxide. BEI polished surface.

had undergone prehydration during storage, and on investigation of the cement storage system it was found that cement had been recently delivered, at which time any old cement in the bottom of the storage hopper was intermixed with the fresh cement. These prehydrated regions were therefore assumed to be either; part of the recent delivery which had undergone prehydration while in storage at the cement manufacturers, or during delivery; or cement which had been prehydrated in the storage hopper, and was inaccesible until the cement was mixed with the recent delivery.

The significance of these observations is that as has already been stated, the microstructure contains large regions of calcium hydroxide, and regions of more densely packed unhydrated cores and also, as plate 5.15 shows air has been entrained around these lumps. The possible effects of these features on the mechanical properties of HCP of this type will be discussed in section 6A.I.v.

5B CRACK PATHS IN HCP

Previous work (Walsh et al, 1974; Grudemo, 1978) on determining crack paths through HCP have centred around studies of fracture surfaces, and have suggested a number of possible crack path elements; calcium hydroxide cleavage; fracture between calcium hydroxide and C-S-H, and between inner product C-S-H and anhydrous cores. These observations have been investigated by examination of complementary fracture surface pairs. A BEI examination of introduced crack paths in slices of HCP describes a number of crack path elements, and quantifies these various elements.

5B.I EXAMINATION OF COMPLEMENTARY FRACTURE SURFACE PAIRS

Much the same as a general fracture surface observation of HCP (see section 5A), this technique uses a pair of complementary fracture faces and allows assumptions about the complementary part of a fracture element to be confirmed, in particular it can be seen (plate 5.17) that fracture occurs predominantly through C-S-H and calcium hydroxide, and that this fracture is "intra-component" rather than along boundaries between C-S-H and calcium hydroxide.

Plate 5.17 is a low magnification image of a fracture surface and includes several different crack path elements; inner product C-S-H [B & B′]; calcium hydroxide [C & C′]; outer product C-S-H [D & D′]; and pores, in this case containing AFt [E & E′]. At higher magnification (plate 5.18), cleavage through a large region of

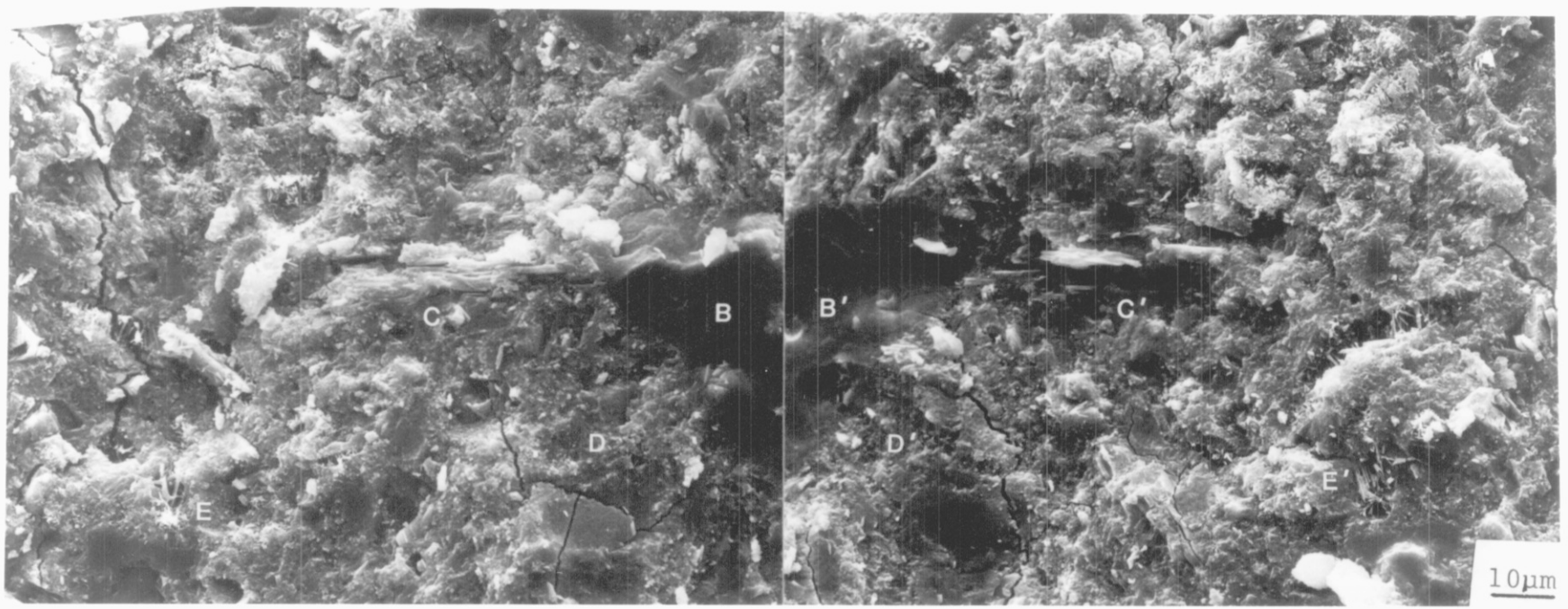


Plate 5.17 HCP fracture surface showing typical fracture elements; B & B´, inner product C-S-H; C & C´, calcium hydroxide; D & D´ outer product C-S-H; E & E´, pore containing AFt. SEI complementary fracture surfaces.

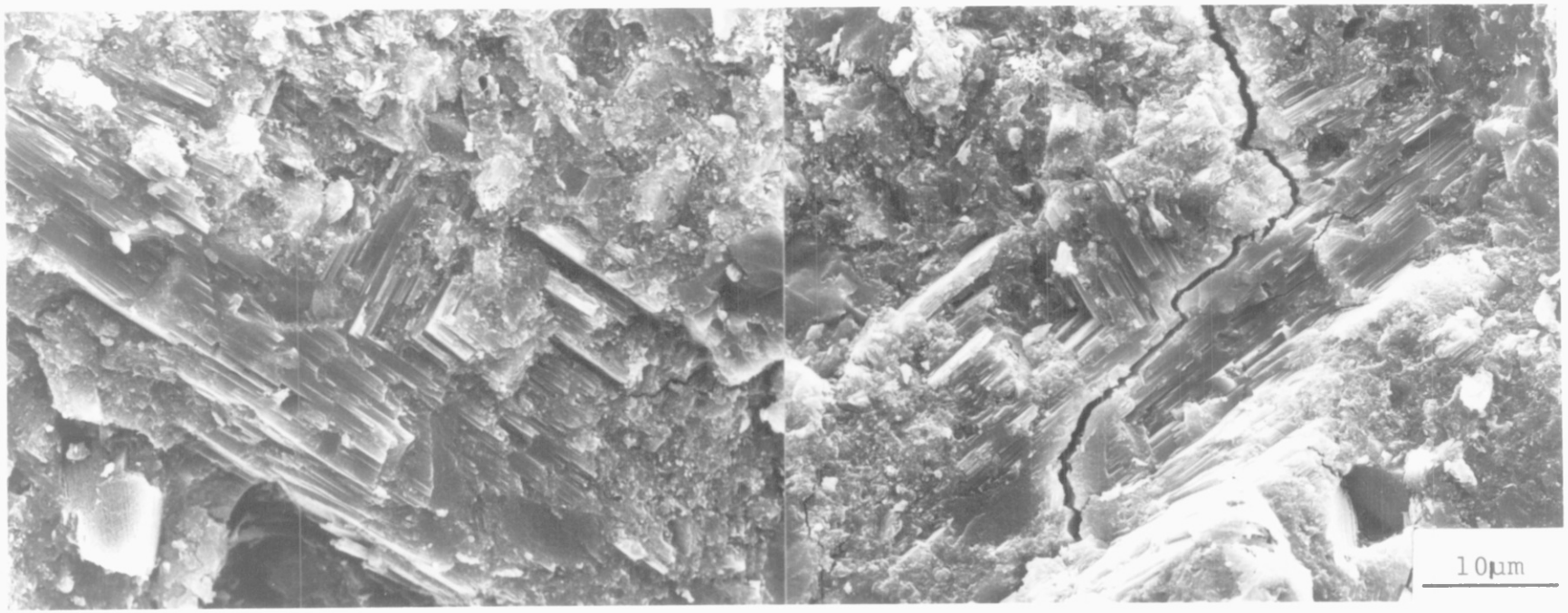


Plate 5.18 Fracture through a mass of calcium hydroxide showing two distinct crystallographic orientations. SEI complementary fracture surfaces.

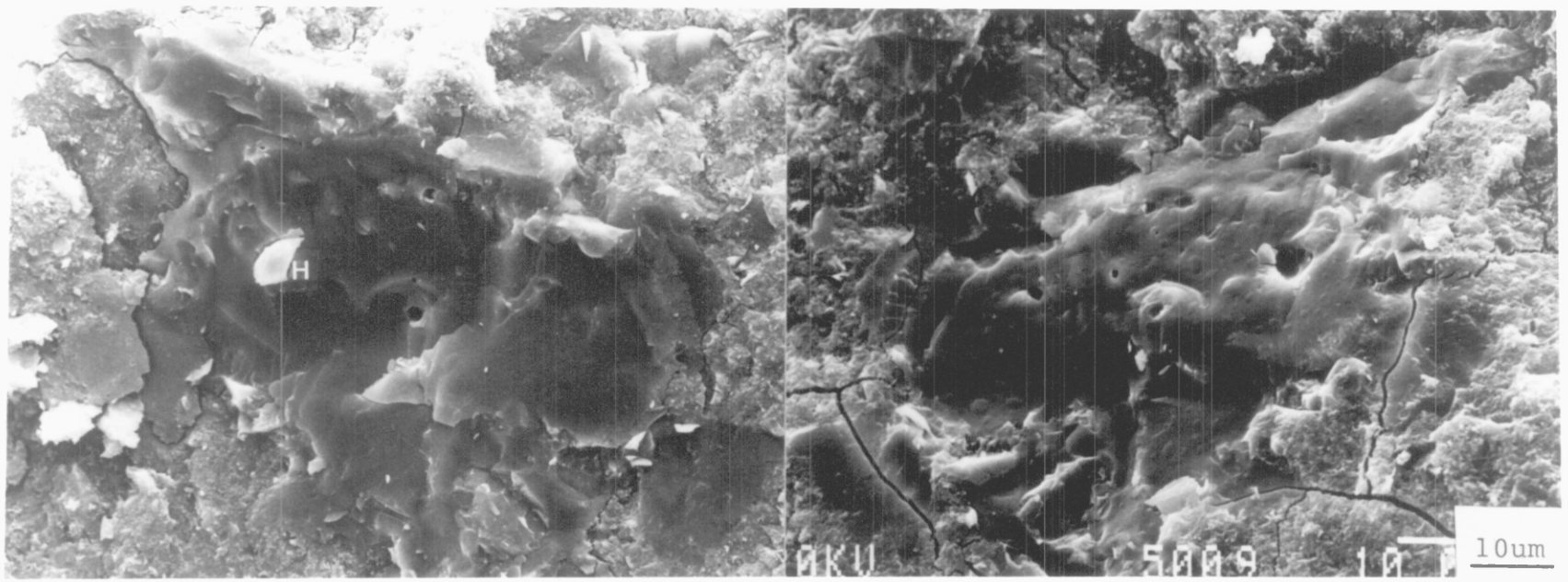


Plate 5.19 Fracture through an extensive mass of inner product C-S-H, which includes an anhydrous core [H]. SEI complementary fracture surfaces.

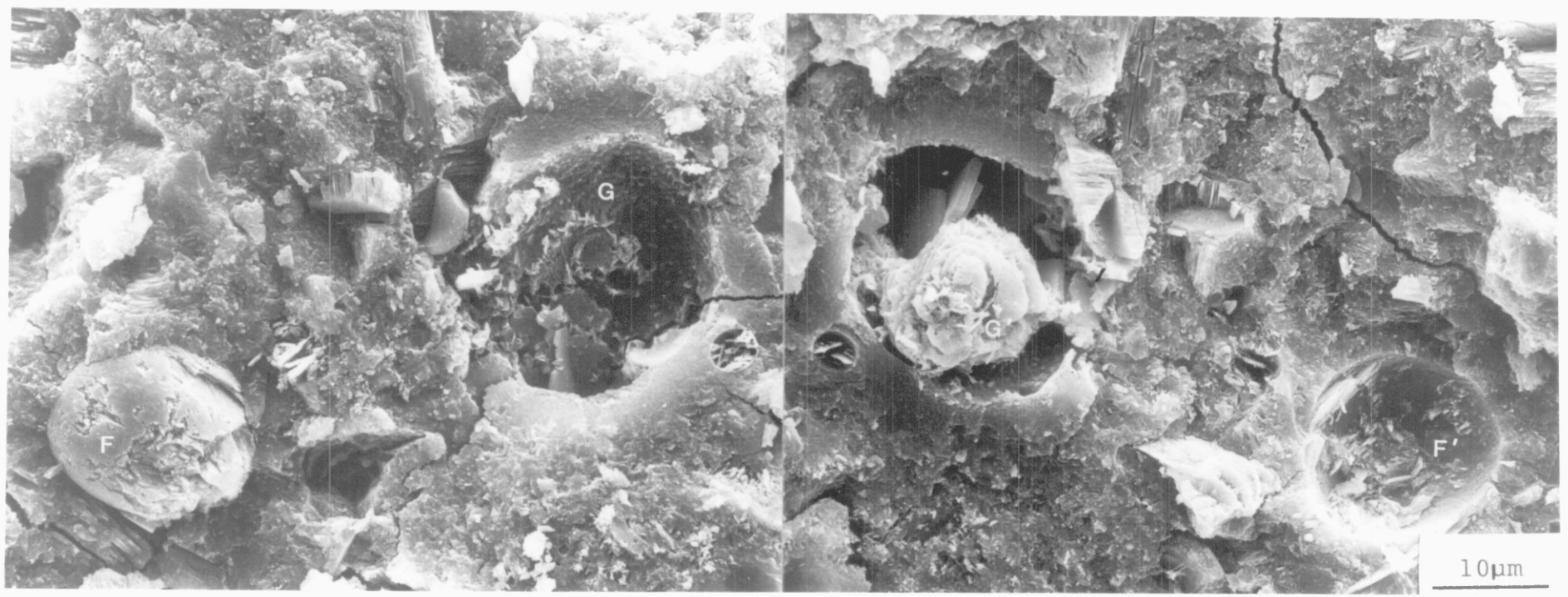


Plate 5.20 Fracture around a "grain" of inner product C-S-H [F & F´], and through an shell of inner product C-S-H to reveal an anhydrous core [G´] and an empty shell [G]. SEI complementary fracture surfaces.

calcium hydroxide can be seen. The calcium hydroxide displays at least two crystallographic orientations, suggesting that at least two regions of calcium hydroxide have grown together. It can be seen that the calcium hydroxide has engulfed several small regions of C-S-H, a feature also observed by Marchese (1977) in C_3S pastes. Fracture within a shell of inner C-S-H is shown in plate 5.19, and here it should be noted that what appears to be a small anhydrous core [H], probably C_2S or interstitial, remains embedded in the C-S-H, and that the C-S-H surface is uneven and contains several small pores.

Plate 5.20 shows several features of interest, in particular showing fracture in and around inner product C-S-H. A "grain" of inner product C-S-H and a surrounding layer of outer product have been separated [F & F′], and it can be seen that the shell of outer product replicates the original "grain" almost exactly, including several fragments which have been pulled from the surface of the "grain". A fracture through a shell of inner product C-S-H is shown [G & G′], and inside the shell an anhydrous core [G], some calcium hydroxide and some AFm [G′] are present. The original grain of cement appears to have consisted of several phases; C_3S which has reacted to form the shell of C-S-H; C_3A which has reacted to form AFm; and C_4AF which constitutes the anhydrous core after the C_3S and C_3A have reacted. Calcium hydroxide is present probably because the shell of inner C-S-H was incomplete allowing an ingress of calcium rich solution into the shell and AFm is the product of C_3A reaction in the presence of limited sulphate. Also of note are the several regions of calcium hydroxide cleavage.

When examining fracture surfaces it is generally the more unusual features which attract attention, however it should be remembered that plate 5.17 shows a typical area of a fracture surface, in which a mass of interpenetrating C-S-H and calcium hydroxide form the majority of the fracture path elements.

5B.II BEI EXAMINATION OF INTRODUCED CRACKS IN POLISHED SURFACES

This newly developed method of examining crack paths involves the introduction of a crack into a slice of HCP which is then polished, and examined in BEI mode of a SEM to identify the components of cement through which the crack is passing. The technique is particularily useful as a crack can be followed over several millimetres to provide a large number of crack path elements which can be analysed semi-quantitatively. Cracks were introduced either by

indentation or growth from a notch (see section 3B.II). No difference in crack pattern was observed between the two methods of introduction. The following micrographs are all of cracks introduced by indentation, whereas the quantitative analysis was performed on cracks grown from a notch.

5B.II.i Drying shrinkage cracking

Before going on to describe cracks which have been introduced [either by indentation or loading of a notched specimen] it is necessary to point out that even with the careful preparation methods used (section 3B.II), that cracking due to drying shrinkage was a major problem which was minimised rather than eliminated. In extreme cases the surface of a specimen would be covered by a network of cracking, where the introduced cracks could not be identified from amongst the drying shrinkage cracks, in which case the specimens were discarded. More commonly the specimens showed only the expected crack pattern, in which case the cracking was assumed to be that introduced by indentation or loading, and was examined as such with the proviso that cracking near crack tips was presumed to be an extension of the original introduced crack by drying shrinkage. No obvious distinction between introduced and drying shrinkage cracking was identified.

5B.II.ii Introduced cracking

BEI examination shows that the majority of the length of a crack passes through C-S-H and calcium hydroxide, deviating around unhydrated cores. In calcium hydroxide the crack often runs in a straight line, suggesting cleavage along the basal plane of the crystalline masses. The cracks in C-S-H are also relatively straight, but deviations are observed.

C-S-H forms the majority of crack path elements but because of the low resolution of BEI it is often only discernible as a grey mass, which may be either outer C-S-H or small sections of inner C-S-H. This is supported by fracture surface examinations (section 5B.I - plate 5.17) which shows extensive areas of featureless C-S-H. Large shells of inner product C-S-H are easily recognised in BEI and show all the features observed on fracture surfaces. Plate 5.21 shows a crack which has divided on encountering an unhydrated core, where one part runs between inner and outer C-S-H (cf. plate 5.06); plate 5.22 shows fracture within a mass of inner C-S-H (cf. plate 5.05); and the right edge of plate 5.23 shows cracking through a shell of

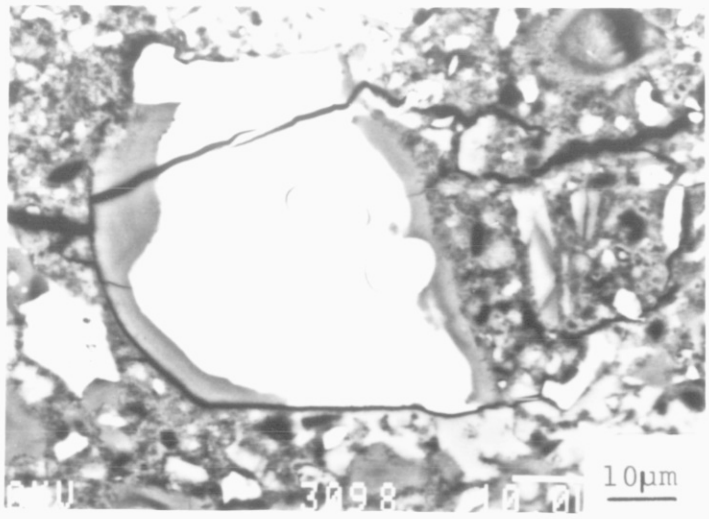


Plate 5.21 Introduced crack dividing and running through an anhydrous core, and between inner and outer product C-S-H. BEI polished surface.

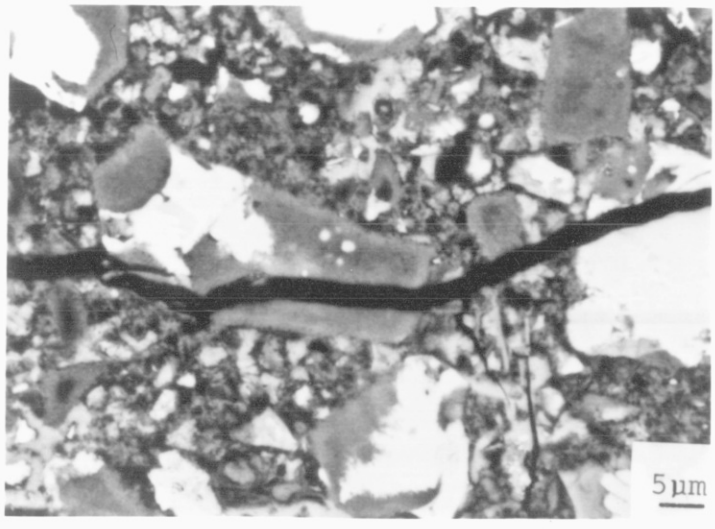


Plate 5.22 Introduced crack running through large mass of inner product C-S-H. BEI polished surface.

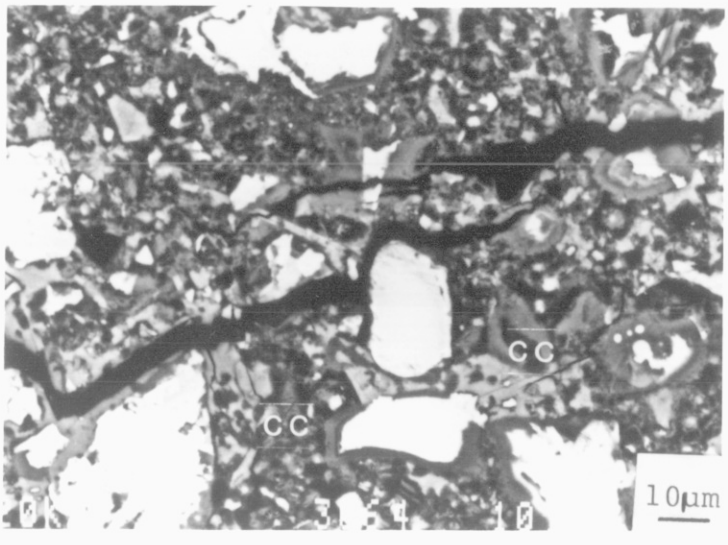


Plate 5.23 Typical features of an introduced crack. BEI polished surface.

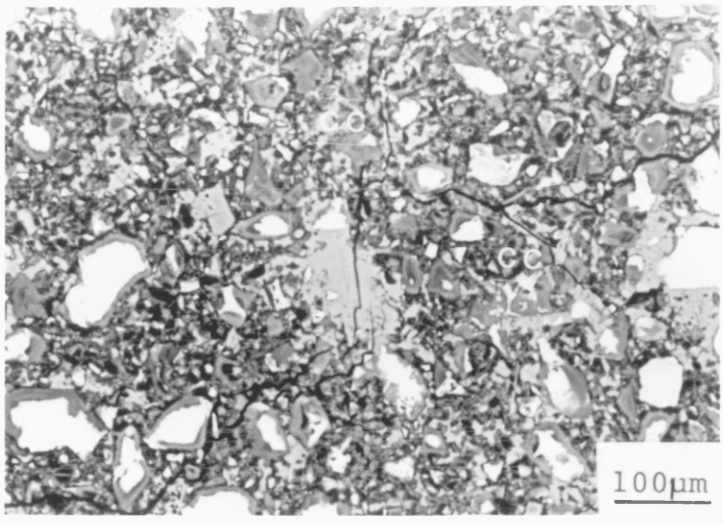


Plate 5.24 Introduced crack running through a large region of calcium hydroxide. BEI polished surface.

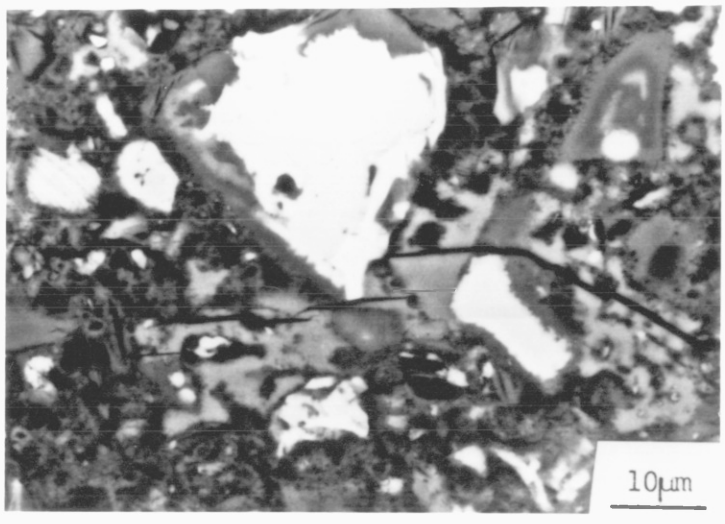


Plate 5.25 Drying shrinkage cracking in calcium hydroxide. BEI polished surface.

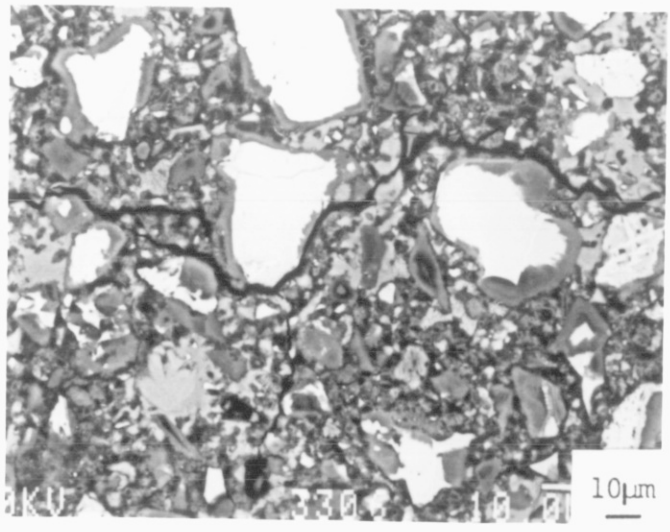


Plate 5.26 Introduced crack tortuosity caused by anhydrous cores.
BEI polished surface.

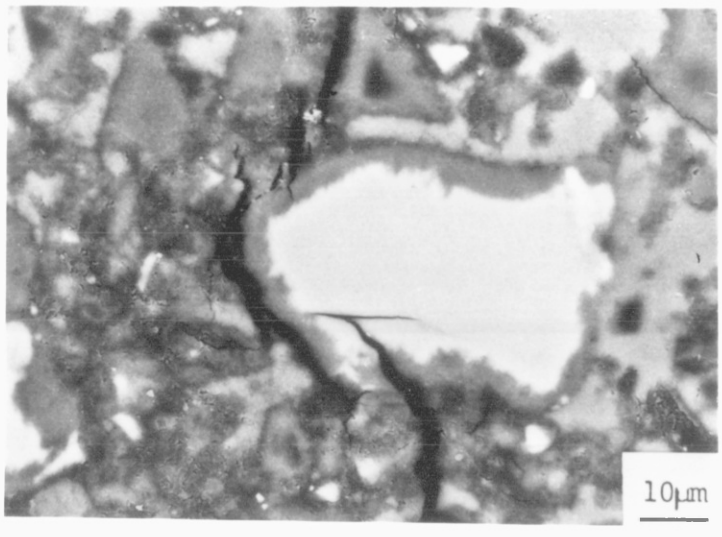


Plate 5.27 Introduced crack entering and passing around an anhydrous core.
BEI polished surface.

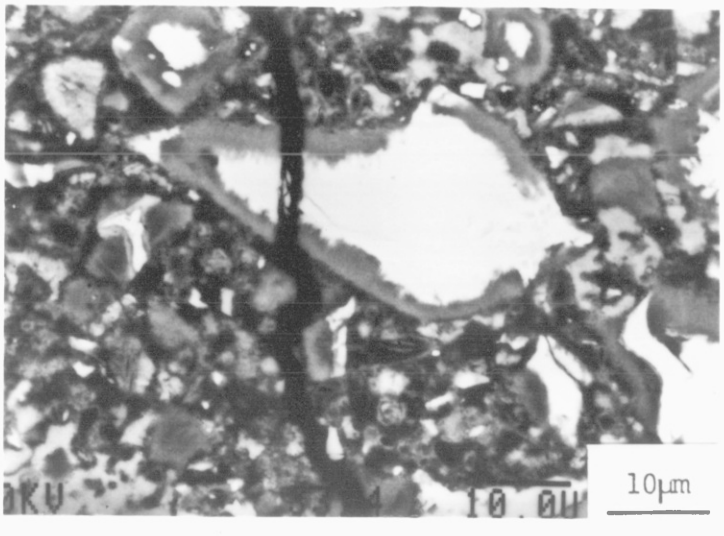


Plate 5.28 Introduced crack passing through an anhydrous core.
BEI polished surface.

innner C-S-H to reveal an unhydrated core (cf. plate 5.03).

Calcium hydroxide is known to cleave easily along its basal plane, and suggests two possible roles for calcium hydroxide in crack growth; firstly it may act as a weak link, promoting crack growth; or secondly, by being susceptible to microcracking it may act as a crack blunter. Polished surfaces, by showing the adjacent regions as well as the crack, show that both of these roles are significant. Plate 5.24 shows a crack passing through a large region of calcium hydroxide [~70um] suggesting that calcium hydroxide is a weak link, but this plate also shows cracks [CC] within calcium hydroxide which are subsidiary to the main crack. This dual role is also seen in plate 5.23 where the crack cleaves through calcium hydroxide [lower left] while subsidiary cracking in calcium hydroxide is occuring elsewhere [CC]. Plate 5.25 [known to be a drying shrinkage crack] shows a pronounced change of direction in the crack path, associated with the change in basal plane orientation, from one region of calcium hydroxide to another. Steps within a crystallite of calcium hydroxide can also be seen, which are an obvious feature of fracture surfaces.

One observation which can only be performed on polished surfaces is the examination of the effect of unhydrated cores on the crack path, because their influence is to deflect cracks away, and they are therefore seldom revealed on fracture surfaces. There is still a remnant of some 20-30% of unhydrated cement after 28 days, and large unhydrated cores can significantly increase the tortuosity of the crack, as they are resistant to cracking (see plate 5.26); although in some cases the crack may enter (plate 5.27) or pass straight through (plate 5.28) an unhydrated core. The cracking of unhydrated cores may be due to severe localised stresses, or as in the case of plate 5.01, the anhydrous grain may have included pre-existing cracks. Small unhydrated remnants, particularily interstitial material, which have no obvious layer of surrounding hydrates, are often exposed by the crack, although these have not been recognised on fracture surfaces.

The role of porosity in determining the crack path appears to be minimal because apart from a small number of large air pores the porosity is generally evenly distributed throughout the component which forms the majority of crack path elements, C-S-H. No interaction between air pores and the crack were observed.

From measurements of the length of crack in various phases from a series of crack path frames a rough quantitative assessment can be

made of the elements of cement through which the crack passes (table 5.01). These figures generally confirm expectations about crack paths in HCP, that C-S-H and calcium hydroxide form the majority of crack path elements [86.4%] and that the majority of cracks are intra-component. The value of 13.6% of the crack involving unhydrated material initially appears high, though on inspection the majority of this is seen to be the crack passing around small fragments of interstitial material rather than through unhydrated phases.

5B.iii In-situ SEM examination of crack growth casued by drying shrinkage in HCP polished surfaces

As mentioned in the previous section drying shrinkage cracks were assumed to extend introduced cracks, and in one particular case the very high vacuum of the SEM caused further drying of the specimen which in turn caused extension of a particular crack over the space of approximately 1 hour. Plate 5.29 shows a sequence of photographs of the crack, which between 20 and 40 minutes appears to have grown by the coalescence of several microcracks ahead of the crack tip as has been suggested by Grudemo (1979), although it must be remembered that these cracks were produced under abnormal conditions i.e. the specimen, and hence the hydration products were drying, and the stresses which caused cracking were tensile surface stresses which were expected to be of roughly the same magnitude across the whole specimen. However it is still of interest to note that the crack appears to run through elements similar to introduced cracks. Of particular note is that the crack opening in C-S-H is in some cases very small, and that the cleavage of the calcium hydroxide on the extreme right of the plate, occured between frames [i.e. relatively rapidly].

Table 5.1 Crack path elements in SENB specimen showing crack extension from sawn notch. The cumulative length [in μm] of a number of crack path elements involving particular phases, with percent of total cracked length [3680μm] in brackets.

	C_3S	C_2S	Inter-stitial	Inner C-S-H	Outer C-S-H	Calcium Hydroxide
C_3S	64[1.8]	-	-	49[1.3]	-	14[0.4]
C_2S	-	40[1.1]	-	-	94[2.6]	18[0.5]
Inter-stitial	-	-	63[1.7]	60[1.6]	162[4.4]	35[0.9]
Inner C-S-H	49[1.3]	-	60[1.6]	147[4.0]	358[9.8]	122[3.4]
Outer C-S-H	-	94[2.6]	162[4.4]	358[9.8]	1540[42.2]	138[3.8]
Calcium Hydroxide	14[0.4]	18[0.5]	35[0.9]	122[3.4]	138[3.8]	746[20.4]
* All components	$\overline{127}$[2.9]	$\overline{152}$[3.5]	$\overline{320}$[7.3]	$\overline{736}$[16.7]	$\overline{2292}$[45.3]	$\overline{1262}$[24.4]
	[13.6]			[86.4]		

Intra-component failure = 71.2%

Inter-component failure = 28.8%

Total Crack Length = 3680μm

End-to-End Crack Length = 2625μm

Tortuosity Factor [Total/End-to-End] = 1.4

* All components is the sum of the crack path elements involving all components with a particular component. As such the total lengths, which are simple sums include crack path elements involving different components twice, i.e. the total length of the all component crack lengths is 4889μm. The percentages of the crack length involving all components with a component are therefore percentages of 4889μm rather than simple sums of the individual percentages [which refer to 3680μm].

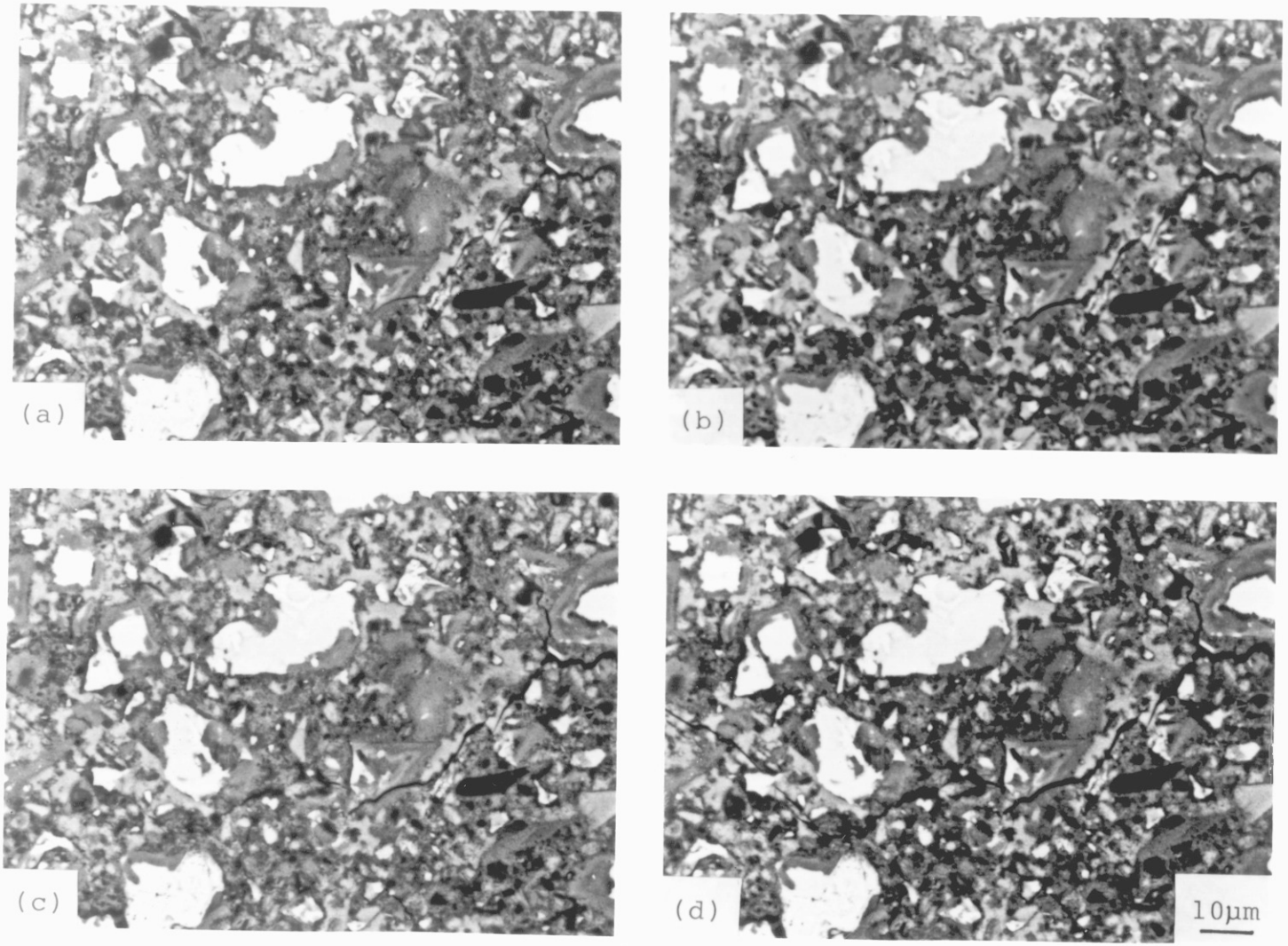


Plate 5.29 Crack growth due to specimen drying shrinkage in the SEM specimen chamber. BEI polished surface.

Time in specimen chamber;
a) 10 mins. b)20 mins.
c) 40 mins. d)60 mins.

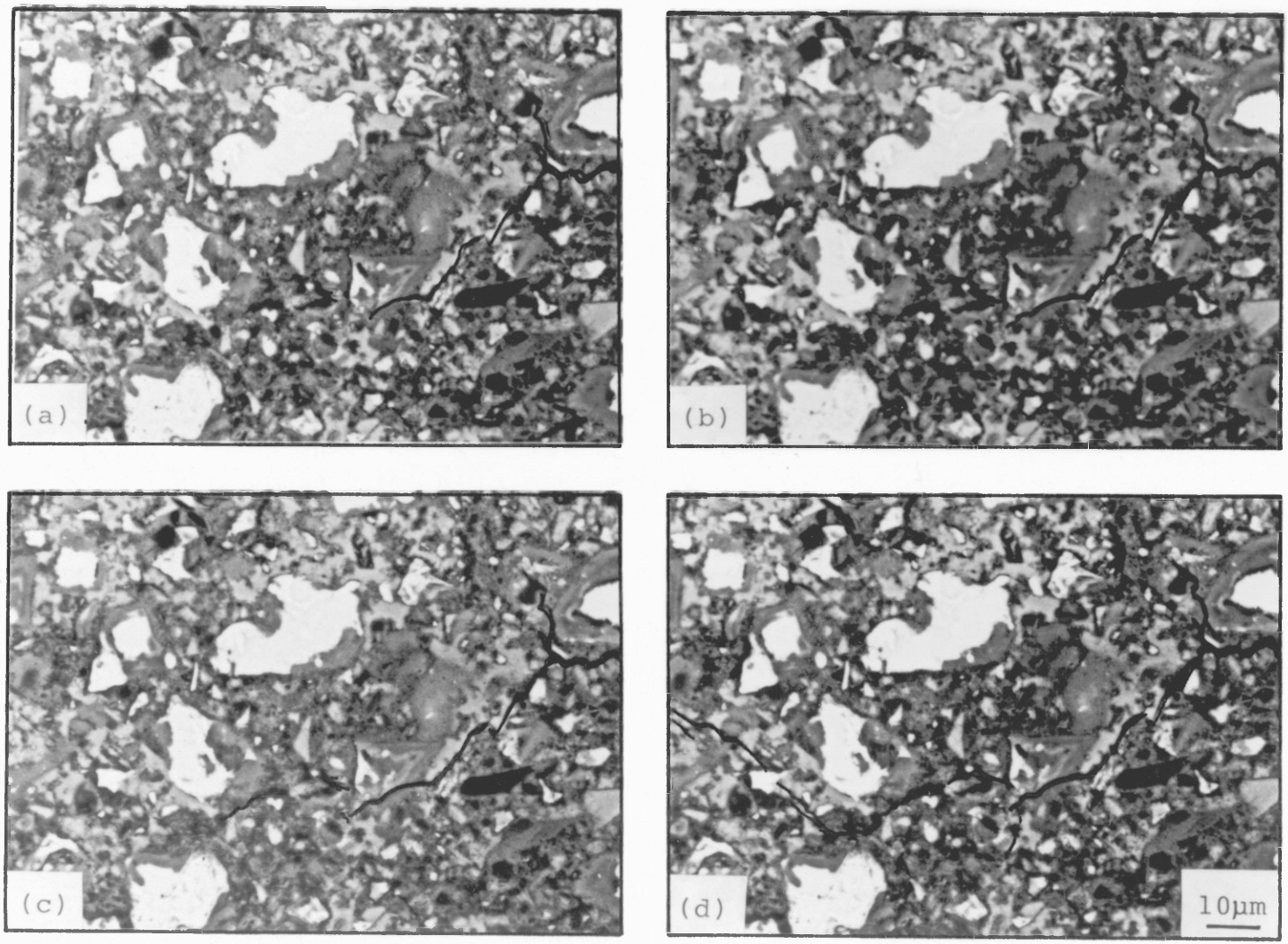


Plate 5.29 Crack growth due to specimen drying shrinkage in the SEM specimen chamber. BEI polished surface.

Time in specimen chamber;
a) 10 mins. b)20 mins.
c) 40 mins. d)60 mins.

5C SUBCRITICAL CRACK GROWTH PARAMETER, n

5C.I DOUBLE TORSION LOAD-RELAXATION

Double torsion measurements were performed on four batches of 28 day old HCP with an original water cement ratio of 0.4. From each batch of cement 5 type I plates and 3 type II plates were cast, and for both types of plate one specimen was used to measure the notch length - compliance relationship leaving the remainder for load-relaxation measurements.

5C.I.i Notch/crack length measurement

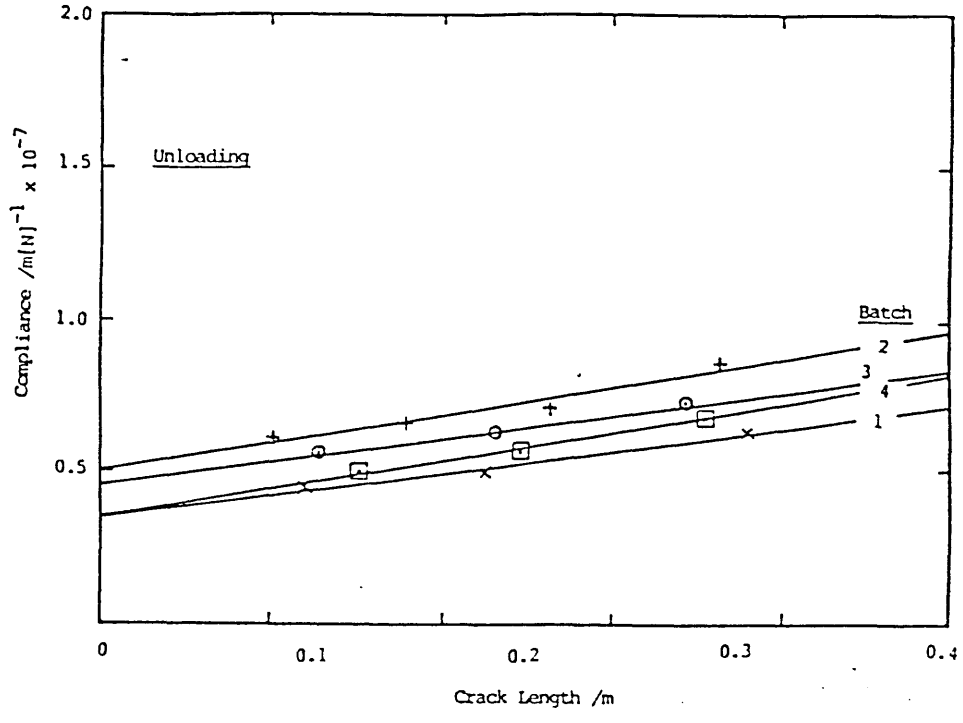
The relationship between notch length [a] and compliance [C] showed the expected linear relationship,

$$C = M_c a + D_c$$

where M_c and D_c are constants.

The slope M_c of compliance-notch length plots was roughly constant at $1.8 \times 10^{-7} m[N]^{-1}$ but the intercept D_c varied from plate to plate (see figure 5.01). Therefore instead of using a single equation which related notch length to compliance, determined from a number of specimens, the compliance of each plate with its initial sawn in notch was measured and the value of D_c was determined assuming a constant value of M_c equal to $1.8 \times 10^{-7} m[N]^{-1}$.

When the specimens had undergone subcritical crack growth the compliance of the specimen was measured to determine the initial crack length for the subsequent measurement of subcritical crack growth. However the scatter in these compliance measurements resulted in ridiculously low values of crack length. To check that crack growth was occuring, the underside [tension face] of a small number of specimens were wiped dry with tissues, and after a few seconds bleeding of water out of the crack onto the dry surface showed the extent of the crack, which was considerably greater than that determined by compliance methods [the drying of the specimen made it unuseable for further testing]. In an attempt to overcome the problem of not knowing the crack length a very approximate calculation was performed, which combined the expected equality between the products of initial crack length [a_i] and initial load [P_i], and final crack length [a_f] and final load [P_f],



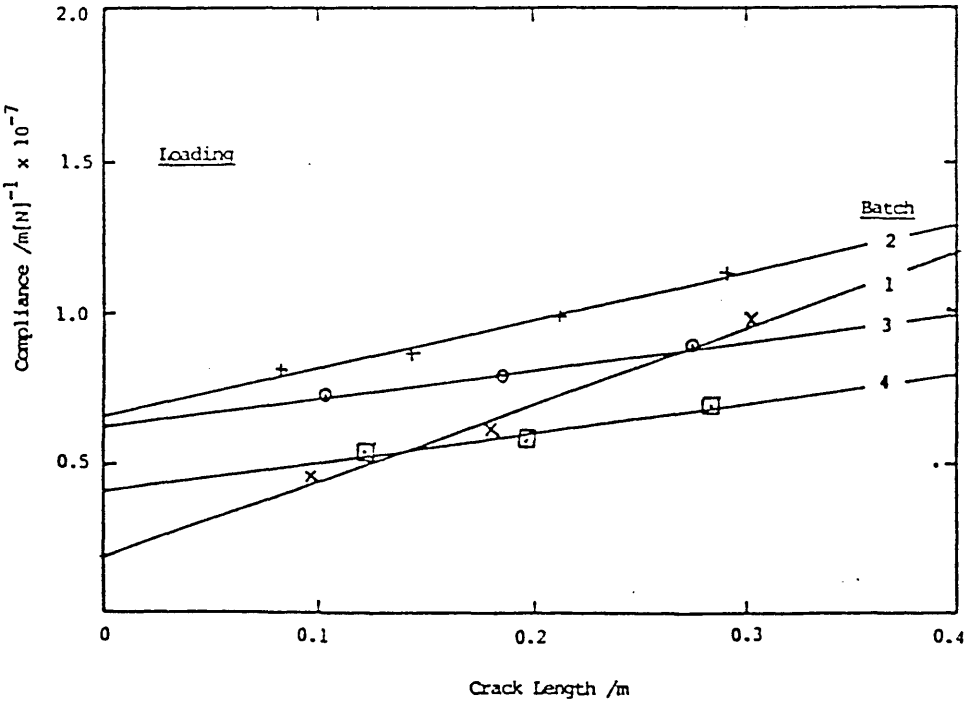


Figure 5.01 Compliance-notch length measurements for Type I DT plates

$$a_i P_i = a_f P_f$$

and the typical crack extensions observed after drying the tensile face of specimens. This method is inaccurate, because it uses the sawn notch as the initial crack length in the first determination, and the value calculated from this in the subsequent determination, and so on. It was felt that the values of crack length determined were useful, and accurate to within 10-20%. As will be pointed out in section 6B.I.ii there were other variations in the V-K determinations which make errors of this magnitude acceptable.

The actual values of crack extension in a load-relaxation were determined as being between 10mm [e.g. 1st load-relaxation of plate 4/I/1] and 30mm [e.g. 5th load-relaxation of plate 4/I/1], resulting in overall crack lengths between 100 and 240mm.

5C.I.ii Load-relaxation measurements

After the initial problems of determining the background component of the measured relaxation, the computer made acquisition and processing of results simple. Typical load-relaxation curves are shown in figure 5.02, and it can be seen that succesive relaxation measurements were perfomed from increasing maximum loads, and that the curves level-off at increasing loads.

In load-relaxation tests Mindess et al (1976) found that all of the background relaxation was due to the testing machine and fixtures. In this test program the first background relaxation was larger than subsequent measurements on a particular plate, and there was variation between plates (see figure 5.03). This suggests that there is a contribution to the background relaxation from the specimen and, as this decreases after the initial measurement, that an irreversible process occurs during testing.

Typical V-K plots (figure 5.04) show that only region I of the theoretical V-K curve (figure 2.04; Evans 1972) is found. The increasing maximum loads used for succesive relaxation measurements result in increasing values of stress intensity, however this is not accompanied by an increase in crack velocity, which is consistently between 3×10^{-5} and $5 \times 10^{-3} ms^{-1}$. This results in an apparent shift of the V-K curves along the stress intensity [K] axis for a particular DT plate, as well as the obvious variation between plates in the

position of V-K curves on the stress intensity axis.The value of critical stress intensity [K_{1c}] was measured on a small number of plates by rapidly loading the plate to failure after a number of relaxation tests had been performed. This was also found to vary from plate to plate [477-580 $kNm^{-3/2}$]. Possible reasons for the increasing values of stress intensity which occured in the same plate, without corresponding increases in crack velocity will be discussed in section 6B.I.ii.c.

Subcritical crack growth measurements were performed on both Type I and Type II specimens from all four batches of cement, despite a number of instances where cracks propagated outside the guiding groove, or ran straight through the specimen on loading, in which cases the results were unusable. The valid test results are shown in table 5.01.

The average value of subcritical crack growth parameter and the V-K intercept for each specimen type and batch are shown in table 5.02. Student t-test values (Weatherburn, 1957), which assess the probability of observed variations between measurements occuring, suggest that there is a significant difference [high value of t] between the two different types of plate, and a less significant difference between batch 1 and the other three batches. The difference between the two plates will be discussed in section 6B.I.i, while the difference between batch 1 and the other batches may be a result of an observed change in the cement (see section 5A.II), and will be discussed in section 6A.I.v.

Table 5.02 Subcritical crack growth parameter values, n and V-K intercept, log [A] values. Particular plates are identified by a three symbol code i.e. X/A/Y, where X is the cement batch, A is the plate type (see section 3A.I), and Y is the particular plate number from a batch. Where multiple runs were performed on a particular plate the results are given in order.

Plate	n	log[A]	Plate	n	log[A]
1/I/2	36	-219	3/I/1	99	-538
			do.	55	-381
1/II/2	70	-382	do.	90	-403
do.	64	-349	do.	72	-445
do.	51	-315	do.	74	-571
			do.	94	-466
1/II/3	60	-364			
do.	48	-295	3/II/3	60	-344
1/II/4	33	-190	3/II/5	36	-207
do.	69	-409			
			4/I/1	64	-399
1/II/5	54	-330	do.	104	-568
			do.	92	-503
2/I/1	64	-565	do.	58	-362
do.	67	-332	do.	34	-214
do.	71	-544	do.	38	-240
do.	95	-441			
do.	81	-461	4/II/4	60	-348
do.	104	-585	do.	70	-410
			do.	43	-319
2/II/5	64	-347			
do.	60	-378	4/II/5	64	-374
do.	32	-187	do.	54	-322

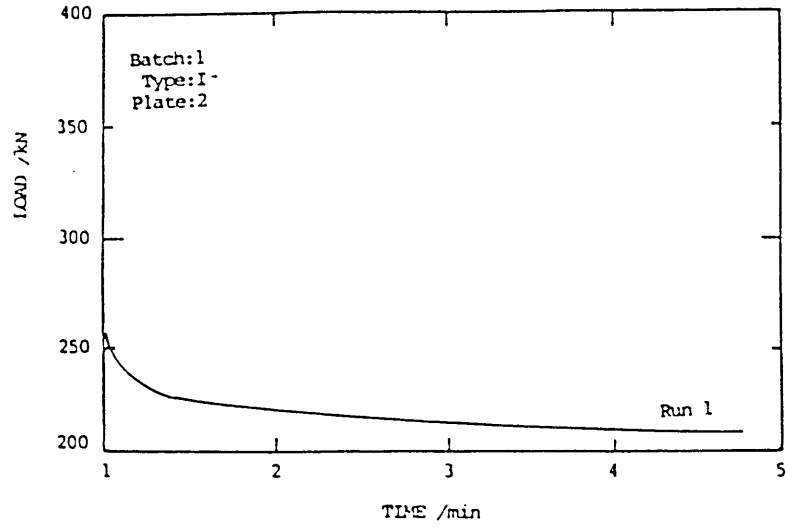
Table 5.03 Average values of the subcritical crack growth parameter, n and the V-K intercept, log[A] for 4 batches of 2 types of double torsion plates. Number of values in average in brackets. t is the value of the "Students-t" test between a particular batch and the other batches, and between plate types.

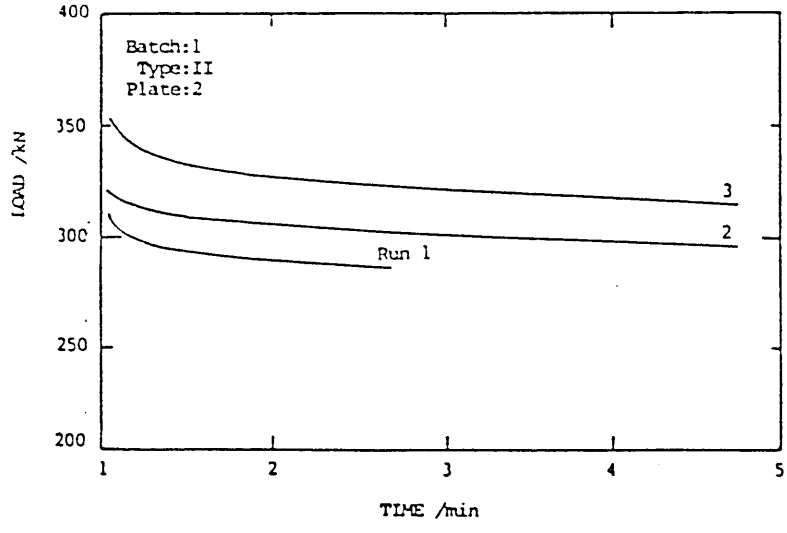
Subcritical crack growth parameter, n

	Type I	Type II	Overall Average	t
Batch 1	36[1]	56[8]	54[9]	1.89
Batch 2	80[6]	52[3]	71[9]	1.22
Batch 3	81[6]	48[2]	72[8]	1.30
Batch 4	65[6]	58[5]	62[11]	0.43
Overall Average	73[19]	55[18]	64[37]	
t	3.02	3.02		

V-K intercept, log[A]

	Type I	Type II	Overall Average	t
Batch 1	-219[1]	-329[8]	-317[9]	2.25
Batch 2	-488[6]	-304[3]	-427[9]	1.59
Batch 3	-467[6]	-276[2]	-419[8]	1.22
Batch 4	-381[6]	-355[5]	-369[11]	0.48
Overall Average	-434[19]	-326[18]	-381[37]	
t	3.34	3.34		





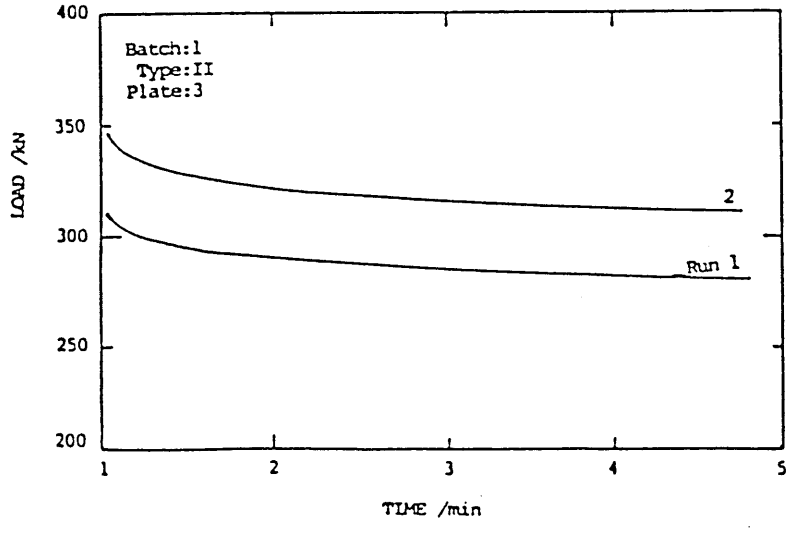
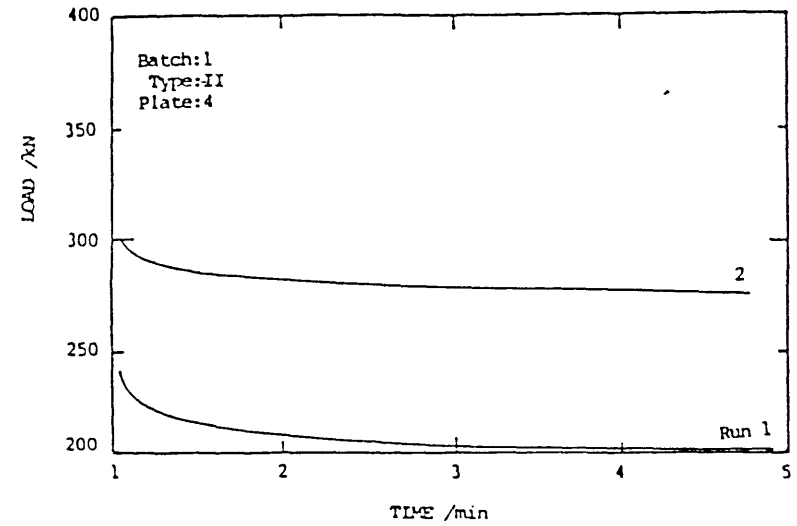


Figure 5.02 Load relaxation curves obtained from DT plates.



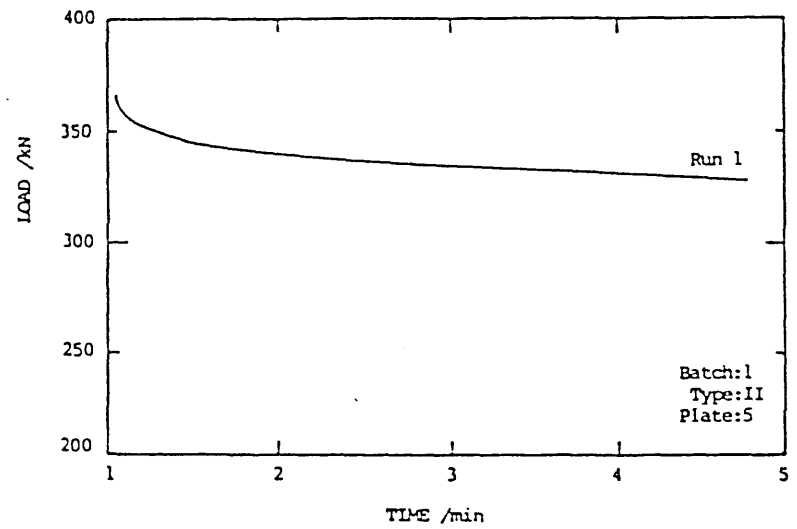
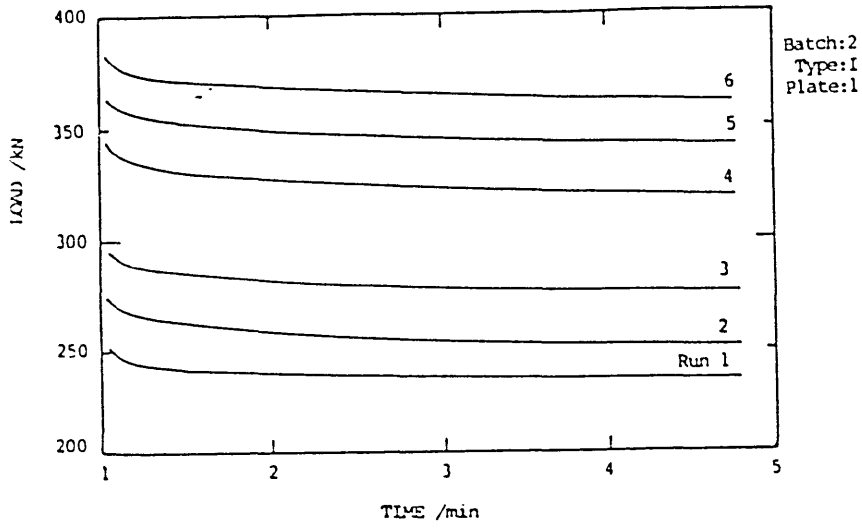


Figure 5.02 contd. Load relaxation curves obtained from DT plates.



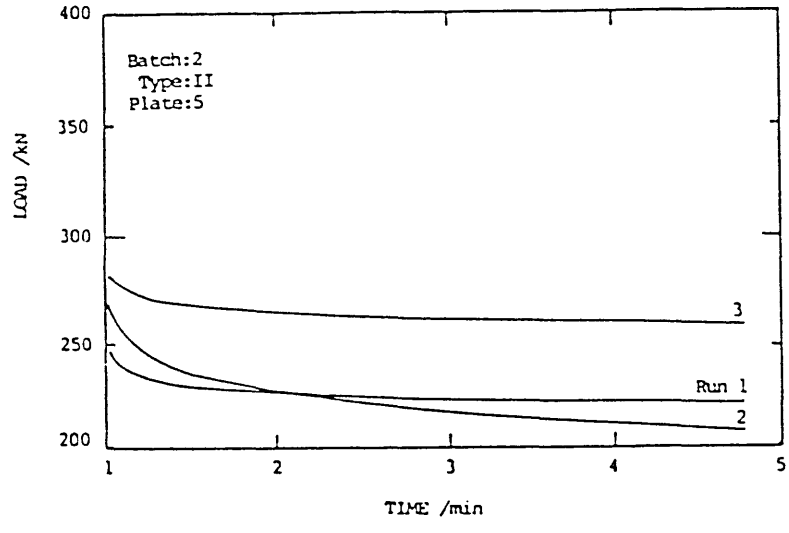
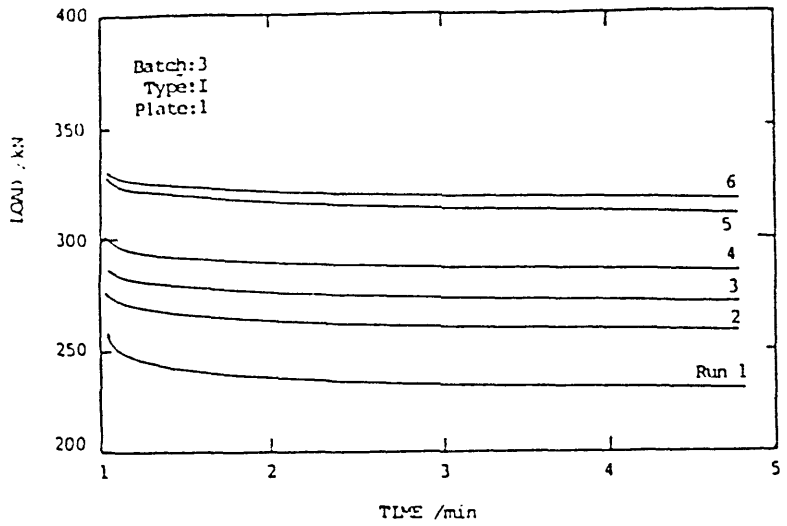
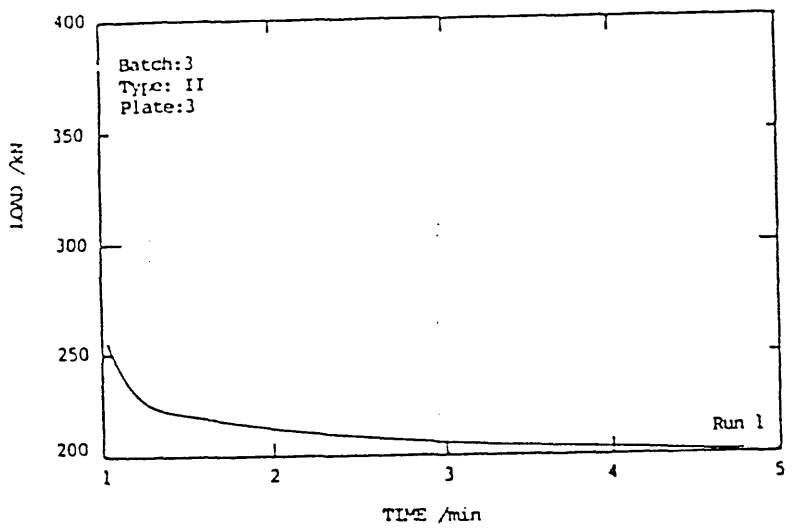


Figure 5.02 contd. Load relaxation curves obtained from DT plates.





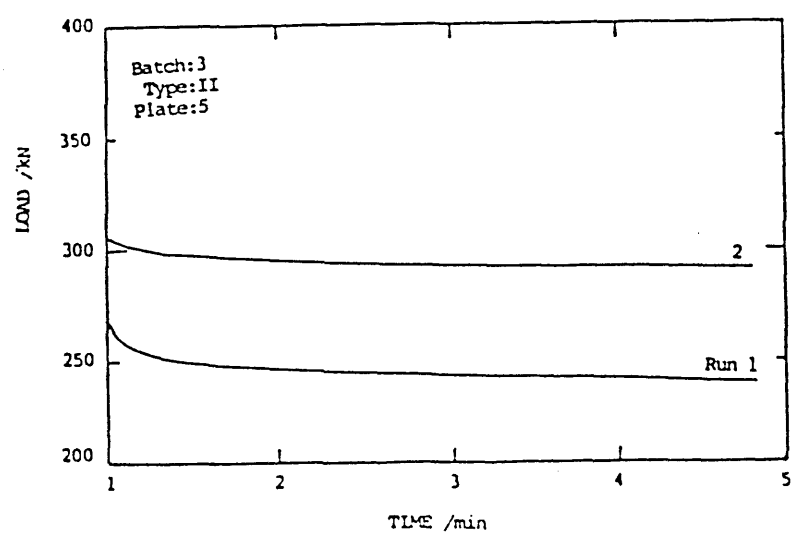
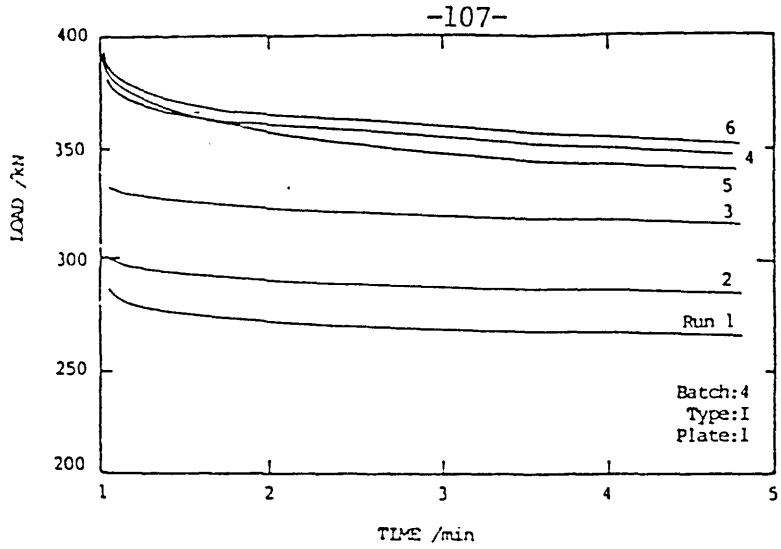
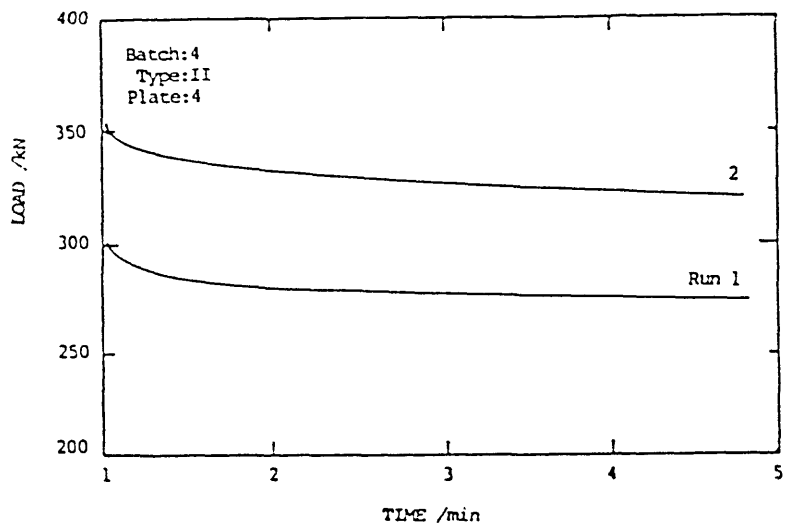


Figure 5.02 contd. Load relaxation curves obtained from DT plates.





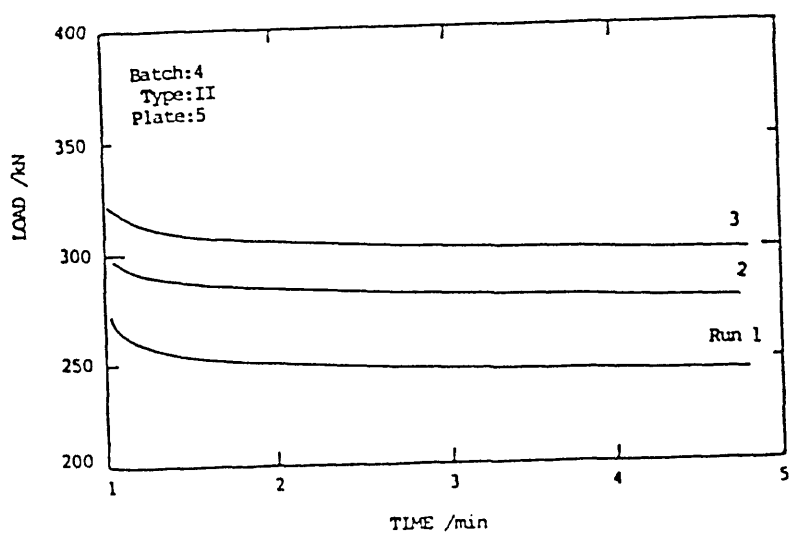


Figure 5.02 contd. Load relaxation curves obtained from DT plates.

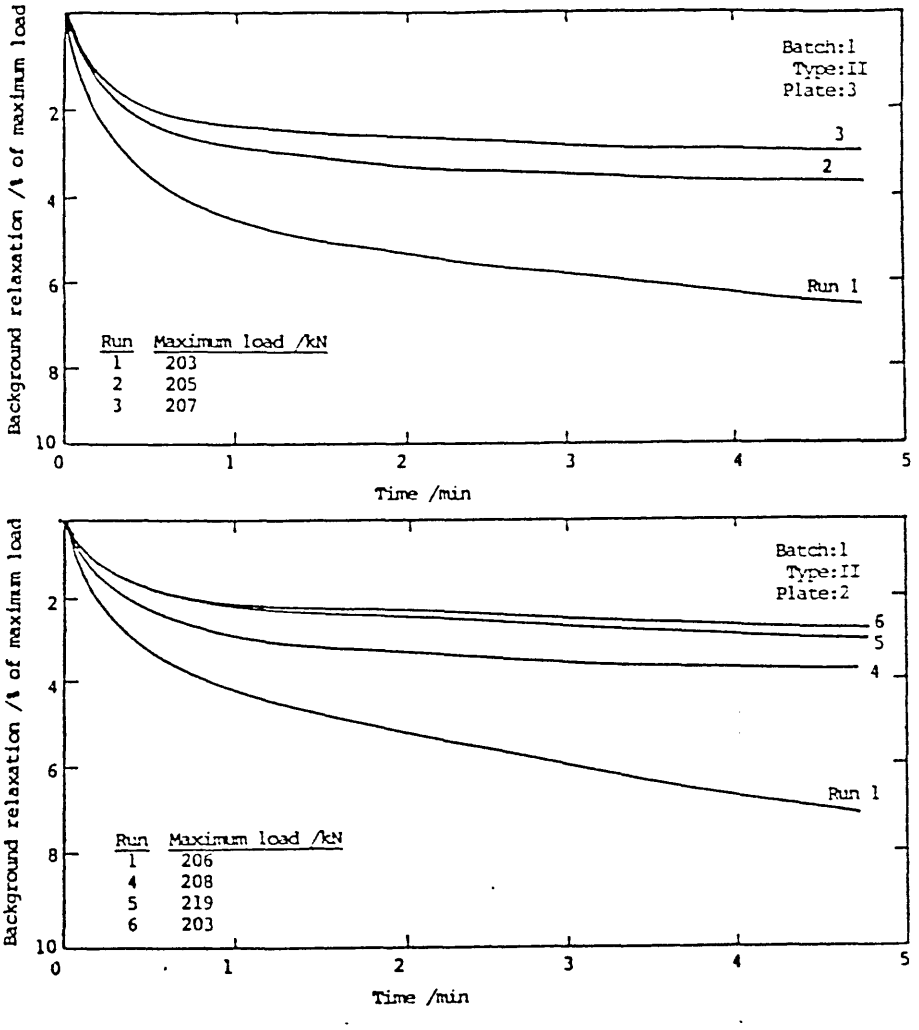


Figure 5.03 Background relaxation curves for DT plates.

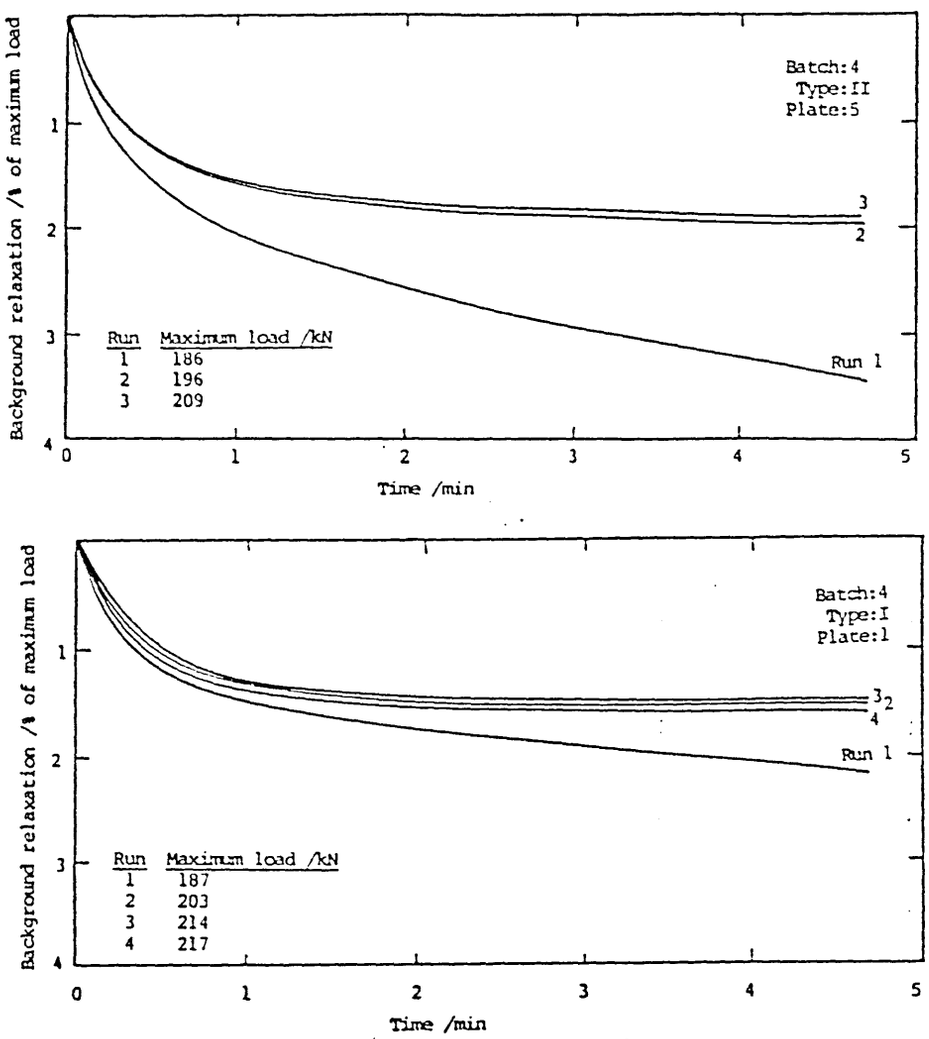
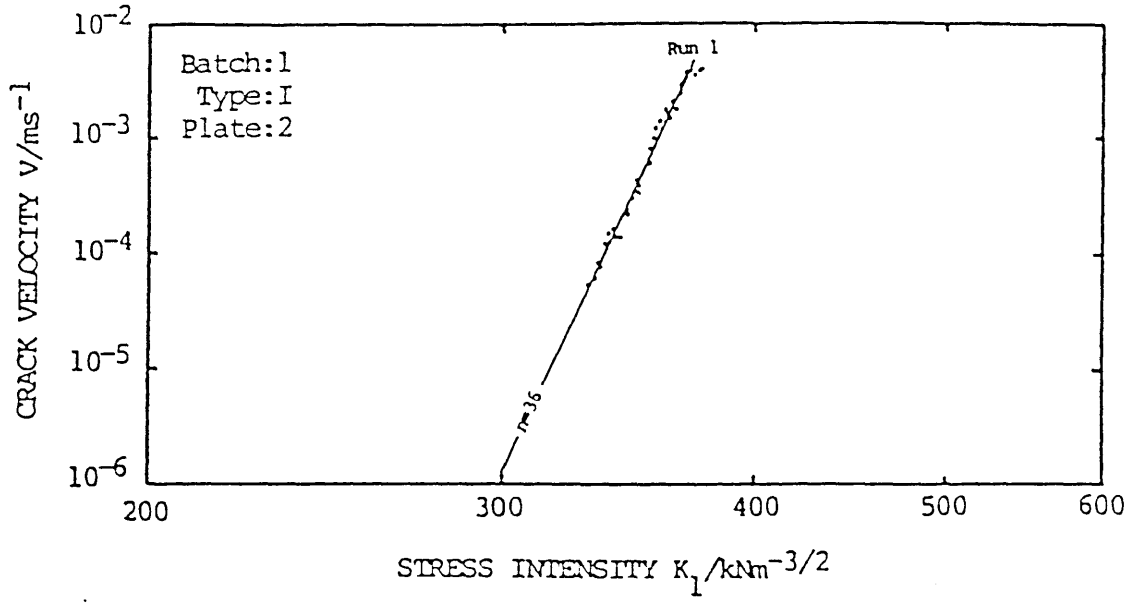


Figure 5.03 Background relaxation curves for DT plates.



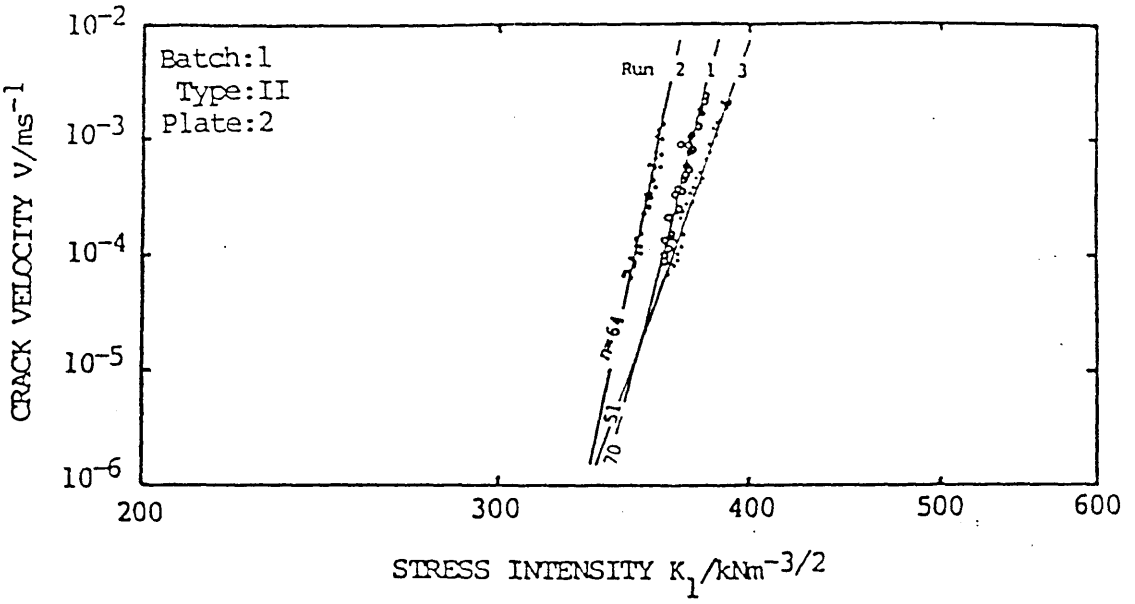
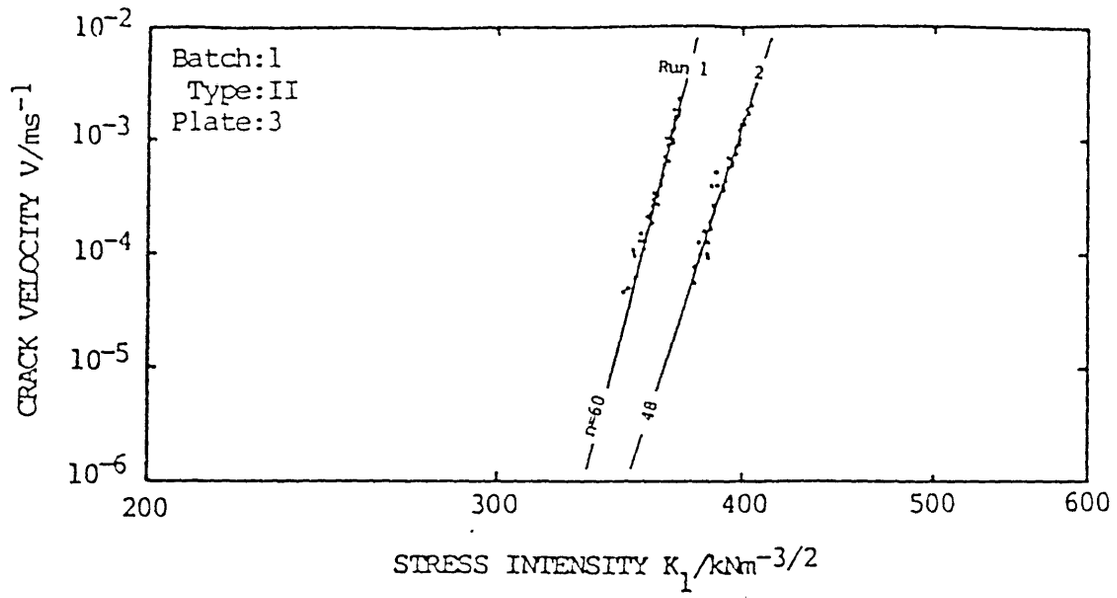


Figure 5.04 Crack velocity-Stress Intensity [V-K] plots determined by load-relaxation in DT plates.



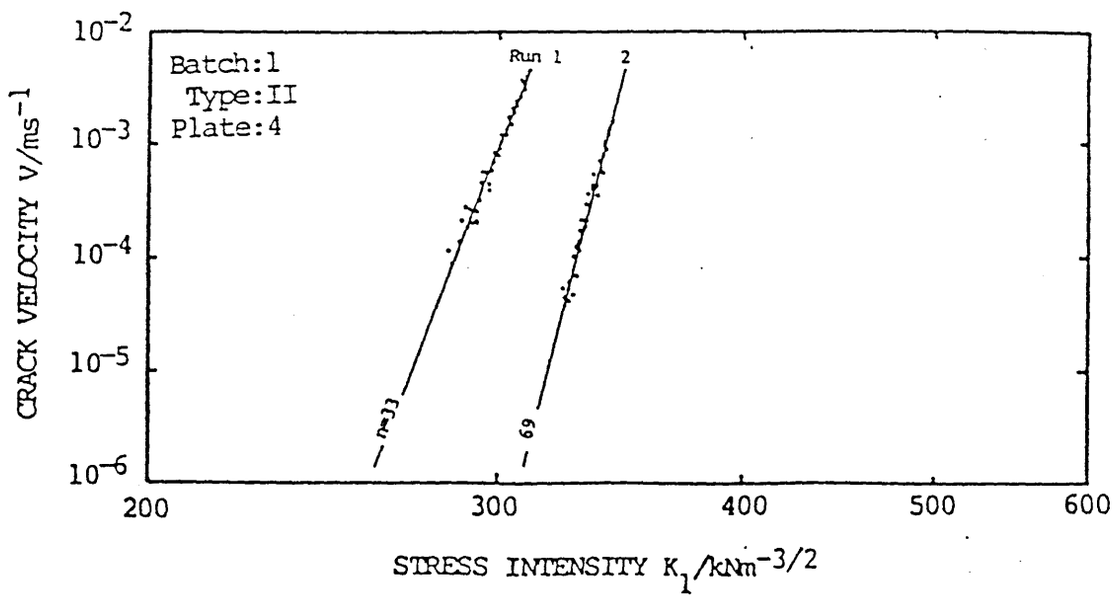


Figure 5.04 contd. Crack velocity-Stress Intensity [V-K] plots determined by load-relaxation in DT plates.

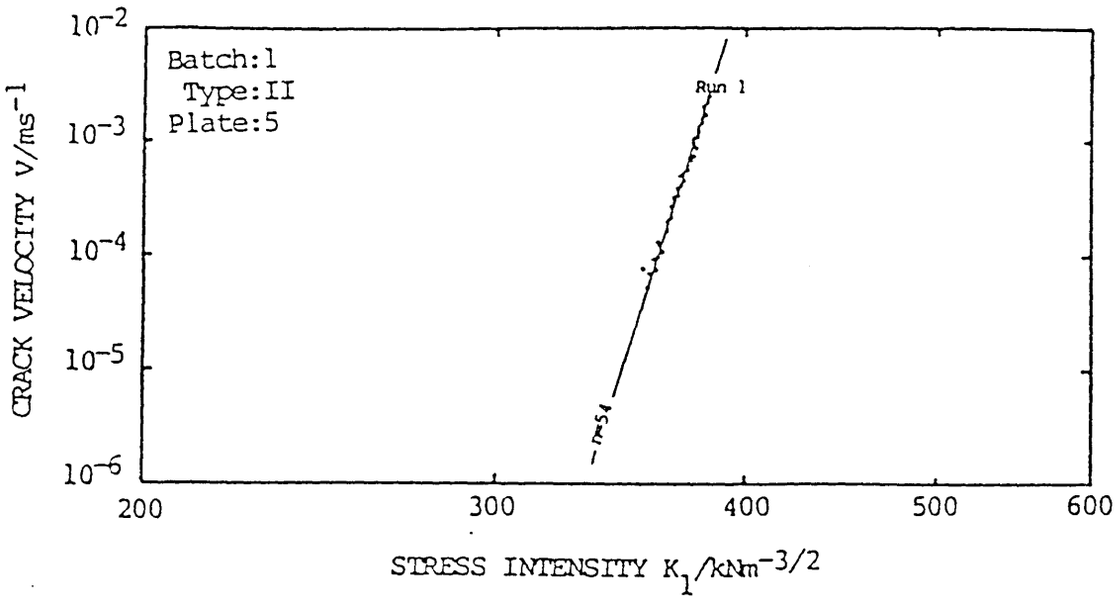
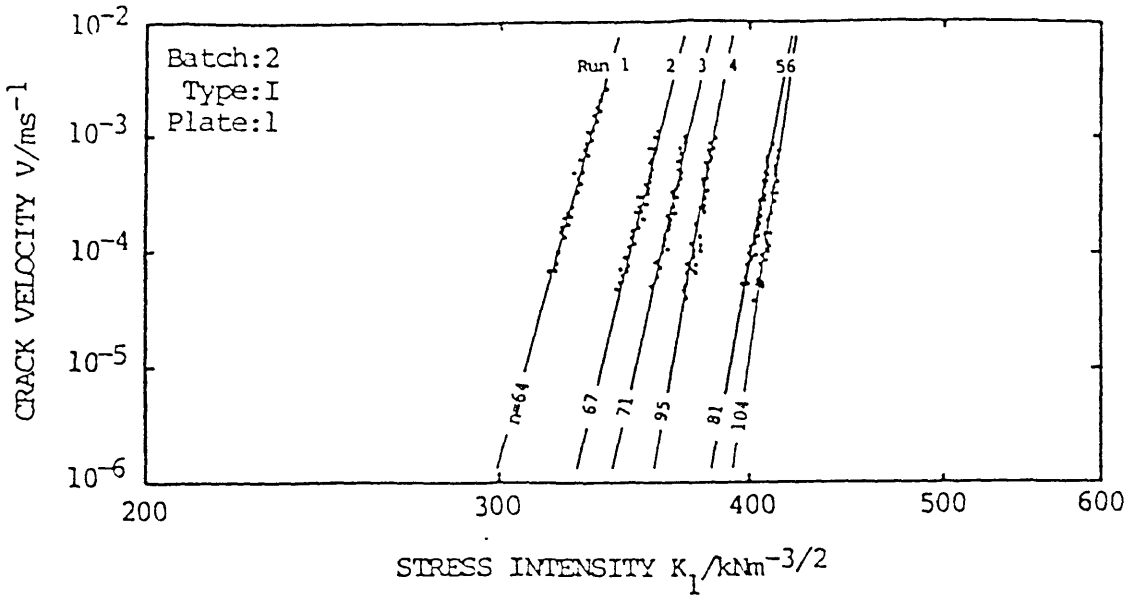


Figure 5.04 contd. Crack velocity-Stress Intensity [V-K] plots determined by load-relaxation in DT plates.



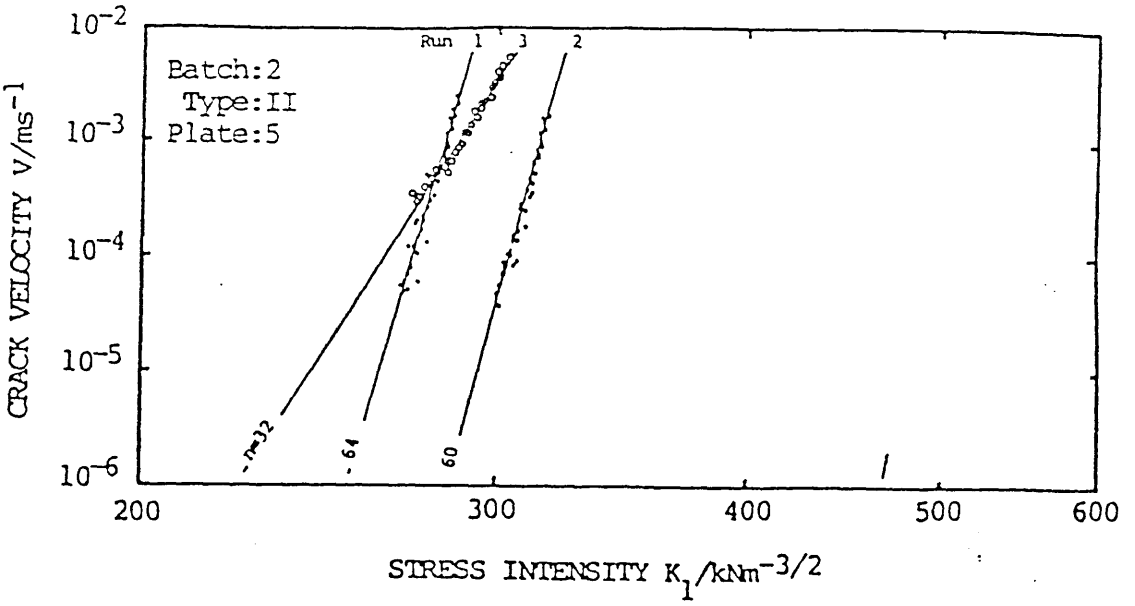
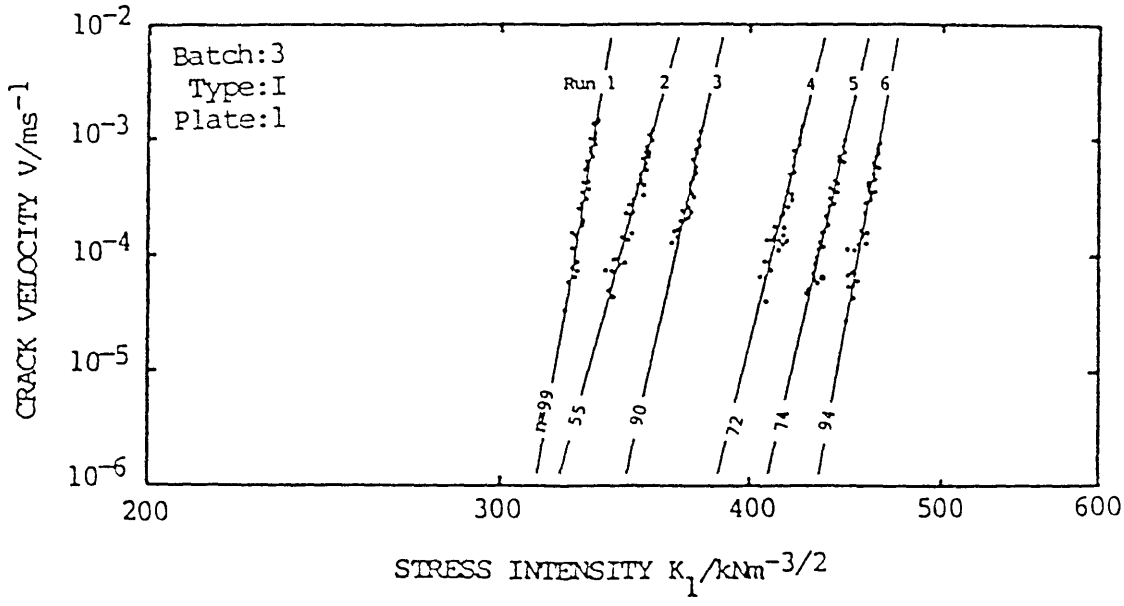


Figure 5.04 contd. Crack velocity-Stress Intensity [V-K] plots determined by load-relaxation in DT plates.



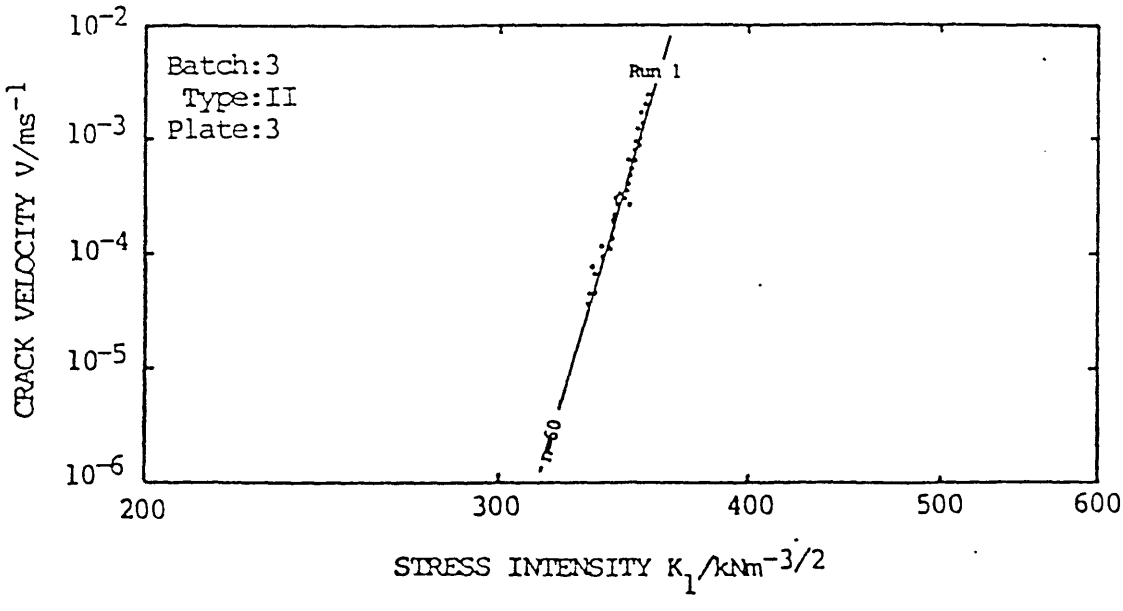


Figure 5.04 contd. Crack velocity-Stress Intensity [V-K] plots determined by load-relaxation in DT plates.

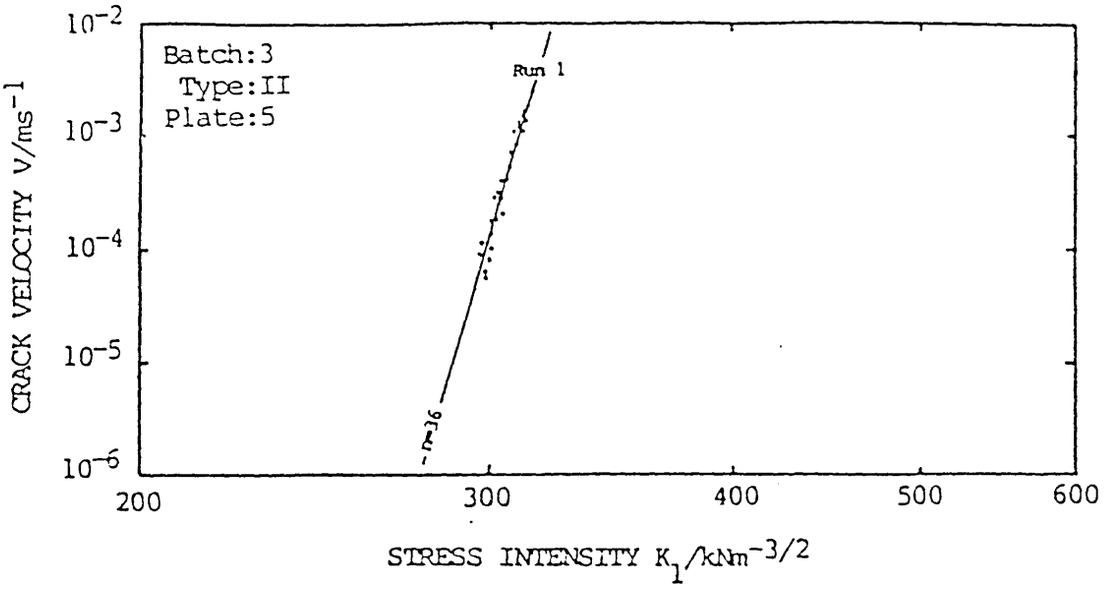
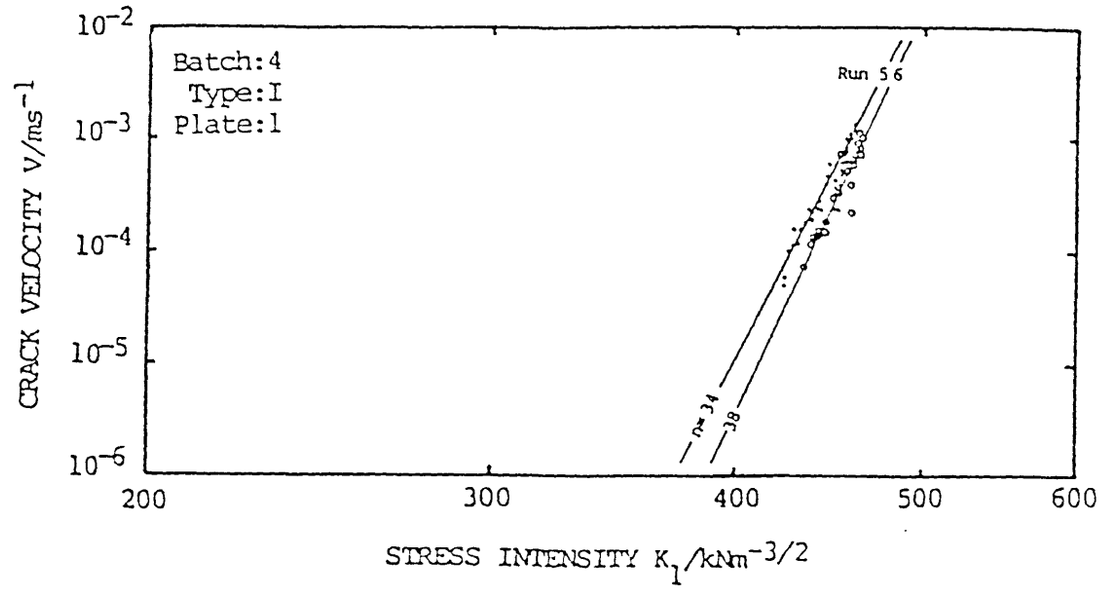


Figure 5.04 contd. Crack velocity-Stress Intensity [V-K] plots determined by load-relaxation in DT plates.



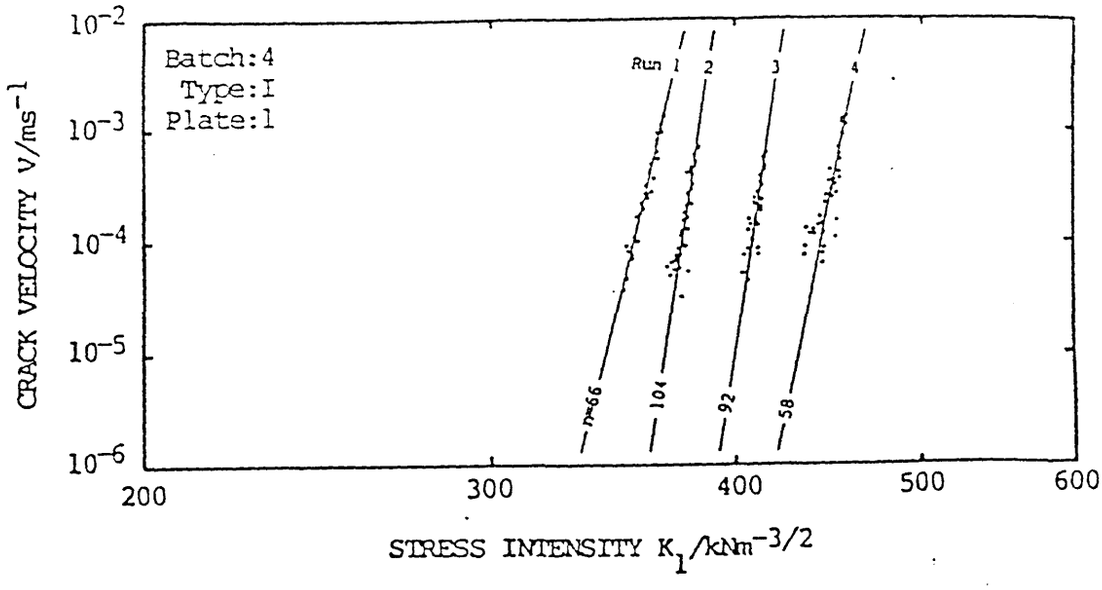


Figure 5.04 contd. Crack velocity-Stress Intensity [V-K] plots determined by load-relaxation in DT plates.

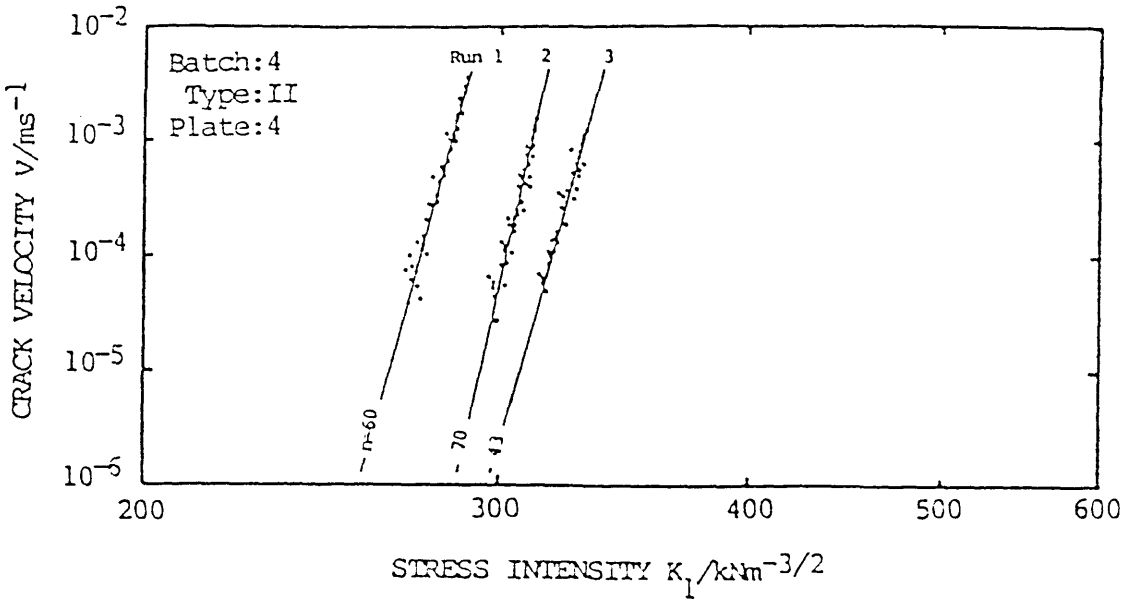


Figure 5.04 contd. Crack velocity-Stress Intensity [V-K] plots determined by load-relaxation in DT plates.

5C.II VARIATION IN CRITICAL STRESS INTENSITY WITH LOADING RATE

Fracture toughness [K_{1c}] was measured on groups of 16 specimens at crosshead speeds [$\dot{x}$] between 8.3×10^{-8} and $2.8 \times 10^{-4} ms^{-1}$. The results are given below, and shown in figure 5.05.

Table 5.04. Crosshead Speed and Median Critical Stress Intensities for 3-point bend SENBs [standard deviation in brackets].

Crosshead speed $\dot{x}$ / ms^{-1}	Median Critical stress intensity K_{1c} / $kNm^{-3/2}$	Batch
8.3×10^{-8}	318.5[24.4]*	4
1.7×10^{-7}	320.0[35.5]*	4
3.3×10^{-7}	333.0[15.7]*	4
1.1×10^{-6}	364.0[30.7]	2
2.8×10^{-6}	365.0[33.8]	2
1.1×10^{-5}	387.5[28.0]	2
2.8×10^{-5}	397.5[44.8]	2
2.8×10^{-5}	408.0[29.0]	3
1.1×10^{-4}	407.0[31.2]	3
2.8×10^{-4}	416.0[23.7]	3

* denotes tested on Instron, all other testing on ESH (see section 3D.II.ii).

Two values of critical stress intensity were measured at a crosshead speed of $2.8 \times 10^{-5} ms^{-1}$ to check how reproducable the results were, and although the second value [$408 kNm^{-3/2}$] appears unusually high compared to the other results it is included in the subsequent calculations. The scatter in the values of K_{1c} for a particular crosshead speed is generally low, as indicated by the values of standard deviation of 30. The only slight discontinuity in the straight line (see figure 5.05) is between those specimens from batch 4, which were tested at the slowest loading rates. The slight drop is regarded as insignificant because: the differences between batches 2, 3 and 4 in the measured values of subcritical crack growth parameters was small; although the testing machine was different, the specimen loading rig was the same for both machines; and the testing inside a thin gauge polythene bag cannot be expected to alter the

measured values as the strain at failure of the HCP was more than accounted for by folds in the polythene.

The slope of a plot of all log [K_{1c}] vs. log [$\dot{x}$] is 0.036, which corresponds to a value of the subcritical crack growth of 27. If separate slopes for the three lowest loading rates, and the seven other rates are calculated separately the values of n were 31 and 36 respectively. This suggests that the value of subcritical crack growth parameter determined by the variation in critical stress intensity with loading rate is approximately 30.

The values of critical stress intensity determined from SENBs were always less [318.5 to 416kNm$^{-3/2}$] than those determined by rapid loading of DT plates [477 to 580kNm$^{-3/2}$], and often less than the stress intensity required for subcritical crack growth (see figure 5.04). The reason for this is unclear, but may be associated with other unexpected behaviour in the DT plates, which is discussed in section 6B.I.ii.

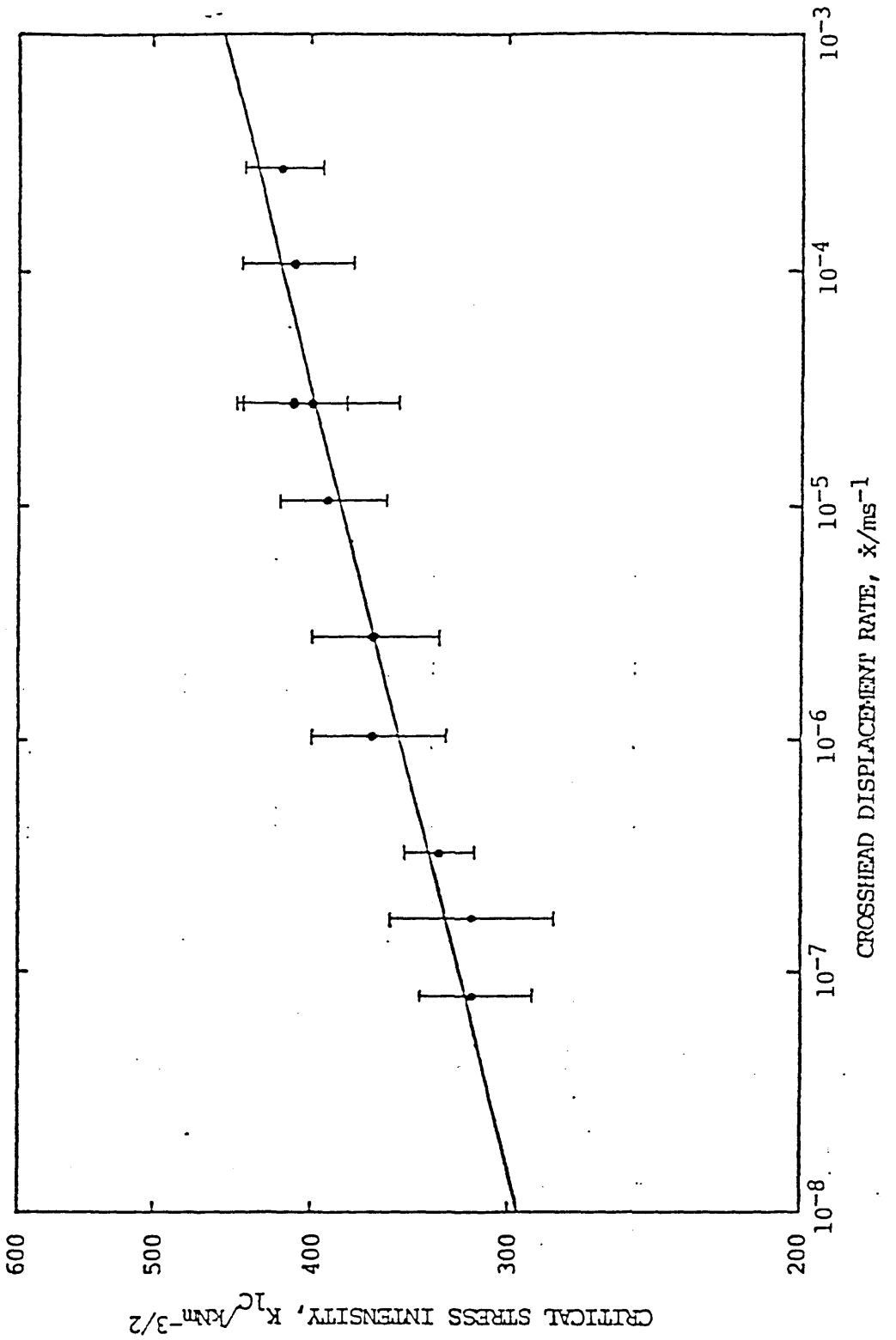


Figure 5.05 Variation in Critical stress intensity with crosshead speed/loading rate.

CHAPTER 6 - DISCUSSION

The mechanical properties of any material can be measured, but they can only be fully understood when the microstructure, and in particular the microstructure involved in crack growth has been characterised. In the case of HCP the mechanical properties have been widely examined, as has the general microstructure. Unfortunately the possibility of studying the microstructural processes occuring during cracking in HCP in the wet state, with the required resolution i.e. in an SEM, has not yet been available.

The present discussion deals with, firstly, the microstructure of HCP, and cracking in that microstructure, and secondly subcritical crack measurements performed on HCP.

6A CRACK PATHS IN HCP AFTER 28 DAYS HYDRATION

A number of cracking mechanisms have been proposed for HCP, which include individual components, but which often do not take into account the overall microstructure of HCP. By examining both fracture surfaces and cracks in polished surfaces it was possible to determine a better overall picture of the cracking process.

6A.I.i The role of unhydrated cement cores

It is clear from examination of polished surfaces that unhydrated cores behave as strong inclusions, the crack path very rarely passing through a core. The proposal (Mindess, 1982) that unhydrated cores act as "micro-aggregate" in a manner analogous to true aggregate in concrete and mortar is therefore in that sense true.

An important feature of aggregate in concrete is that it is often the site for microcrack nucleation, both because the aggregate/matrix bond is relatively weak and because large stress concentrations are built up across this bond during loading due to the very different stiffnesses of aggregate and bond. This propensity to microcracking in concrete leads to a particular failure mode, consisting of the coalition of microcracks in a large [~50mm in a 220mm thick specimen (Reinhardt, 1985)] microcracked zone ahead of the crack.

There is very little to suggest that cracking in HCP occurs in a similar manner. Unlike concrete and mortar, no cracks exist between unhydrated cores and hydrates in HCP which has not been loaded, nor does drying shrinkage promote this type of cracking. Anhydrous cores may be separated from the surrounding hydration products, but these

are not regarded as cracks (see section 6A.I.iii). The observed interactions of introduced cracks with unhydrated core/hydrate bonds are of two types, "C_3S" and "non-C_3S". C_3S, which forms a large part of the unhydrated material, has a surrounding layer of inner C-S-H, with which it appears to be closely associated, and in a number of instances strongly bonded (plate 5.01). The crack tends to pass around the inner C-S-H as well as the underlying C_3S. In the case of the other anhydrous phases in unhydrated cores, there does not appear to be any strongly bonded hydrate, and the crack may pass directly around the anhydrous core. This is seen in plate 5.26, where a crack, entering from the left, passes the first large unhydrated core. This core is predominantly C_3S, which is covered by a layer of inner C-S-H, with a small region of interstitial material at the base of the core; it can be seen that while the crack deviates around the core and inner C-S-H, it passes directly between the interstitial material and the hydrate adjacent to it. On a smaller scale, the crack often passes around fragments [2-3μm] of anhydrous material, which are probably fragments of interstitial material.

It therefore appears that the unhydrated core/hydrate bond in HCP is much stronger than the aggregate/matrix bond in concrete, and does not act as a site for microcrack nucleation. This is consistent with the stress-strain behaviour of HCP, which is much more linear than concrete and mortar. The non-C_3S core/hydrate bond appears to be relatively weak, and therfore susceptible to failure in the immediate vicinity of the crack tip, but not so weak as to be a possible site for microcrack nucleation. It is unfortunate that the ambiguity in the identification of features of 2-3μm has prevented the positive identification of fragments of interstitial material on fracture surfaces, as this would no doubt give a better insight into the bonding of this material to the hydrate matrix.

6A.I.ii The role of hydration products

The two main hydration products, C-S-H and calcium hydroxide, are the components through which cracks generally pass [86.4% of the crack length, see table 5.01]. This is to be expected, because the hydration products are likely to be much weaker than the unhydrated material. On the other hand, very little is known about the relative strengths of C-S-H and calcium hydroxide, except that calcium hydroxide appears to be particularly susceptible to fracture along its basal plane. A variation in strength with orientation is assumed

to occur in calcium hydroxide, because of ease of cleavage along the basal plane. However the stress fields in HCP are too complex to assume that the load across the basal plane will be simply a function of the orientation of the crystallite. Indeed plate 5.24 shows the crack passing through a massive area of calcium hydroxide in which the cleavage plane is oriented almost perpendicular to the direction of crack growth.

At early ages [<7 days] fracture occurs through low-density C-S-H and water filled space (Berger et al, 1973, Walsh et al, 1974) [a process often ambiguously described as inter-granular fracture]. At later ages the fracture surfaces reveal both calcium hydroxide and C-S-H, there are two possible reasons for this. The first, hydration has proceded to a stage where due to the intergrowth of calcium hydroxide and C-S-H the crack path would be extremely tortuous if it were to pass through C-S-H alone; the second, that as hydration continues the C-S-H becomes stronger by becoming increasingly compact, so that in a number of situations calcium hydroxide now offers the path of least resistance.

It is important to understand that while the molecular structure, gel porosity and hence density, of C-S-H remain relatively constant throughout hydration, the amount of micro porosity in the C-S-H decreases with hydration. The model of the structure of HCP suggested in section 2B.II was of a water-filled space between cement grains, which was filled by hydrates, in particular outer product C-S-H and calcium hydroxide, to form a bonded structure. As hydration continues the space available for hydration product is reduced, and the outer product C-S-H becomes increasingly compact, i.e. the micro porosity present decreases. It is the decrease in micro porosity which increases the strength of HCP with increasing age by increasing the amount of bonding within the outer product C-S-H gel.

The present microstructural examination has shown that at 28 days of age a decrease in the micro porosity in C-S-H and hence an assumed increase in strength has occured (see Appendix n). It was very uncommon to observe high micro porosity fibrillar morphology outer product C-S-H (see plate 5.08), which is commonly seen in young pastes (Dalgleish et al, 1980). The predominant morphology of outer product C-S-H was the compact, low micro porosity material of plate 5.07. Grudemo (1979) observed that the amount of calcium hydroxide exposed by fracture increased as the water cement ratio decreased. This would be explicable by a lower micro porosity in the C-S-H

formed in pastes with low water/cement ratios, because of the initially smaller space for hydrate growth. The micro porosity of inner product C-S-H is assumed to be relatively constant, and less than that of outer product C-S-H. Polished surfaces show that the crack tends to deviate around the inner product C-S-H, and passes through outer product C-S-H, confirming the supposition of low micro porosity and high strength for the inner product.

Polished surfaces also show that there is a high degree of intergrowth of calcium hydroxide and C-S-H. We are thus presented with a hydrate matrix consisting of C-S-H which varies in strength with density, and calcium hydroxide which we assume shows some variation in strength with crystallite orientation. The crack path tends to pass through regions of relative weakness, low density C-S-H and suitably oriented calcium hydroxide (plates 5.23) wherever possible but, because these weak links are intergrown with stronger regions [including unhydrated cores], fracture through a stronger region (plate 5.22) will sometimes take place.

The quantitative image analysis of crack paths showed that in general there was very little crack growth along boundaries, and in particular C-S-H/calcium hydroxide boundaries, which suggests that the intergrowth of C-S-H and calcium hydroxide produces a strong physical, if not chemical, bond. Where BEI examination cannot resolve the detail of the interface between C-S-H and calcium hydroxide, SEI examination of fracture surfaces (plate 5.09) shows that there is not an obvious discontinuity between C-S-H and calcium hydroxide, an observation also made by Marchese (1977) for samples of C_3S paste.

There are suggestions in the micrographs that microcracking is occuring in calcium hydroxide in the vicinity of the main crack (CC on plate 5.23 & 5.24), which is effectively blunting the crack. It is not possible to state categorically that these cracks occured during the growth of the introduced crack, rather than subsequently due to drying shrinkage. However it does seem reasonable that the inhomogeneities in the microstructure could lead to microcracking, e.g. in the case of the right-most region of cracked calcium hydroxide [CC] in plate 5.23, the two unhydrated cores adjacent to the calcium hydroxide may have caused a high local stress field, sufficient to initiate cracking. It has been suggested (Beaudoin, 1982) that calcium hydroxide may act as a crack arrestor, but no evidence of this has been observed.

Plate 5.29 shows the extension of a crack by the formation of

microcracks due to drying shrinkage. The microcracks, 2-3um long, form in C-S-H in a zone 20um ahead of the crack tip, before the crack rapidly proceeds to pass through a region of calcium hydroxide. Even at the stage when the crack has passed out of the field of this micrograph (plate 5.29d) there are regions in the C-S-H adjacent to the initial crack tip where the crack does not appear to have opened. Although the processes of fracture in dry HCP might be expected to be different from those occuring in wet HCP [and despite the unusual stress field produced by drying shrinkage] it is significant that the crack does not proceed as a single continuous crack.

It is interesting to compare these observations with those of Higgins & Bailey (1976) who observed a crack pattern in wet HCP, which had been wedge loaded, consisting of a number of microcracks 100um long, which in turn consist of smaller microcracks [20-30μm] which coalesce to form a growing crack. The limit of resolution suggested by Higgins & Bailey for their observations was a crack opening of 0.1μm, and it is not unreasonable to suggest that the microcrack units 20-30μm long were made up of yet smaller units.

6A.I.iii The role of porosity

Porosity is important in determining the crack pattern in HCP, in particular it appears that variation in the micro porosity of C-S-H can alter its strength significantly (see above). The exact nature of this porosity is difficult to ascertain, it is only identifiable in the SEM as a result of the differing degree of disruption which occurs in the drying process.

The suggested interactions between cracks and larger scale porosity [i.e. that which is not seen to be significantly altered during drying] have been: as crack initiators due their stress concentrating effect (Alford, 1981); as crack arrestors by rounding the crack tip.

There are a number of possible causes of large pores in HCP. Starting at the lower limit, there are capillary pores, which is originally water filled space which has not been filled with hydration products. These pores range in size up to 10μm, and have ill defined and often convoluted boundaries. These pores may act in either of the above roles. However their small size, and the existence of larger inhomogeneities in the structure of HCP suggests that capillary pores can only act as major sites of crack initiation, or crack arrest in combination with a number of features. More probably this type of pore

simply reduces strength by reducing the overall bonding of HCP. No confirmation of either crack initiation, or arresting was gained by microstructural examination. The resolution on polished surfaces was not sufficient, and fracture surfaces generally reveal a number of capillary pores but it is not possible to state their effect.

Shells of inner C-S-H, the product of C_3S hydration, are often present in HCP. The particular morphologies of these shells are varied, they may contain an anhydrous core which is either strongly (plate 5.01) or weakly (plate 5.03) bonded to the shell, or they may be empty. The shell is not necessarily continuous, because of the presence of non-C_3S phases in the anhydrous cement grain. Polished surfaces show that these features occur in abundance (plate 5.26), and it has been suggested that empty shells, or the gaps which occur between shell and anhydrous cores may be regarded as porosity [2-20μm]. It is questionable if conventional measurements of porosity such as mercury intrusion (Sereda et al, 1980) detect all of this type of porosity, and furthermore this porosity tends to disappear with continuing hydration. Grudemo (1979) has suggested that these pores may act as crack blunters by rounding the crack tip. Figure 5.29 includes a branch of the main crack [top right] which appears to terminate in a shell of C-S-H. On the other hand, the main crack in plate 5.29a ends in an inner C-S-H shell, and proceeds to grow out of it (plate 5.29b). This type of porosity is highly specific to shells of inner C-S-H, and as such must be expected to be highly influenced by the shell which is relatively strong. It seems to be an unnecessary complication to include this feature of HCP as porosity, and it is more valid to associate the mechanical properties of HCP with the inner product C-S-H rather than the associated porosity.

The largest pores in HCP are the result of entrained air, and vary in size from 0.1-1mm, they are generally spherical, and are often lined with calcium hydroxide (Bache et al, 1966) which may be a continuous mass or a number of crystallites (Barker et al, 1984). Once again two possibly contrasting roles have been proposed for these pores, namely crack initiators, based on a strength sensitivity to the largest air void [cf notch-sensitivity] (Alford, 1981); and crack arrestors, based on the observation of lower critical stress intensity in de-aired HCP (Eden & Bailey, 1984). Fracture surfaces invariably include some air pores, but in polished surfaces with introduced cracks the crack does not seem to interact with large air voids; in one case a crack ran within 60μm of a 200μm air void

without deviating.

It is possible that both crack initiation, and crack arresting may occur, the role being determined by the specific structure of the material around the air void. As previously stated the properties of the various components of HCP can vary considerably, and whereas a mass of calcium hydroxide surrounding an air void whose basal plane is aligned perpendicularily to the maximum applied load would be susceptible to fracture, a dense layer of C-S-H and unhydrated cores merely coated by calcium hydroxide crystals would not.

6A.I.iv Summary of the microstructural aspects of cracking in HCP

The microstructure of HCP is highly complex, and even by using complementary microscopical techniques it is not possible to ascertain the exact processes of cracking in HCP. It is also particularly dangerous to itemise the roles of the various components of the microstructure without taking into account the interactions that occur between them. It is also particularly significant that the material in the planes above and below those exposed on fracture surfaces and polished surfaces may influence the crack more than those which are visible. Fracture surfaces and polished surfaces make it obvious that tortuosity is present in three dimensions.

Fracture through HCP takes place predominantly through C-S-H and calcium hydroxide, because they are generally the weakest phases. However the strength of these two phases can vary, the strength of C-S-H depends on its microporosity, and that of calcium hydroxide with its orientation relative to the basal plane, so that no phase can be described as the stronger or weaker. Local changes which vary the strength, and the fact that C-S-H and calcium hydroxide grow as an interpenetrating mass, suggest that it is more reasonable to regard the hydrates en masse.

The idea of the hydrates forming a pseudo-homogeneous matrix recalls the concrete analogy. As described the anhydrous cores generally act as strong inclusions, but there are situations where the crack path does pass through an anhydrous core. The presence of a pre-existing crack in the core may cause this, but it is also possible that the local stress intensity could be sufficiently increased by features in the microstructure to fracture anhydrous material. The bonding between unhydrated cores and hydration products is sufficiently good to prevent the occurence of microcrack nucleation, probably because the strength of inner product C-S-H is

sufficient to act as a binder between the cores and the other hydrates.

Porosity is known to decrease the strength of HCP by decreasing the continuity of the system, but beyond that the interaction of larger scale porosity with cracks is not so well understood. The crack arresting mechanisms of porosity postulated are highly tentative, and at the moment require positive experimental evidence. The suggestion that large air voids in HCP represent critical flaws (Alford, 1981) is probably valid up to a point, but below a threshold value it is possible that critical flaws in HCP may be made up of less obvious flaws. It should be noted that the shape of a flaw significantly alters the stress concentration at the crack tip, so that in a material such as HCP where there are a large number of discontinuities, a combination of these discontinuities, capillary pores, high micro porosity C-S-H, etc. could be the major stress concentrator.

6A.II THE EFFECT OF PREHYDRATED CEMENT MICROSTRUCTURE

Analysis of the subcritical crack growth results (see section 5C.I.ii) suggests that there is a difference between batch 1, and batches 2, 3 and 4 of cement. This may be a result of the lumpy microstructure of batches 2, 3 and 4 (see section 5A.II, plates 5.15 & 5.16). The effect of the lumps is difficult to imagine, the calcium hydroxide surrounding the lumps could if favourably oriented provide a path of relative weakness, or act as a site for microcracking around the crack, and hence effective crack blunting. The higher concentration of anhydrous particles in the lumps will act as relatively strong areas, but it is unclear what the nature of the hydration products in the lumps is. Hydration products are obviously visible, suggesting that water was able to penetrate into the lumps and allow hydration, but the higher density of anhydrous cores suggest that there is not the same amount of hydration product as in the bulk of the specimen. A decrease in the amount of hydration product would under normal circumstances suggest a weaker structure, however in this case the the decrease in available space, caused by the closer packing of anhydrous particles may be associated with low micro porosity C-S-H, and a corresponding increase in strength.

Direct observation of fracture faces of both DT and SENB specimens, identified the lumps, but did not show any deviation in the crack path due to them, nor were they identifiable on SEM micrographs of fracture surfaces.

6B SUBCRITICAL CRACK GROWTH

6B.I Load-Relaxation in Double Torsion plates

The measurement of subcritical crack growth using the method of load-relaxation in Double torsion [DT] plates is usually a relatively straightforward procedure. However, the use of this test method, in the present study of HCP, has identified a number of problems which question the applicability of the test method to this material. After a discussion of the basic results these problems will be highlighted, and their influence on the results examined.

6B.I.i V-K curves

The values of crack velocity [V] and stress intensity [K] when plotted as V-K curves showed only the linear relationship of Region I of the theoretical V-K curve. The coefficient of correlation of the straight line through these plots was good [$\sim$0.97], but there was considerable scatter in the values of slope, n [average = 64, standard deviation = 20].

Errors must be expected in any experimental work, due to inaccuracies in measurements, and in the particular case of HCP, because of local variations in the structure. However the scatter in the values of subcritical crack growth parameter is much larger than that in measurements of critical stress intensity [at any particular loading rate] by 3-point bend tests on SENBs. This suggests that the scatter is partly due to the test method, and in particular the necessity to determine two curves, the overall relaxation and the background component of that relaxation, and the subtraction of the latter from the former. In the initial determinations of the V-K curves, where the background was overestimated by 20%, the values of n were overestimated by 50%. This uncertainty over the exact extent of the background relaxation, and the unexpected reduction in background relaxations which occured in subsequent testing of individual plates, implies that background relaxation measurements may be subject to significant error and are probably the main cause of scatter in the calculated values of subcritical crack growth parameter. To improve the background relaxation determination it will be necessary to first, determine the cause of the variation in background relaxation, and second, characterise this variation and its effect.

Statistical analysis of the results by Students t-tests suggest

that there are significant difference between the two different sizes of plates, and between batches 1 and batches 2, 3, and 4 of cement. The difference in the width and thickness of the two plate types is small [type I, 22 x 190 x 450; type II 24 x 170 x 300], the major difference being the increased length of the type I plate, although as mentioned later (section 6B.I.ii.d.) the difference in the thickness to width ratio may be significant. In both types of plates the crack lengths used were within the most conservative estimate of the range of crack lengths which prevent possible end effects (Shetty & Virkar, 1979). The results from the type I plates were generally gathered from 6 tests on the same plate whereas the type II plates were tested a maximum of three times, but the results showed no trend towards higher or lower values with the number of repetitions (see table 5.02). The suggestion that the difference between batches of cement may be a result of the lumps in the microstructure of batches 2, 3 and 4 is not supported by the observation of fracture surfaces of these batches, which suggests that the lumps have little effect on the crack path.

As the variations cannot be satisfactorily explained, the implications of the t-test results may not be valid. The high values of the parameter t may merely reflect a large amount of scatter, rather than identify positive variations between either the type of plates, or the batches of cement.

Despite the high degree of scatter in the result, it is believed that the average value of slow crack growth parameter, 64, which was within the values determined by other workers (see table 6.01) has some significance.

Table 6.1 Values of n, the slow crack growth parameter determined for HCP by load-relaxation in double torsion plates and the variation in strength with loading rate for beams.

Test method	n	Comments
DT (Nadeau et al, 1974)	36	w/c=0.5, 3-4 months, HESPC*
DT (Mindess et al, 1974)	76.2	w/c=0.4, 4-6 months, HESPC
DT (Mindess et al, 1977)	34.2	w/c=0.4, HESPC
Beam (Mindess et al, 1977)	17.7	w/c=0.4, HESPC
DT (Brown, 1983)	26.7	28 days
Beam (Mindess, 1984)	36	w/c=0.3, 50 days, OPC
DT (Present work)	69	w/c=0.4, 28 days, OPC
Beam (Present work)	27	w/c=0.4, 28 days, OPC

* HESPC = High early strength Portland Cement.

6B.I.ii The applicability of the load-relaxation method of determination of the subcritical crack growth parameter

A possible reason for the wide range of values determined by this, and previous load-relaxation measurements, may be errors in the background relaxation determination, as discussed. Other observations during the present work suggest that the properties of HCP may make this test method inherently unsuitable.

6B.I.ii.a Compliance-crack length relationship

The derivation of the relationships between applied load, rate of change of load, stress intensity and crack velocity (Evans, 1972) are based on the assumption that the compliance of the DT plate is linearly related to the crack length. The compliance of HCP DT plates with sawn notches was found to follow this relationship, but the compliance of plates containing cracks produced by slow crack growth did not. The compliance in this latter case remained more or less constant, increasing only slightly with increasing crack length.

This is difficult to explain, because under conditions of fixed displacement a decrease in load [load-relaxation], is a manifestation of an increase in compliance. This implies that the error must be in the measurement of compliance. The compliance was measured before each background measurement, 2 minutes after unloading from the previous load-relaxation measurement. The settling time was included because time dependant changes in load [up to 0.01kN in the 30s] were observed after unloading. This time may not have been sufficient, and have resulted in a superposition of the increasing applied load, and the time dependant load increase, which led to the nearly constant compliance measurement [a similar, inverted, superposition could occur during the unloading compliance measurement]. This explanation is highly speculative, proposed as it is in the context of no previous examples of this type of behaviour, and as a fault in experimental technique. The error in the measurement of compliance is possibly preventable. Of much greater significance is the time dependant variation in load, which appears to dependant on the previous load history of the specimen.

6B.I.ii.b The variation in the background relaxation with repeated relaxation measurements

Mindess (1974) stated that the background relaxation which

occured during load-relaxation tests on HCP was attributable solely to the testing machine and fixtures. In the present work the variation in the background relaxation between plates, and the decrease after the initial load-relaxation measurement on an individual plate suggests that the specimen contributes to the background relaxation. The change in background relaxation also suggests that the contribution from the specimen is changing with repeated loading.

It is well known that HCP is susceptible to creep (Soroka, 1979). A number of possible mechanisms for creep have been suggested, e.g. movement of inter-layer water (Feldman & Sereda (1970), and the displacement of C-S-H sheets relative to another (Bentur et al, 1979), and although the exact mechanisms are not clear, it is apparent that there are reversible and irreversible components. The decrease in background relaxation which occurs after the first load relaxation tests may be explained by creep in the specimen. In the first background relaxation measurements the applied load results in both elastic deformation, and reversible and irreversible creep in the torsion arms of the DT plate. The irreversible creep in the torsion arms is a significant contribution to a large background relaxation. The first load-relaxation measurement, which takes place at almost twice the load of the background relaxation, is likely to include some irreversible creep which will remove a number of the possible sites for irreversible creep at the lower load used for the subsequent background measurement, resulting in a lower background relaxation. Once again no previous incidences of this type of behaviour have been reported.

6B.I.ii.c The systematic shift of the V-K curves to higher stress intensity [K] values

As well as the large scatter in the value of the subcritical crack growth parameter, there was a systematic shift of the V-K curves towards higher stress intensities [K] with repeated measurement on a particular plate. The increased stress intensity [25% for plate 4/I/1] is obviously a result of increasing the applied load, and it is the absence of a corresponding increase in crack velocity [V] which is of interest. This behaviour is effectively an increased resistance to crack growth, a rising R-curve (see section 2B.III.ii), and has also been observed in alumina (Pletka et al, 1979). Although unexplained by Pletka et al, the observations

of Hubner & Jillek (1977), and Knehans & Steinbreich (1982) suggest that increased resistance to crack growth in alumina is caused by crack branching, which reduces the effective stress intensity at individual crack tips.

There are a number of possible causes for a rising R-curve in HCP. A zone of microcracking has been suggested (Grudemo, 1979) and has been discussed at length in sections 2C.III.ii, 5B.II.ii and 6A.I.ii, where it was proposed that a small zone of microcracking, of constant width [upto 300um] may accompany macrocrack propogation. A zone of microcracking of these dimensions would not explain the continued increase in the stress intensity required for a particular rate of crack growth, which was observed. According to Evans & Faber (1984) an R-curve approaches a maximum after a crack extension of approximately five times the width of the microcracked zone. If this were true for HCP, in plate 4/I/1 where the V-K curve is continuing to shift after five relaxation measurements, with an accompanying overall crack extension of 120mm, the implied width of the microcracked zone is 24mm. This does not appear to be realistic. Wittman & Zaitsev (1972) suggested that stress concentrations at crack tips were redistributed by creep, and as this creep is localised to the small region of high stress concentration around the crack tip, it will be left behind as a wake as the crack grows. This wake, like a microcrack wake would involve a dilational strain, but is unlikely to alter significantly the local elastic modulus of the material, and as such is not considered likely to be responsible for the V-K shift.

[The likely stress relaxation around the crack tip by creep may decrease the value of the subcritical crack growth parameter. If the creep responsible for redistributing the stresses were more effective at higher loads, then the crack velocities at high loads would be reduced, reducing the slope of the V-K plot, i.e. the subcritical crack groth parameter.]

Another possible cause of the V-K shift is a change in profile of the crack front. Trantina (1977) showed that a 10% decrease in the maximum stress intensity would occur with a change in crack front orientation from 45^{o} to 30^{o}. A change in the profile of the crack front from that sawn-in, to a more stable shape may occur. It is not possible to state whether a change in the crack front profile is occuring, because no method of retaining the DT crack profile has been developed for HCP. However, it must be expected that a change in

crack profile would occur either relatively quickly, i.e. in the first test, after which the shift along the stress intensity axis would cease, or throughout testing, which would be at such a slow rate that the change would not result in a shift as pronounced as that observed.

The previous possible explanations for the increased resistance to crack growth have examined possible changes in the crack, and suggested that neither a microcracking/creep wake nor changes in the crack profile, occur to an extent which would result in the observed V-K shift. A number of other mechanisms for increasing the resistance to crack growth can occur, which are not directly related to the crack. The direction of crack growth in the DT plates was vertical with respect to the orientation in which they were cast, which could have lead to the occurence of segregation, i.e. a settling of cement particles to the bottom part of the mould. This could lead to a gradient of decreasing local w/c ratio, and hence decreasing porosity and increasing strength towards the bottom of the plate. While segregation undoubtedly does occur, it is minimised in this case by using a relatively low w/c ratio [0.4] and limited vibration following casting. Grudemo (1977) suggests that segregation is only significant in the top and bottom 5% of a specimen, and therefore would not result in continual shift of the V-K curves along the stress intensity axis.

In the previous sections (6B.I.ii.a & 6B.I.ii.b) it was suggested that significant time dependant load changes occured after loading and unloading, and that there was a decrease in the susceptibility to irreversible creep of the DT plate during background relaxation. The background relaxation measurements, while not perfect, are sufficiently good to prevent such large shifts in the V-K curves. The suggestion that creep is occuring during background relaxation implies that creep can occur in HCP at relatively low loads. Unlike the highly localised creep which is responsible for the reduction of stress concentrations at crack tips (Wittman & Zaitsev, 1972 see above), it is suggested that the creep occurs in the length of the torsion arms of the DT plate which are transmitting the load to the crack tip. The resulting specimen would therefore be one in which the increasing resistance to cracking, the rising R-curve, was caused by an increasing length of torsion arm susceptible to creep.

It is well known that creep occurs in HCP, the significant point is that a rising R-curve, caused by an increasing susceptibility to

creep has not been previously reported. In the case of previous determinations of V-K curves for HCP by load-relaxation, only two (Nadeau et al, 1974), or a maximum of three (Mindess et al, 1974) measurements per plate were performed, making it less likely that a shift in the V-K curves would be noticed. The only V-K curves identified by previous workers as being obtained from a single plate, are identified by Nadeau et al, and indeed there is a very slight shift towards higher values of stress intensity for the second measurement. The absence of an increase in the value of critical stress intensity with increasing crack growth observed by Brown (1972) may be explained by the DCB specimens which were used which, because of the larger cross section transmitting the load to the crack tip, are less likely to be susceptible to creep than the DT plates used in this work.

6B.I.ii.d Summary of proposed processes occuring during load-relaxation measurements

It is not disputed that subcritical crack growth occured in the load-relaxation measurements which were performed. It is also clear that there were considerable time dependant load changes when a DT plate was either loaded or unloaded, and that the V-K curves shifted towards higher stress intensity [K] with repeated testing of the same plate.

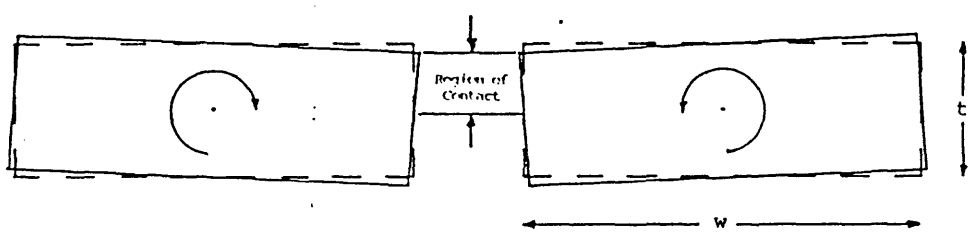
It is therefore suggested that under an applied load the DT plates underwent creep as well as subcritical crack growth, and that the amount of creep increased with increasing crack length. This creep decreased the amount of crack growth which occured. [This may also explain the higher value of K_{1c} determined from DT plates than SENBs, because the load applied to the DT plate resulted in creep as well as crack growth, although the high loading rate was expected to eliminate creep]. Under these circumstances the values of subcritical crack growth parameter which are measured will be overestimated, because the effective stress intensity which is causing the low velocity crack growth is lower than that determined by simple elastic theory. The extent of this overestimate is difficult to estimate, as the variation in the susceptibilty of the specimen to creep will probably depend on the length of torsion arm susceptible to creep [i.e. the crack length] and the previous loading history of the particular specimen [i.e. the amount of previous creep in any particular section of the torsion arms]. The values of subcritical

crack growth parameter determined in the present work are therefore overestimates of the real subcritical crack growth parameter. As will be discussed in section 2C.III the value of subcritical crack growth parameter determined by load relaxation methods is also increased by inhomogeneities in a material.

The determinations of V-K plots are performed for two reasons, the first is to estimate the possible lifetime of components subjected to sustained load, and the second is to determine the corrosion mechanisms responsible for the subcritical crack growth. What must be assessed is whether it is worthwhile to determine V-K plots for HCP by load-relaxation in DT plates.

The susceptibility of the torsion arms of a DT plate to creep is determined by the relative loads necessary to cause crack growth, and creep in the torsion arms. The load necessary for crack growth depends on the thickness of material under the guiding groove, and the susceptibility of the torsion arms to creep depends on their thickness to width ratio. It may therefore be possible to determine V-K curves from specimens which have high thickness to width ratios, and deep guiding grooves. Unfortunately there are significant problems involved with thick plates, the first is that calculations of the stress intensity assume thin plates Fuller (1979), and although corrections can be made for thick plates these do not take into account the presence of a region of contact, with accompanying contact stresses in the upper region of the crack (see figure 6.01), which in plates of increasing thickness will become increasingly significant. The second problem which may occur in DT plates with a large thickness to width ratio is increased shear stress in the torsion arms (Hillerborg, 1983), making the specimen susceptible to failure by shear.

In order to determine the DT plate shapes which would be suitable for determination of V-K curves by load-relaxation it would be necessary to perform comparative tests on a number of specimen shapes. However, some indications of the required specimen shape can be deduced from the present work, and the work of Nadeau et al (1974) and Mindess et al (1974). The thickness to width ratio of the DT plates used have been, 1:8.5 [present work, type I plate], 1:7 [present work, type II plate], 1:7.5 [Mindess et al] and 1:6 [Nadeau et al], and in all these cases a guiding groove [half the thickness of the specimen], was present in the upper side of the plate (see figure 6.01), the surface likely to contain contact stresses.



End view of DT plate.

Figure 6.01 Schematic, exploded diagram of double torsion plate, showing the presence of a region of contact.

The indication of creep, by the shift in the V-K curves, in the present study suggests that this thickness to width ratio of the DT plates is beyond an upper limit for worthwhile testing, given the relative thickness of material under the guiding groove. Thickness under groove/thickness [t_n/t] = 0.55:1 and 0.58:1 for the type I and type II plates respectively. The observations byMindess et al (1974) that the specimen does not contribute to the background relaxation suggests that at a thickness to width ratio of 1:7.5 creep has been eliminated by decreasing the relative thickness under the groove t_n/t to 0.50:1. This may be so at the loads used for background measurements, but at the higher loads of the load-relaxation test it is not possible to discount creep without examining the V-K curves obtained from repeated testing of a single DT plate. It must also be remembered that the samples of Mindess et al were tested at an age of 4-6 months, when the susceptiblity to creep would probably be slightly reduced. It is interesting to note that in the two comparable groups of load-relaxation measurements using DT plates of different thickness to width ratio [i.e. Nadeau, Mindess & Hay (1974) and Mindess, Nadeau & Hay (1974), and the type I and type II plates in the present work], the lower value of subcritical crack growth parameter was measured in the plates with the higher thickness to width ratio (see tables 5.04 and 6.01). This may be a reflection of the decreased susceptibility to creep of the DT plates, but is highly tentative, and may be better explained by other as yet unknown factors.

Evans et al (1974) suggested that the minimum thickness to width ratio which did not result in an underestimation of the critical stress intensity [K_{1c}], due to contact stresses, in DT plates was 1:8. This was determined for plates with guiding grooves on the lower side of the DT plate. The measurements performed on HCP DT plates have always had the guiding groove on the upper side, i.e. reducing the effects of contact stresses, it therefore seems reasonable to assume that the limiting criterion should be a value of the thickness under the notch [rather than overall thickness] to width ratio of not less than 1:8. This criterion was satisfied in all of the above mentioned plates used for testing HCP.

The failure of a specimen by shear is only likely in DT plates with very high values of thickness to width ratio [~1:4] and this mode of failure can be prevented by reducing the thickness of material under the guiding groove (Hillerborg, 1983).

Returning to the question of the applicability of load-relaxation

in DT plates as a method of determining V-K curves. It appears that the reduction of the amount of material under the guiding groove is a good method for preventing creep in the torsion arms, errors due to to contact stresses and failure by shear, and as such may provide specimens which are suitable for this test method. By placing the guiding groove on the upper surface the effects of contact stresses are minimised, and, as the load required for crack growth in the DT plate is reduced, susceptibility to creep and failure by shear are reduced. With the very limited specimen shapes available the shape criteria appear to be a thickness to width ratio of approximately 1:7, with a relative thickness under the groove of 0.5:1, and a thickness under the groove to width ratio no greater than 1:8. However, as stated earlier these suggestions require a thorough testing programme to confirm their efficacy. As well as the effects mentioned above, the production of HCP DT plates containing deep guiding grooves must be examined, and the stress concentrating effects of these grooves must be more fully understood.

If a suitable DT specimen shape cannot be found for HCP then it will be necessary to directly determine the V-K curve for HCP using other types of specimen, such as double cantilever beams [DCBs]. Unfortunately these specimens require a measurement of crack length in order to determine crack velocity, which in the case of HCP where the crack cannot readily be followed by optical methods will rely on the variation of the compliance of the specimen.

6B.II DETERMINATION OF THE SUBCRITICAL CRACK GROWTH PARAMETER BY THE VARIATION IN CRITICAL STRESS INTENSITY WITH LOADING RATE

The value of the subcritical crack growth parameter determined from the variation of the critical stress intensity K_{1c} measured on 3-point bend SENBs was 27, much lower than that determined by load-relaxation in DT plates. This was to be expected, because as outlined in section 2C.III the variation in K_{1c} with loading rate tends to give a lower value of subcritical crack growth parameter, which is assumed to be a value more representative of the material. The value of subcritical crack growth parameter determined by load-relaxation in DT plates is probably increased by the increasing susceptibilty to creep which accompanies crack growth (see section 6B.I.i.d).

The effect of creep on the measurement of critical stress intensity may manifest itself in two inter-related ways. First, the effect of creep during the measurement of K_{1c}, and second, the

effect of creep during the load-relaxation of DT plates on the measured value of K_{1c} of beams made from these plates. It is highly likely that some creep will occur during the loading to failure of notched beams, but it is assumed that this will be confined to the region of high stress concentration around the crack tip, unlike DT plates where creep also occured in the bulk of the specimen. Wittman & Zaitsev (1972) suggested that a redistribution of the stress concentration at crack tips could occur by creep. Sagar Dwivedi & Pratt (1984) have also suggested that creep occurs in HCP at low strain rates but at high loading rates the creep processes cannot occur fast enough, and a transition to creep-free bahaviour occurs. In addition [in a manner analogous to the increased slow crack growth at low loading rates], the amount of creep which can occur prior to failure will be greater at lower loading rates.

These observations combine to suggest that the measurements of K_{1c} at low load rates will be accompanied by a greater amount of creep, which will, by decreasing the stress concentration at the crack tip, increase the measured value of K_{1c}. The increased critical stress intensity at lower loading rates will decrease the slope of the V-K plot, which will in turn increase the value of the subcritical crack growth parameter.

The loading history of each beam is likely to be different, according to its original position in the DT plate, the load history of the plate, and the fact that the notched edge of the beam was not consistently either the upper or lower face of the DT plate. This variation in previous load history, and hence creep history is important because it will affect the susceptibility of the beam to creep during the measurement of K_{1c}. As a beam is undergoing loading the variation in susceptibility to creep might affect the capacity of the beam to redistribute stress concentrations around the crack tip. This would be reflected in a high degree of scatter in the results, which in comparison to other workers (Mindess & Nadeau, 1977; Mindess, 1984) is not present. It is therefore assumed that the previous loading of the beams [as DT plates] does not effect the measurements of K_{1c}. This is explicable because the creep processes which are expected to occur in the beams are those which are limited to the much higher stress concentrations around the crack tip. The susceptibility of the beams to this type of creep is unlikely to be significantly affected by the creep which occured at much lower stresses in the torsion arms of DT plates during load-relaxation.

6B.III VARIATION IN THE SUBCRITICAL CRACK GROWTH PARAMETER DUE TO MICROSTRUCTURE AND TEST TECHNIQUE

The presence of inhomogeneities resistant to crack growth in the microstructure of a material result in a higher value of subcritical crack growth parameter when determined by load-relaxation in DT plates, than that determined by the variation in strength/critical stress intensity with loading rate (Pletka & Wiederhorn, 1982). The highly inhomogeneous nature of HCP, and in particular, the observation that cracks in HCP pass through all types of component (see section 5B.II.ii) make this a likely cause of some of the disparity between the two methods used to determine the subcritical crack growth parameter in this work.

The increasing resistance to crack growth with increasing crack growth, due to the increased susceptibility of the test specimen to creep also results in an increase in the value of subcritical crack growth parameter measured by load-relaxation in DT plates.

The relaxation of stress concentrations around the crack tip by creep will result in an increase in the subcritical crack growth parameter measured by the variation in critical stress intensity with loading rate, and possibly a small decrease in the value measured by load-relaxation.

The above phenomena make it clear that the subcritical crack growth parameter is not a material constant for HCP, but it is worthwhile examining the practical situations in which the subcritical crack growth parameter might be applied, i.e. the determination of specimen lifetime under sustained load. In the case of cement, a practical case would involve a concrete structure, in which tensile stresses are eliminated as much as possible, and lifetime predictions would require an adaptation of the subcritical crack growth parameter to take compressive failure into account.

In a realistic practical application the applied load would be such that the specimen lifetime would hopefully be a number of years. Under these circumstances the rate of creep in the bulk of the specimen, due to bulk stresses would be vanishingly small. However, the processes of creep responsible for redistributing the stress concentrations around crack tips are confined to a small area, and will therefore continue to occur as the crack grows. If the process of crack growth is assumed to include the redistribution, by creep, of stress concentrations around the crack tip then so long as the subcritical crack growth parameter is determined at rates of crack

growth which allow creep to occur then the values of subcritical crack growth parameter so determined will be valid for practical applications. This assumption seems reasonable when the overall lifetime of a specimen is compared to the short time spent at the high rates of crack growth necessary to preclude creep from the cracking process. In the present determination of subcritical crack growth parameter by the variation of K_{1c} with loading rate no transition to creep-free crack growth was implied by a decrease in the value of K_{1c} determined at the highest rates of loading, as seen by Mindess (1984) and Sagar Dwivedi & Pratt(1984). The value of subcritical crack growth parameter so determined is therefore assumed to be valid for prediction of specimen lifetimes under sustained loading. No discontinuity in the V-K curves at high crack velocity was observed, which suggests that a crack velocity which was creep free had not been reached, however the presence of other irregularities in the determination of the V-K curves may have overshadowed this effect.

The other errors present in the determination of subcritical crack growth parameter by load-relaxation, the effect of inhomogeneities and an increasing susceptibility to creep in the specimen cannot be regarded as likely to affect subcritical crack growth in practice, and the high value [64] of subcritical crack growth parameter resulting from these effects must be regarded as a serious overestimate.

As the determination of subcritical crack growth parameter by the variation in critical stress intensity with loading rate is not overinfluenced by inhomogeneities or a varying susceptibility to creep the value [27] determined by this method will be used in the following calculation of specimen lifetimes (see below).

6B.IV PREDICTION OF SPECIMEN LIFETIME UNDER SUSTAINED LOAD

The predicted specimen lifetimes of 3-point bend SENBs containing various sizes of edge notch were determined for a variety of applied loads (see figure 6.02). The calculations were made using the value of slow crack growth parameter determined by the variation of critical stress intensity (see Appendix 3), and were compared to an intrinsic strength of $15MNm^{-2}$. The value of intrinsic strength of $15MNm^{-2}$ was chosen, in the absence of any measurement of the modulus of rupture, as a somewhat arbitrary value, suggested by the value deduced by Higgins & Bailey (1976). The assumed values of K_{1c} and an intrinsic strength, of $0.45MNm^{-3/2}$ and $15MNm^{-2}$ respectively suggest a maximum intrinsic Griffith flaw of 0.3mm, and the curve for a beam

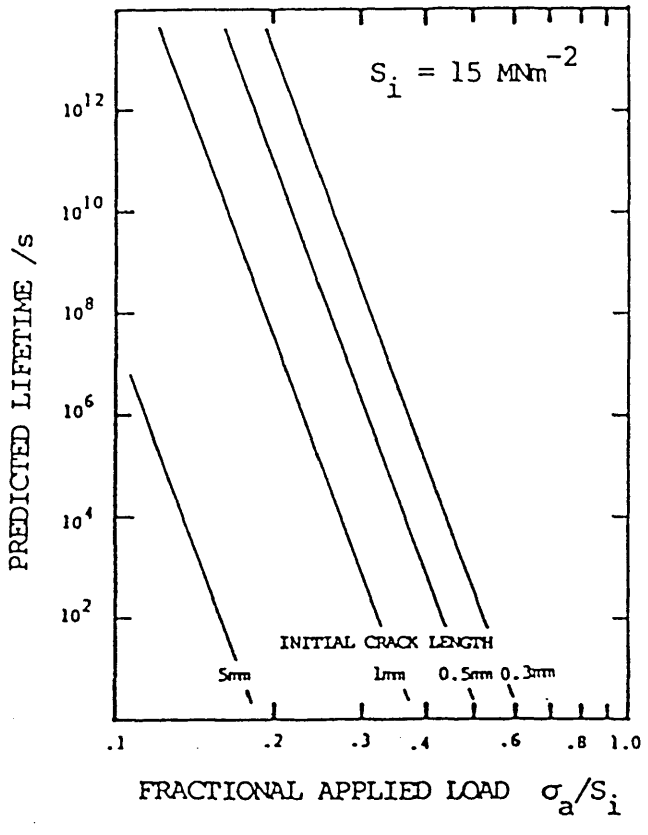


Figure 6.02 Predicted lifetimes of single edge notched beams under a sustained load.

containing a 0.3mm flaw therefore represents an un-notched beam.

It should be emphasised that the calculations of predicted lifetime are based on the assumption of the Griffith criterion for failure and as such are not necessarily accurate for HCP, which may be better characterised by a tied-crack failure criterion. However, it was felt to be an adequate assessment at the present time, when there is not an exact analytical description of the failure of HCP.

6B.V STRESS CORROSION

In the present work all testing was performed in the same water saturated state, and therefore can only give limited indications about possible stress corrosion mechanisms.

The measured value of the subcritical crack growth parameter [27] is similar to silica glass, in which the attack of silicate bonds by OH^- has been proposed (Wiederhorn & Johnson, 1973) as the stress corrosion mechanism. Beaudoin (1985a) has proposed a similar mechanism for HCP, in which OH^- ions attack silicate bonds in C-S-H. Microscopic evidence (see section 5B.II.ii) shows that both C-S-H and calcium hydroxide are involved in the cracking process, which suggests that if a silicate attack by OH^- is responsible for the variation in slow crack growth that calcium hydroxide cleavage is unaffected, or much less affected, by chemical environment than C-S-H. This may be the case, as the basal plane bonding in calcium hydroxide is suggested to be a very weak covalent bond (Tabor, 1981), much weaker than the bonding in C-S-H, and therefore breakable by thermal rather than chemical energy.

The dimensions of the DT plates [1 x 38 x 76mm] used by Beaudoin (1985a&b) suggest, according to the criterion determined in section 6B.II.ii.d, that the plates would be susceptible to significant creep. However, it is believed that the effects of different testing environments on V-K curves would be consistent, and the overall conclusions therefore remain valid.

CHAPTER 7 - CONCLUSIONS AND SUGGESTIONS FOR FURTHER WORK

7A MICROSTRUCTURE OF, AND CRACK PATHS IN HCP

The observed microstructure of HCP was very much that expected from previous workers examinations. It was found particularly useful to examine both fracture surfaces and polished surfaces, using secondary electron and back-scattered electron imaging techniques respectively. Fracture surfaces showed the morphology of the various components, and polished surfaces showed the distributions of these components.

The characterisation of HCP microstructure from back-scattered electron images of polished surfaces is a very useful technique, but has not been widely used by other workers. The HCP examined in the present work was 28 day old 0.4 w/c OPC, which showed the main hydration products, C-S-H and calcium hydroxide, as often inter-penetrating masses. Calcium hydroxide was present in a wide range of crystallite sizes, and presumably orientations. Some variation in porosity within C-S-H [in particular between inner and outer product C-S-H] was indicated by variations in back-scattered electron intensity.

Examination of crack paths in polished surfaces showed that the crack was made up of a number of crack path elements, predominantly C-S-H and calcium hydroxide. The crack deviated around anhydrous cores in all but a few instances. This suggests that crack growth proceeded through the hydrated mass by a collection of relatively weak links, i.e. C-S-H with high micro porosity and preferentially oriented calcium hydroxide, except in a small number of instances where the local structure prevented this.

Examination of this specific material has provided a number of insights into the interaction of cracks with microstructure, and it also suggests a great deal of further work using this technique. The present work has suggested that improvements in the strength of HCP could be achieved by alterations in the microstructure of the hydrates, which are responsible for the bonding in HCP and therefore its strength. These improvements will be a decrease in the micro porosity of C-S-H, and an alteration in the microstructure of calcium hydroxide to prevent large expanses susceptible to basal cleavage.

A number of techniques have been used for improving the strength of HCP: lower w/c ratio (Grudemo, 1979), which results in a lower micro porosity C-S-H, and by reducing the water-filled space reduces

the possible extent of calcium hydroxide crystallites; increased degree of hydration by increasing cement fineness (Yudenfreund et al, 1972), which again decreases micro porosity in C-S-H; and hot-pressing (Roy & Gouda, 1973), which combines a decrease in micro porosity, a removal of large calcium hydroxide crystallites, and a high proportion of unhydrated material. In all of these cases microscopical examination was limited to examination of fracture surfaces. While fracture surfaces are ideal for examining morphology, it must be remembered that when produced by slow fracture, the surfaces show the weakest path, and other measurements [degree of hydration, quantitative X-ray analysis, porosimetry] which characterise the bulk microstucture give no information about the distribution of components. On the other hand polished surfaces are representative of the structure, and image analysis (Scrivener et al, 1985) allows quantitative assessment of the amounts and distribution of anhydrous material and calcium hydroxide, and by implication C-S-H. Extension of the examination of polished surfaces to include introduced cracks can provide a quantitative measure of the microstructural components involved in fracture, and by comparison with the uncracked microstructure should provide an insight into the possible methods of improving the strength of HCP.

Specific work which should be undertaken is the examination of the variation in microstructure and crack path with age and w/c ratio. The strength of HCP is known to increase with increasing age and decreasing w/c ratio, because of a decrease in overall porosity. However, it is also known that a transition from a predominantly C-S-H to a C-S-H and calcium hydroxide fracture path occurs, at different ages for different w/c ratios. This transition should be relatively easy to detect in the microstructure of introduced cracks in polished surfaces, and, because it will be obvious, it may be possible to detect variations in the structure of C-S-H, which at present are not identifiable. Beyond this the technique could be used to characterise the modifications in microstructure which result in an increase in strength.

A number of other high strength cement based materials have been produced in which small amounts of strong hydrate bond very strong anhydrous cores, so that both hydrate and anhydrous material are significant contributors to strength. Hot-pressing may be regarded as an example of this, but more interesting are recent developments in which the hydrates are modified by either, the addition of long-chain

polymers ["MDF" (Birchall et al, 1981)], or very fine silica [0.1um-"DSP" (Hjorth, 1983)]. Examination of these materials, particularly crack paths within them, may also provide information on possible mechanisms of improving the strength of more conventional HCP.

HCP is primarily used in concrete, and the examination of polished sections of concrete could provide the same type of information about concrete, particularly methods of improving its mechanical properties. In the case of concrete the main area of interest should initially be the aggregate/matrix bond, rather than the HCP, because it is in this region that the characteristic microcracking associated with concrete failure is nucleated. It has been suggested that the bond material often responsible for microcrack nucleation is calcium hydroxide. The examination of introduced cracks in polished sections of concrete could easily confirm this suggestion. More fruitfully, introduced cracks could identify those features of concrete, and in particular high strength concrete, which prevent bond failure. Subsequent to examination of the aggregate/matrix bond, the possible improvements in HCP could be applied to concrete.

7B SUBCRITICAL CRACK GROWTH IN HCP

Measurement of subcritical crack growth in HCP by the variation in the critical stress intensity of single edge-notched beams with loading rate provided a result [subcritical crack growth parameter =27] which is believed to be valid for prediction of specimen lifetime under sustained tensile load.

The subcritical crack growth data obtained by load relaxation in double torsion plates was not regarded as a valid measurement of the materials properties. The reasons for this are probably two-fold, the first is the over large influence that inhomogeneities have on load relaxation measurements, and the second is the indication that the double torsion specimens became more susceptible to creep, and as a result more resistant to crack growth, as crack growth occured. The first of the reasons was expected from other researchers work, and the reason for using two different methods to determine the subcritical crack growth parameter was to confirm this expectation. It was not possible to quantify the effect of the two reasons for error, however, it is believed that the second reason, the increasing resistance of the specimen to crack growth was at least as significant as the first.

As load relaxation in double torsion plates is much the easiest

way of determining the subcritical crack growth parameter it is believed that further work on subcritical crack growth in HCP should be done to determine a specimen shape which does not have a variable crack growth resistance, by testing a number of double torsion plates of different shape. Subsequent to this it should be possible to determine the effect of inhomogeneities on the measurement of the subcritical crack growth parameter, which if still significant will unfortunately discount this method of testing for lifetime predictions. The determination of stress corrosion processes, by performing load relaxation experiments in different environments is unlikely to be influenced by the effect of inhomogeneities, unless the environment significantly alters the resistance to crack growth of the inhomogeneities relative to the bulk.

The initial intention of relating microstructure to mechanical properties, in particular subcritical crack growth, has become somewhat overshadowed by the difficulties involved in the load relaxation measurements, but it is believed to be worthwhile to continue examining subcritical crack growth, hopefully by load relaxation in double torsion plates, in particular to determine the mechanisms of stress corrosion.

7C COMPUTING

The use of computers to acquire and process load relaxation data proved to be indispensable. Without the speed of calculation which the computer provided the calculation [and re-calculation after the adjustment of the background correction] would have been increased the amount of time spent on calculation considerably. This allowed a large number of V-K curves to be determined which made the indications of errors more obvious.

The computer programs were all succesful, although a number of minor alterations were necessary once the testing program had begun. The success of the programs, and the relative ease of programming suggest that a computer should be used to control the testing machine, as well as log data from it. It would be relatively simple to write specific programs which could perform the whole series of measurements [compliance, background and load relaxation] necessary for subcritical crack growth measurements. The attempt to measure the effect of repeated loading up to the point at which rapid crack growth occured was unsuccesful because it required rapid unloading of the specimen once crack growth had begun. This task could probably

be better controlloed by a computer, which would be better at detecting non-linearity in the load deflection curve and could activate changes in loading extremelt quickly.

The above suggestions for control of the testing machine are specific ideas which would involve communication between testing machine and computer only. More generally, a basic program which allows the user to "program" the testing machine and log data, directly from the testing machine and possibly a number of other outputs [e.g. strain gauges, temperature sensors etc.], is not unreasonable.

APPENDIX 1 - CHARACTERISATION OF THE ORDINARY PORTLAND CEMENT USED THROUGHOUT THIS WORK

AI Characterisation techniques

The cement used throughout this project was an Ordinary Portland Cement [OPC] supplied to Imperial College Department of Civil Engineering in batches of 6 tonnes from Blue Circle Industries plc. As the cement was supplied in batches, detailed chemical analyses were not regarded as worthwhile.

The cement was characterised by a number of qualitative techniques: isothermal conduction calorimetry; compressive strength measurements at 7 and 28 days; and microstructural examination.

AI.i Isothermal conduction calorimetry

Isothermal conduction calorimetry measures the variation in heat output during thr hydration of cement. The heat is derived fron the hydration reactions, and has been used to characterise the hydration of cement by a number of workers (Pratt & Ghose, 1983).

In the present work the cement produced a "normal" calorimeter curve (see figure A1.1), i.e. an initial high heat output [peak 1] followed by an induction period of a few hours, during which only a small amount of heat is given out, followed in turn by a renewed high heat output [peak 2] which includes a small shoulder [peak 3]. This typical characteristic confirmed the expectation that the cement was a typical OPC. The slightly lower than "normal" height of peak 2 suggests that a small amount of prehydration may have occured.

AI.ii Compressive strength measurements

The compressive strength of 22mm cubes, made from Double Torsion plates, was measured at 7 and 28 days for a single casting. The measured strengths of $38MNm^{-2}$ [7 days] and $58MNm^{-2}$ [28 days] compare favourably to other values at these ages (Bye, 1983).

AI.iii Microstructural examination

Characterisation of the microstructure of hardened cement paste is well developed in this research group (Dalgleish et al, 1980; Pratt & Ghose, 1983; Scrivener, 1984). Examination of fracture surfaces, of pastes ranging in age from 7 to 50 days, and more beneficially 28 day old polished surfaces has shown all the features

expected in a typical cement paste, and an absence of anything unfamiliar. At 28 days, polished surfaces show that, C_3S and C_3A have reacted strongly, and that there are significant amounts of these phases remaining, together with C_2S and C_4AF.

AII Characteristics of the OPC used

The above characterisation techniques have shown that the cement used throughout this work was a typical OPC. The presence of lumps in some of the batches used for the casting of the Double Torsion plates which provided the bulk of the results presented was unfortunate, but is not regarded as having significantly altered the properties of the HCP produced from it.

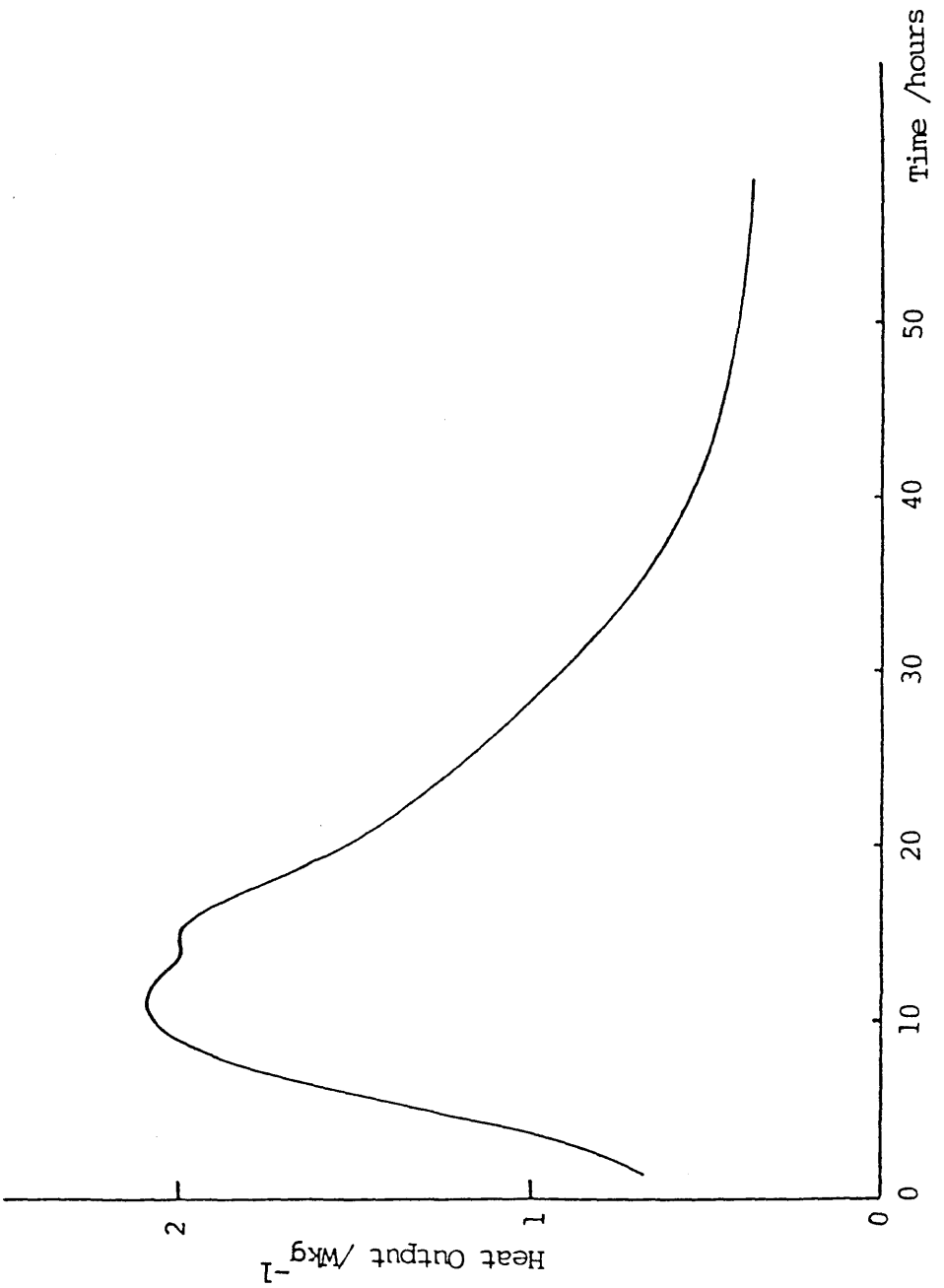


Figure A1.1 Isothermal calorimeter output for hydrating cement.

APPENDIX 2 - COMPUTER PROGRAMS AND FLOWCHARTS

RELMEAS-Acquires load relaxation data.

BACK-Creates a background correction file from a background relaxation measurement.

BACKOFF-Corrects a load-relaxation file for background relaxation.

ALL-Calculates stress intensity, crack velocity and subcritical crack growth parameter.

PROGRAM LISTING:

RELMEAS

```
10  ONERR  GOTO 60000
20  HIMEM: 38400
30 D$ =  CHR$ (4):B$ =  CHR$ (7):
     SL$ = "═══════════
     ═══════════"
40 A =  - 16240:B =  - 16239:KB =
     - 16384:KC =  - 16368:C = 2
     56:K% = 10240:L = 0
50 Q = 3000: DIM L%(Q),C(6)
60  TEXT : HOME : SPEED= 255: VTAB
     5: PRINT "CATALOG OF DATA DI
     SC": PRINT D$;"CATALOG,D2"
70  PRINT : INVERSE : PRINT "WHAT
      IS THE RELAXATION FILENAME?
     " SPC( 48): NORMAL : INPUT "
     REL ";Z$:Z$ = "REL " + Z$
80 O$ = D$ + "OPEN" + Z$:C$ = D$ +
     "CLOSE" + Z$:A$ = D$ + "APPE
     ND" + Z$:R$ = D$ + "READ" +
     Z$:W$ = D$ + "WRITE" + Z$:
90  HOME : VTAB 5: INVERSE : PRINT
     "ENTER SPECIMEN PARAMETERS
                    " SPC( 40): NORMAL
     : PRINT
100  PRINT  SPC( 11)"LOAD RANGE(k
     N) ": PRINT  SPC( 16)"WIDTH(
     mm) ": PRINT  SPC( 11)"MOMEN
     T ARM(mm) ": PRINT  SPC( 12)
     "THICKNESS(mm) ": PRINT "THI
     CKNESS UNDER NOTCH(mm) "
110  PRINT " INITIAL CRACK LENGTH
     (mm)"
120  VTAB 8: FOR I = 1 TO 6: HTAB
     27: INPUT "";C(I): NEXT
130  HOME : VTAB 5: PRINT "BEFORE
      AND AFTER THE TEST THE 'ZER
     O'": PRINT "MUST BE CHECKED,
     THEREFORE": GOSUB 1000
140  HOME : VTAB 10: FLASH : PRINT
     "PRESS S WHEN YOU ARE READY
     TO START": NORMAL
150  IF  PEEK (KB) <  > 211 THEN
      GOTO 150
160  POKE KC,0: HOME : VTAB 10
170  PRINT  SPC( 10)"LOGGING HAS
     BEGUN": PRINT  SPC( 4)"PRESS
      'I' (SHIFT I) TO TRUNCATE"
180  PRINT : PRINT  SPC( 7)"0000
     DATA POINTS LOGGED"
190  FOR I = 0 TO Q: FOR J = 1 TO
     5: POKE A,L:L% = L% +  PEEK
     (A) +  PEEK (B) * C: FOR K =
     1 TO 2: NEXT : NEXT :L%(I) =
     L%:L% = 0
200  VTAB 13: HTAB (12 -  LEN ( STR$
     (I))): PRINT I: IF  PEEK (KB
     ) <  > 161 THEN  NEXT
210  IF I <  > Q + 1 THEN Q = I: HOME
     : POKE KC,0: VTAB 9: PRINT  SPC(
     10)"LOGGING TRUNCATED"
220  PRINT " DO YOU WANT VALUES D
     UMPED TO DISC?"
230  IF  PEEK (KB) = 206 THEN  POKE
     KC,0: GOTO 990
240  IF  PEEK (KB) <  > 217 THEN
     230
250  POKE KC,0: HOME : VTAB 5: PRINT
      SPC( 8)"FINAL ZERO CHECK": GOSUB
     1000
260  VTAB 10: PRINT  SPC( 40): VTAB
     10: PRINT  SPC( 8)"DUMPING T
     O DISC"
270  PRINT O$: PRINT W$: PRINT SL
     $: PRINT SL$: FOR I = 1 TO 6
     : PRINT C(I): NEXT : PRINT Q

280  FOR I = 0 TO Q: PRINT L%(I):
      NEXT
290  PRINT C$
990  END

1000  PRINT : PRINT  SPC( 5)"1.SE
     T ZERO LOAD": PRINT  SPC( 5)
     "2.PRESS 'Z' TO START CHECK"

1010  IF  PEEK (KB) <  > 218 THEN
     1010
1015 ZC = ZC + 1
1020  POKE KC,0: FOR I = 1 TO 25:
      POKE A,L:V = V +  PEEK (A) +
      PEEK (B) * C: NEXT :ZC%(ZC)
      = V / 5:V = 0
1030  IF ZC < 2 THEN  RETURN
1033  IF ZC%(1) = 0 AND ZC%(2) =
     0 THEN  RETURN
1035 ZC% = ZC%(1)
1040  IF (ZC%(2) - ZC%(1)) / (ZC%
     (2) + ZC%(1)) <  = .2 THEN Z
     C% = (ZC%(1) + ZC%(2)) / 2: RETURN
1050 ZB% = (ZC%(2) - ZC%(1)) / Q:
      IF ZB% < 0 THEN ZB% = ZB% +
     1
1060  PRINT ZB%,ZC%: RETURN
59990  END
60000  PRINT C$: PRINT Z$" IS CLO
     SED":ER =  PEEK (222):LI =  PEEK
     (218) + 256 *  PEEK (219): PRINT
     : PRINT "ERROR DETECTED ON L
     INE ";LI: PRINT B$: PRINT "T
     YPE";ER
```

PROGRAM LISTING:

RELMEAS

```
10  ONERR  GOTO 60000
20  HIMEM: 38400
30 D$ =  CHR$ (4):B$ =  CHR$ (7):
     SL$ = "═══════════════════
     ═══════════════"
40 A =  - 16240:B =  - 16239:KB =
      - 16384:KC =  - 16368:C = 2
     56:K% = 10240:L = 0
50 Q = 3000: DIM L%(Q),C(6)
60  TEXT : HOME : SPEED= 255: VTAB
     5: PRINT "CATALOG OF DATA DI
     SC": PRINT D$;"CATALOG,D2"
70  PRINT : INVERSE : PRINT "WHAT
      IS THE RELAXATION FILENAME?
     " SPC( 48): NORMAL : INPUT "
     REL ";Z$:Z$ = "REL " + Z$
80 O$ = D$ + "OPEN" + Z$:C$ = D$ +
     "CLOSE" + Z$:A$ = D$ + "APPE
     ND" + Z$:R$ = D$ + "READ" +
     Z$:W$ = D$ + "WRITE" + Z$:
90  HOME : VTAB 5: INVERSE : PRINT
     "ENTER SPECIMEN PARAMETERS
                    " SPC( 40): NORMAL
     : PRINT
100  PRINT  SPC( 11)"LOAD RANGE(k
     N) ": PRINT  SPC( 16)"WIDTH(
     mm) ": PRINT  SPC( 11)"MOMEN
     T ARM(mm) ": PRINT  SPC( 12)
     "THICKNESS(mm) ": PRINT "THI
     CKNESS UNDER NOTCH(mm) "
110  PPRINT " INITIAL CRACK LENGTH
     (mm)"
120  VTAB 8: FOR I = 1 TO 6: HTAB
     27: INPUT "";C(I): NEXT
130  HOME : VTAB 5: PRINT "BEFORE
      AND AFTER THE TEST THE 'ZER
     O'": PRINT "MUST BE CHECKED,
     THEREFORE": GOSUB 1000
140  HOME : VTAB 10: FLASH : PRINT
     "PRESS S WHEN YOU ARE READY
     TO START": NORMAL
150  IF  PEEK (KB) <  > 211 THEN
      GOTO 150
160  POKE KC,0: HOME : VTAB 10
170  PRINT  SPC( 10)"LOGGING HAS
     BEGUN": PRINT  SPC( 4)"PRESS
      '!' (SHIFT 1) TO TRUNCATE"
180  PRINT : PRINT  SPC( 7)"0000
     DATA POINTS LOGGED"
190  FOR I = 0 TO Q: FOR J = 1 TO
     5: POKE A,L:L% = L% +  PEEK
     (A) +  PEEK (B) * C: FOR K =
     1 TO 2: NEXT : NEXT :L%(I) =
     L%:L% = 0
200  VTAB 13: HTAB (12 -  LEN ( STR$
     (I))): PRINT I: IF  PEEK (KB
     ) <  > 161 THEN  NEXT
210  IF I <  > Q + 1 THEN Q = I: HOME
     : POKE KC,0: VTAB 9: PRINT  SPC(
     10)"LOGGING TRUNCATED"
220  PRINT " DO YOU WANT VALUES D
     UMPED TO DISC?"
230  IF  PEEK (KB) = 206 THEN  POKE
     KC,0: GOTO 990
240  IF  PEEK (KB) <  > 217 THEN
     230
250  POKE KC,0: HOME : VTAB 5: PRINT
      SPC( 8)"FINAL ZERO CHECK": GOSUB
     1000
260  VTAB 10: PRINT  SPC( 40): VTAB
     10: PRINT  SPC( 8)"DUMPING T
     O DISC"
270  PRINT O$: PRINT W$: PRINT SL
     $: PRINT SL$: FOR I = 1 TO 6
     : PRINT C(I): NEXT : PRINT Q

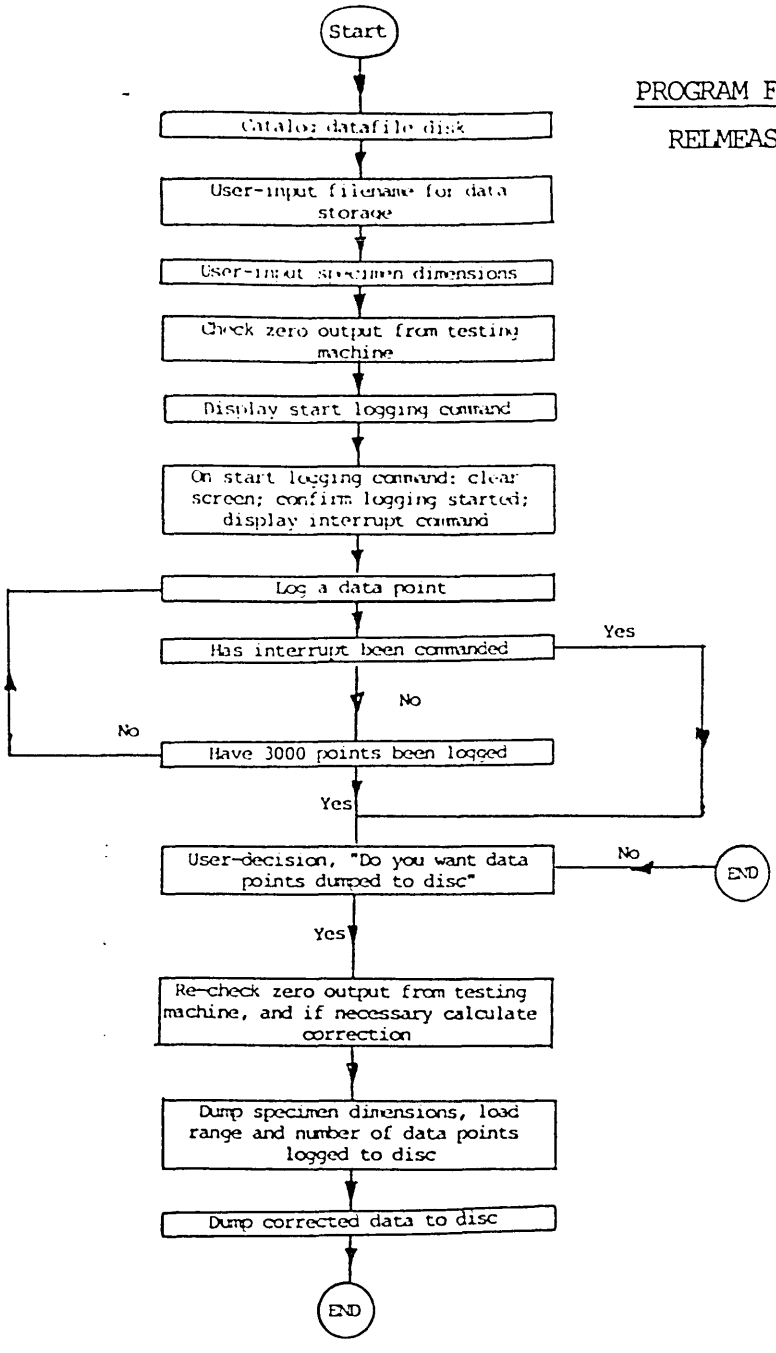
280  FOR I = 0 TO Q: PRINT L%(I):
      NEXT
290  PRINT C$
990  END

1000  PRINT : PRINT  SPC( 5)"1.SE
     T ZERO LOAD": PRINT  SPC( 5)
     "2.PRESS 'Z' TO START CHECK"

1010  IF  PEEK (KB) <  > 218 THEN
     1010
1015 ZC = ZC + 1
1020  POKE KC,0: FOR I = 1 TO 25:
      POKE A,L:V = V +  PEEK (A) +
      PEEK (B) * C: NEXT :ZC%(ZC)
      = V / 5:V = 0
1030  IF ZC < 2 THEN  RETURN
1033  IF ZC%(1) = 0 AND ZC%(2) =
     0 THEN  RETURN
1035 ZC% = ZC%(1)
1040  IF (ZC%(2) - ZC%(1)) / (ZC%
     (2) + ZC%(1)) <  = .2 THEN Z
     C% = (ZC%(1) + ZC%(2)) / 2: RETURN
1050 ZB% = (ZC%(2) - ZC%(1)) / Q:
      IF ZB% < 0 THEN ZB% = ZB% +
     1
1060  PRINT ZB%,ZC%: RETURN
59990  END
60000  PRINT C$: PRINT Z$" IS CLO
     SED":ER =  PEEK (222):LI =  PEEK
     (218) + 256 *  PEEK (219): PRINT
     : PRINT "ERROR DETECTED ON L
     INE ";LI: PRINT B$: PRINT "T
     YPE";ER
```

PROGRAM FLOWCHART:

RELMEAS



PROGRAM LISTING:

BACK

```
10  GOTO 1000
20  REM SMOOTHING & DISC DUMP
30 C1 = 3:C2 = 12:C3 = 17:C4 = 35

40  HOME : VTAB 5: HTAB 12: PRINT
     "SMOOTHING "
50  FOR S = 1 TO 3
60  VTAB 5: HTAB 22: PRINT S
70 I = 2:S1 = ( - 3 * L%(I - 2) +
     12 * L%(I - 1) + 17 * L%(I) +
     12 * L%(I + 1) - 3 * L%(I +
     2)) / 35
80 I = 3:S2 = ( - 3 * L%(I - 2) +
     12 * L%(I - 1) + 17 * L%(I) +
     12 * L%(I + 1) - 3 * L%(I +
     2)) / 35
90 N = Q - J: FOR I = 4 TO N - 3:
     S3 = ( - C1 * L%(I - 2) + C2
      * L%(I - 1) + C3 * L%(I) +
     C2 * L%(I + 1) - C1 * L%(I +
     2)) / C4:L%(I - 2) = S1:S1 =
     S2:S2 = S3: NEXT
100 L%(N - 4) = S2:L%(N - 3) = S3

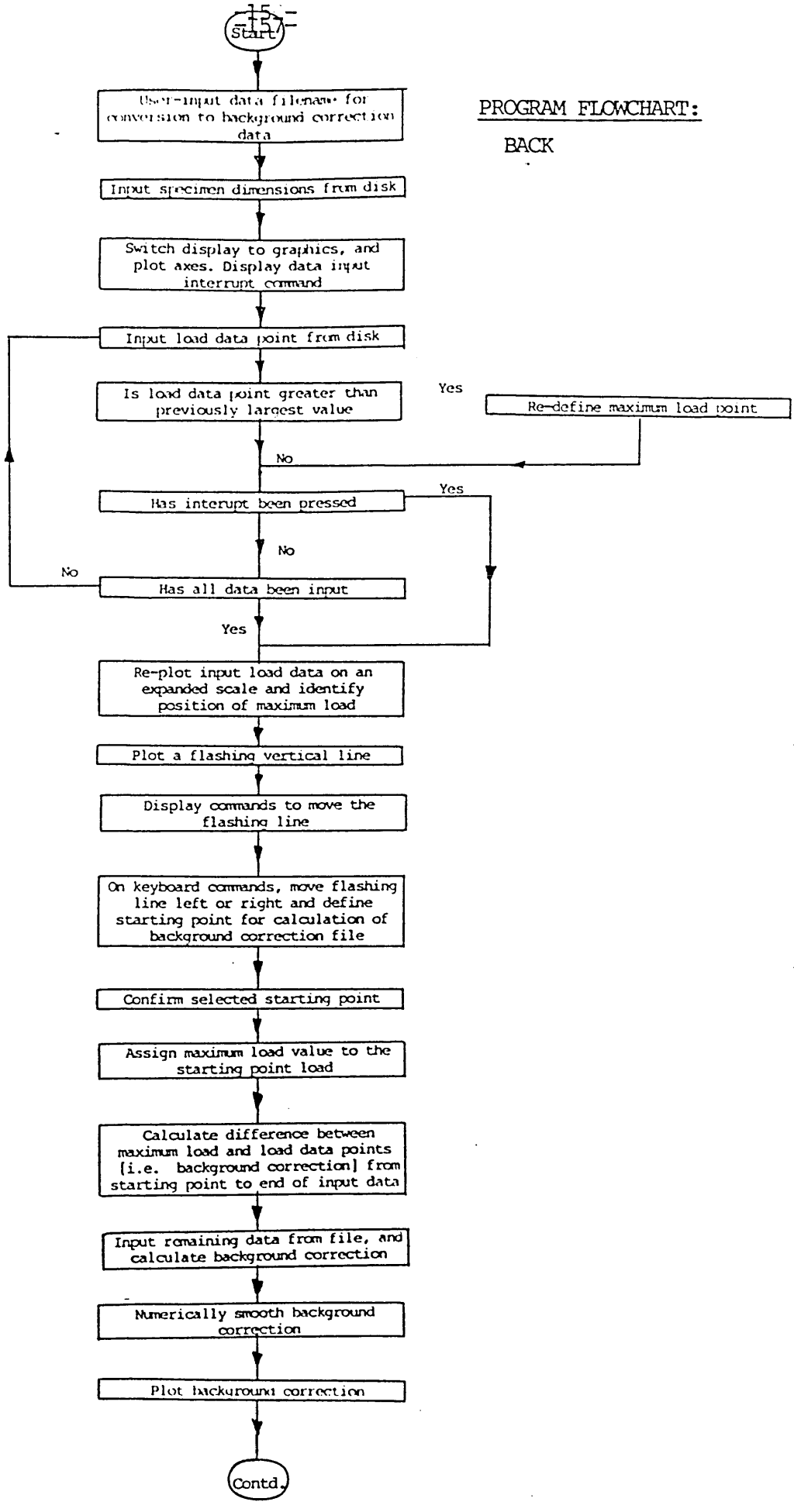
110  NEXT
500  PRINT D$;"DELETE";Z$: PRINT
     O$"X": PRINT W$"X": PRINT SM
     %: PRINT N: FOR I = 0 TO N: PRINT
     L%(I): NEXT : PRINT C$"X"
999  END
1000  ONERR  GOTO 60000
1010  LOMEM: 16384
1020  TEXT : HOME : SPEED= 255
1060 SA% = 16384:DV = 256:C = 256
     :D = 20480
1070 D$ =  CHR$ (4):B$ =  CHR$ (7
     ):KB =  - 16384:KC =  - 1636
     8
1080  REM ************************
     **
1090  PRINT "CATALOG OF FILES": PRINT
     D$;"CATALOG,D2": PRINT : INPUT
     "ENTER FILENAME:REL B";Z$:Z$
      = "REL B" + Z$
1110  REM ************************
     **
1120 O$ = D$ + "OPEN" + Z$:C$ = D
     $ + "CLOSE" + Z$:W$ = D$ + "
     WRITE" + Z$:R$ = D$ + "READ"
      + Z$: IF Z$ = ZB$ THEN  RETURN

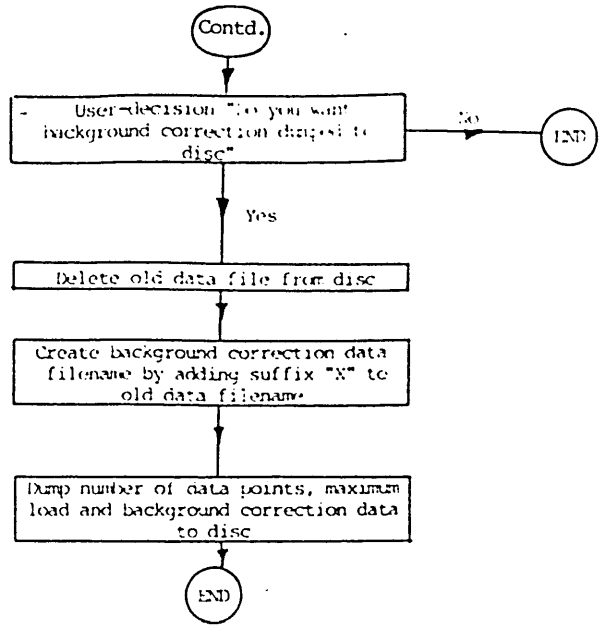
1130  REM ************************
     **
1140  HGR : HCOLOR= 7: HPLOT 0,0 TO
     0,150: HPLOT  TO 250,150
1150  HOME : VTAB 21: PRINT "PRES
     S '1' TO TRUNCATE PLOT"
1160  PRINT O$: PRINT R$: INPUT J
     $: INPUT J$: INPUT LR: INPUT
     WW: INPUT WM: INPUT TT: INPUT
     TN: INPUT NN: INPUT Q
1168  DIM L%(Q)
1170  FOR I = 0 TO Q: INPUT L
1180  IF L > LM% THEN LM% = L:NM =
     0:NM(NM) = I: GOTO 1200
1190  IF L = LM% THEN NM = NM + 1
     :NM(NM) = I
1200  HPLOT 250 * I / Q,150 - (15
     0 * L / D)
1210 N = I
1215 L%(I) = L
1220  IF  PEEK (KB) <  > 161 THEN
      NEXT
1230  POKE KC,0
1240  REM ************************
     *
1250  HGR : HPLOT 0,0 TO 0,150: HPLOT
     0,150 TO 250,150
1260  FOR I = 0 TO N: HPLOT 250 *
     I / N,150 - (150 * L%(I) / L
     M%)
1270  NEXT
1280  REM ************************
     *
1290  FOR I = 0 TO NM: HPLOT 250 *
     NM(I) / N,0 TO 250 * NM(I) /
     N,150: NEXT
1300 NM$ = "THIS IS THE MAXIMUM":
      IF NM > 0 THEN NM$ = "THESE
      ARE THE MAXIMA"
1310  VTAB 21: PRINT NM$
1320  REM ************************
     *
1330  PRINT "USE ARROW KEYS <- ,
     -> TO IDENTIFY       STARTING
      POINT,AND 'S' TO SELECT IT"
1340 J =  INT (N / 2)
1350  FOR I = 0 TO NM: IF J = NM(
     I) THEN CS = 0: GOTO 1370
1360  NEXT :CS = 7
1370  FOR I = 0 TO 7 STEP 7: HCOLOR=
      ABS (CS - I): HPLOT J * 250
      / N,0 TO J * 250 / N,150: NEXT

1380 PK =  PEEK (KB): IF PK < 128
      THEN 1350
1390  HCOLOR= 7: HPLOT 250 * J /
     N,150 - (150 * L%(J) / LM%)
1400  POKE KC,0: IF PK = 211 THEN
     1470
1410  IF PK = 149 THEN J = J + 1
1420  IF PK = 136 THEN J = J - 1
1430  IF J < 0 THEN J = 0
1440  IF J > N THEN J = N
1450  GOTO 1350
1460  REM ************************
     *
1470  FOR I = 0 TO NM: HCOLOR= 0:
     X = 250 * NM(I) / N: HPLOT X
     ,0 TO X,150: HCOLOR= 7: HPLOT
     X,150 - (150 * L%(NM(I)) / L
     M%): NEXT
1480  HPLOT 250 * J / N,0 TO 250 *
     J / N,150
1490  HOME : VTAB 21: PRINT "THIS
      IS THE STARTING POINT": PRINT
     "PRESS 'A' TO ACCEPT IT AND
     CONTINUE        OR 'C' TO CH
     ANGE IT"
1500  IF  PEEK (KB) = 193 THEN  POKE
     KC,0: GOTO 1540
1510  IF  PEEK (KB) = 195 THEN  POKE
     KC,0: GOTO 1370
1520  GOTO 1500
1530  REM ************************
     *
1540  TEXT : HOME : VTAB 5: HTAB
     11: PRINT "LOADING FROM DISC
     "
1550 SM% = L%(J)
1560  HIMEM: 38400
1570  FOR I = J TO N:L%(I - J) =
     SM% - L%(I)
1580  NEXT
1590  IF N = Q THEN 20
1600  FOR I = N + 1 TO Q: PRINT R
     $: INPUT L%:L%(I - J) = SM% -
     L%
1620  NEXT
1630  GOTO 20
59999  END
60000 ER =  PEEK (222):LI =  PEEK
     (218) +  PEEK (219) * 256
60010  NOTRACE
60020  PRINT C$: PRINT Z$;" IS CL
     OSED": PRINT "TYPE ";ER;" ER
     ROR ON LINE ";LI
```

PROGRAM FLOWCHART:

BACK




Contd.
User-decision "Do you want background correction data to disc"
No
END
Yes
Delete old data file from disc
Create background correction data filename by adding suffix "X" to old data filename
Dump number of data points, maximum load and background correction data to disc
END

PROGRAM LISTING:

BACKOFF

```
10  ONERR  GOTO 60000
20  HIMEM: 38400
30  LOMEM: 16384
40 D = 20480:KB =  - 16384:KC =  -
    16368
50 D$ =  CHR$ (4):B$ =  CHR$ (7):
    KB =  - 16384:KC =  - 16368
60  TEXT : HOME
70  PRINT "CATALOG OF FILES": PRINT
    D$;"CATALOG,D2": PRINT : INPUT
    "ENTER BACKGROUND FILENAME:R
    EL B";Z$:ZB$ = "REL B" + Z$:
     INPUT "ENTER RELAXATION FIL
    ENAME:REL ";Z$:ZR$ = "REL " +
    Z$
1000  HOME : VTAB 21: PRINT "LOAD
     RELAXATION PLOT.       PRES
    S '!' TOTRUNCATE PLOT, AND S
    ELECT STARTING POINT"
1010 Z$ = ZR$: GOSUB 5000
1020  HGR : HCOLOR= 3: HPLOT 0,0 TO
    0,150 TO 250,150 TO 250,0 TO
    0,0
1030  PRINT O$: PRINT R$: INPUT J
    $: INPUT J$: INPUT LR: INPUT
    WW: INPUT WM: INPUT TT: INPUT
    TN: INPUT NN: INPUT Q
1040  DIM L%(Q)
1050  FOR I = 0 TO Q: INPUT L
1060  IF L > LM% THEN LM% = L:NM =
    0:NM(NM) = I: GOTO 1080
1070  IF L = LM% THEN NM = NM + 1
    :NM(NM) = I
1080  HPLOT 250 * I / Q,150 - (15
    0 * L / D)
1090 N = I
1100 L%(I) = L
1110  IF  PEEK (KB) <  > 161 THEN
     NEXT
1120  POKE KC,0
1130  REM ********************
    *
1140  HOME
1150  HGR : HPLOT 0,0 TO 0,150 TO
    250,150
1160  FOR I = 0 TO N: HPLOT 250 *
    I / N,150 - (150 * L%(I) / L
    M%)
1170  NEXT
1180  REM ********************
    *
1190  FOR I = 0 TO NM: HPLOT 250 *
    NM(I) / N,0 TO 250 * NM(I) /
    N,150: NEXT
1200 NM$ = "THIS IS THE MAXIMUM":
     IF NM > 0 THEN NM$ = "THESE
     ARE THE MAXIMA"
1210  VTAB 21: PRINT NM$
1220  REM ********************
    *
1230  PRINT "USE ARROW KEYS <- ,
    -> TO IDENTIFY      STARTING
     POINT,AND 'S'TO SELECT IT"
1240 J =  INT (N / 2)
1250  FOR I = 0 TO NM: IF J = NM(
    I) THEN CS = 0: GOTO 1270
1260  NEXT :CS = 7
1270  FOR I = 0 TO 7 STEP 7: HCOLOR=
     ABS (CS - I): HPLOT J * 250
     / N,0 TO J * 250 / N,150: NEXT

1280 PK =  PEEK (KB): IF PK < 128
     THEN 1250
1290  HCOLOR= 7: HPLOT 250 * J /
    N,150 - (150 * L%(J) / LM%)
1300  POKE KC,0: IF PK = 211 THEN
    1370
1310  IF PK = 149 THEN J = J + 1:
     HPLOT 250 * (J - 1) / N,150

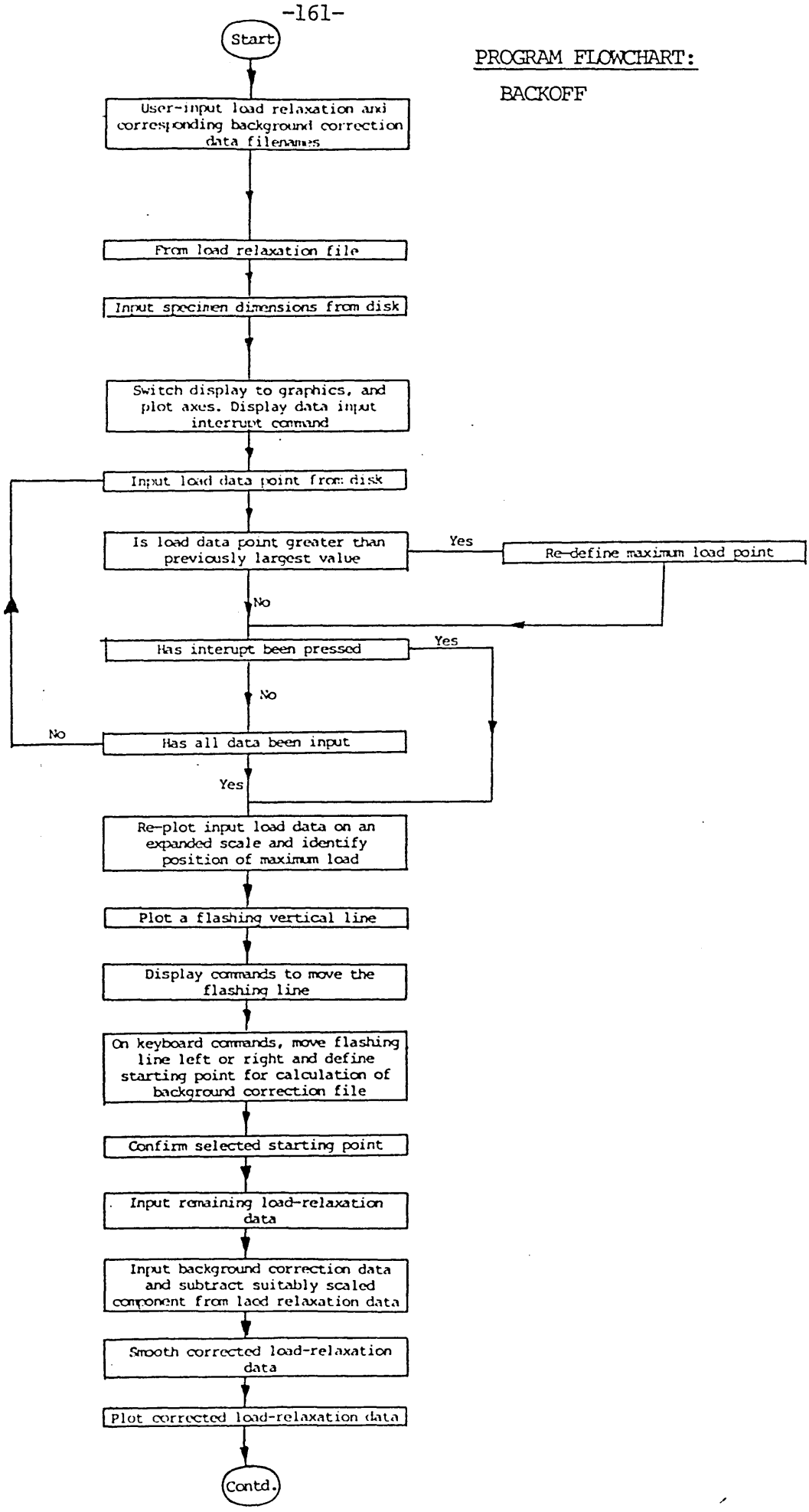
1320  IF PK = 136 THEN J = J - 1:
     HPLOT 250 * (J + 1) / N,150
1330  IF J < 0 THEN J = 0
1340  IF J > N THEN J = N
1350  GOTO 1250
1360  REM ********************
    *
1370  FOR I = 0 TO NM: HCOLOR= 0:
    X = 250 * NM(I) / N: HPLOT X
    ,0 TO X,150: HCOLOR= 7: HPLOT
    X,150 - (150 * L%(NM(I)) / L
    M%): NEXT
1380  HPLOT 250 * J / N,0 TO 250 *
    J / N,150
1390  HOME : VTAB 21: PRINT "THIS
     IS THE STARTING POINT": PRINT
     "PRESS 'A' TO ACCEPT IT AND
    CONTINUE        OR 'C' TO CH
    ANGE IT"
1400  IF  PEEK (KB) = 193 THEN  POKE
    KC,0: GOTO 1440
1410  IF  PEEK (KB) = 195 THEN  POKE
    KC,0: GOTO 1270
1420  GOTO 1400
1430  REM ********************
    *
1440  TEXT
1450 RM% = L%(J)
1460  FOR I = J TO N:L%(I - J) =
    L%(I): NEXT
1470  IF N = Q THEN 1510
1480  HOME : VTAB 5: HTAB 8: PRINT
    "INPUTTING REMAINING DATA"
1490  FOR I = N + 1 TO Q: PRINT R
    $: INPUT L%(I - J)
1500  NEXT
1510 Z$ = ZB$: GOSUB 5000
1520  HOME : VTAB 5: HTAB 8: PRINT
    "LOADING BACKGROUND DATA"
1530  PRINT O$: PRINT R$: INPUT B
    M%: INPUT BN
1540 RA = RM% / BM%:N = Q - J
2000  IF BN >  = N THEN  FOR I =
    0 TO N: INPUT BL%:L%(I) = L%
    (I) + RA * BL%: NEXT : PRINT
    C$: GOTO 3000
2010  FOR I = 0 TO BN: INPUT BL%:
    L%(I) = L%(I) + RA * BL%: NEXT
    : PRINT C$: FOR I = BN + 1 TO
    Q:L%(I) = L%(I) + RA * BL%: NEXT

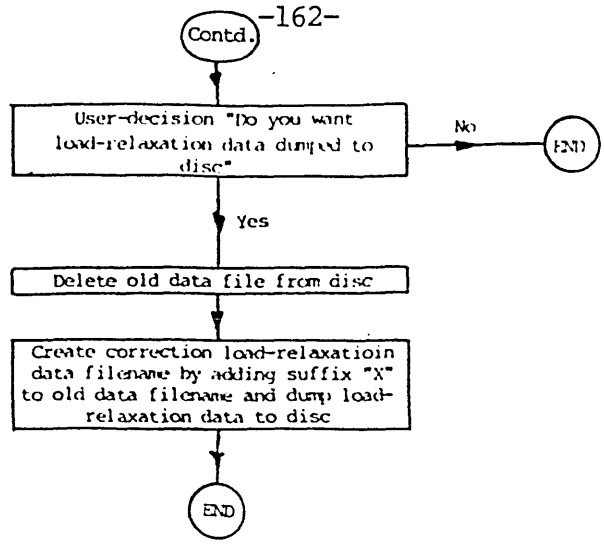
3000  REM SMOOTHING:DISC DUMP
3010 C1 = 3:C2 = 12:C3 = 17:C4 =
    35
3020  HOME : VTAB 5: HTAB 12: PRINT
    "SMOOTHING "
3030  FOR S = 1 TO 3
3040  VTAB 5: HTAB 22: PRINT S
3050 I = 2:S1 = ( - 3 * L%(I - 2)
     + 12 * L%(I - 1) + 17 * L%(
    I) + 12 * L%(I + 1) - 3 * L%
    (I + 2)) / 35
3060 I = 3:S2 = ( - 3 * L%(I - 2)
     + 12 * L%(I - 1) + 17 * L%(
    I) + 12 * L%(I + 1) - 3 * L%
    (I + 2)) / 35
3070  FOR I = 4 TO N - 3:S3 = ( -
    C1 * L%(I - 2) + C2 * L%(I -
    1) + C3 * L%(I) + C2 * L%(I +
    1) - C1 * L%(I + 2)) / C4:L%
    (I - 2) = S1:S1 = S2:S2 = S3
    : NEXT
3080 L%(N - 4) = S2:L%(N - 3) = S
    3
3090  NEXT
3100  HOME : VTAB 21: PRINT "PLOT
    TING 'PURE RELAXATION' !!"
3110  HGR : HPLOT 0,0 TO 0,150 TO
    250,150 TO 250,0 TO 0,0
3120  FOR I = 1 TO N STEP  INT (N
     / 250 + 1):X = 250 * I / N:
    Y = (LM% - L%(I)) / 10
3130  IF (X > 0 AND X < 250) AND
    (Y > 0 AND Y < 150) THEN  HPLOT
    X,Y
3140  NEXT
3150  HOME : VTAB 21: PRINT "DO Y
    OU WANT THIS DATA DUMPED TO
    DISC?  "
3160  IF  PEEK (KB) = 206 THEN  POKE
    KC,0: END
3170  IF  PEEK (KB) = 217 THEN  POKE
    KC,0: GOTO 3190
```

```
3180  GOTO 3160
3190 ZS = ZR$ + "X": GOSUB 5000: PRINT
     DS"DELETE"ZR$: PRINT OS: PRINT
     WS: PRINT LR: PRINT WW: PRINT
     WM: PRINT TT: PRINT TN: PRINT
     NN: PRINT N: FOR I = 0 TO N:
      PRINT LN(I): NEXT : PRINT C
     $
4990  END
5000 OS = DS + "OPEN" + ZS:CS = D
     $ + "CLOSE" + ZS:WS = DS + "
     WRITE" + ZS:RS = DS + "READ"
      + ZS: RETURN
59999  END
60000 ER =  PEEK (222):LI =  PEEK
     (218) +  PEEK (219) * 256
60020  PRINT CS: PRINT ZS;" IS CL
     OSED": PRINT "TYPE ";ER;" ER
     ROR ON LINE ";LI
```

PROGRAM FLOWCHART:

BACKOFF




Contd.
User-decision "Do you want load-relaxation data dumped to disc"
No
END
Yes
Delete old data file from disc
Create correction load-relaxatioin data filename by adding suffix "X" to old data filename and dump load-relaxation data to disc
END

PROGRAM LISTING:

ALL

```
10  ONERR  GOTO 60000
20  HIMEM: 38400
30  LOMEM: 16400
40 D$ =  CHR$ (4):B$ =  CHR$ (7):
     KB =  - 16384:KC =  - 16368
50 D = 40960
60 SP$ = "
                                  "
70  TEXT : HOME : SPEED= 255:TI =
     .12
80  PRINT "CATALOG OF FILES": PRINT
     D$;"CATALOG,D2": PRINT : INPUT
     "ENTER FILENAME  REL ";Z$:ZK
     $ = "KV " + Z$:Z$ = "REL " +
     Z$
90 O$ = D$ + "OPEN" + Z$:C$ = D$ +
     "CLOSE" + Z$:A$ = D$ + "APPE
     ND" + Z$:R$ = D$ + "READ" +
     Z$:W$ = D$ + "WRITE" + Z$:
100  IF ZZ = 1 THEN  RETURN
110  HOME
120  PRINT O$: PRINT R$: INPUT LR
     : INPUT WW: INPUT WM: INPUT
     TT: INPUT TN: INPUT NL: INPUT
     Q: DIM L%(Q)
130  IF WW < 1 AND WM < 1 THEN 15
     0
140 WW = WW * 1E - 3:WM = WM * 1E
     - 3:TT = TT * 1E - 3:TN = T
     N * 1E - 3:NL = NL * 1E - 3
150 EPY = 1 - .6302 * (2 * TT / W
     W) + 1.2 * (2 * TT / WW) *  EXP
     ( - 3.14159 * WW / (2 * TT))
     :MU = .22
160  HOME : VTAB 21: PRINT "INPUT
     TING RELAXATION DATA FROM FI
     LE"
170  INPUT L%(0):LM% = L%(0):LI =
     LM% * LR / D
180  HGR : HCOLOR= 3: HPLOT 0,0 TO
     0,150 TO 250,150 TO 250,0 TO
     0,0
190 CX = 250 / Q:CY = 140 / LM%
200  FOR I = 1 TO Q: INPUT L: IF
     L > LM% THEN L%(I) = LM%: GOTO
     220
210 L%(I) = L
220 PC = PC + 1: IF PC = 5 THEN P
     C = 0: HPLOT CX * (I),L%(I) /
     (20 * SF)
230  NEXT : PRINT C$
240  REM *** SMOOTHING ***
250 C1 = 3:C2 = 12:C3 = 17:C4 = 3
     5
260  HOME : VTAB 21: PRINT "SMOOT
     HING RELAXATION DATA"
270  FOR S = 1 TO 2
280 I = 2:S1 = ( - 3 * L%(I - 2) +
     12 * L%(I - 1) + 17 * L%(I) +
     12 * L%(I + 1) - 3 * L%(I +
     2)) / 35
290 I = 3:S2 = ( - 3 * L%(I - 2) +
     12 * L%(I - 1) + 17 * L%(I) +
     12 * L%(I + 1) - 3 * L%(I +
     2)) / 35
300 N = Q: FOR I = 4 TO N - 3:S3 =
     ( - C1 * L%(I - 2) + C2 * L%
     (I - 1) + C3 * L%(I) + C2 *
     L%(I + 1) - C1 * L%(I + 2)) /
     C4:L%(I - 2) = S1:S1 = S2:S2
      = S3: NEXT
310 L%(N - 4) = S2:L%(N - 3) = S3

320  NEXT
330 NP = 50: IF Q < 250 THEN NP =
      INT (Q / 5)
340  HOME : VTAB 21: INVERSE : PRINT
     " ";: NORMAL : PRINT " DO YO
     U WANT V-K PAIRS CALCULATED
     AT  ";: INVERSE : PRINT " "
350  VTAB 22: PRINT " ";: NORMAL
     : PRINT " 1.LINEAR / 2.LOGAR
     ITHMIC INTERVALS    ";: INVERSE
     : PRINT " ": NORMAL
360 OL =  PEEK (KB) - 176: IF OL <
     1 OR OL > 2 THEN 360
370  POKE KC,0
380  HOME : VTAB 21: PRINT "HOW M
     ANY V-K CALCULATIONS DO YOU
     WANT?  ";: PRINT "(MAX. = ";
     NP;" ) ";: INPUT "";NP
390  DIM V(NP),K(NP),X(NP),Y(NP)
400  HOME : VTAB 21: PRINT "POINT
      NO.": PRINT "V=" SPC( 18)"K
     =": RETURN
410  IF OL = 2 THEN 490
420 ST% =  INT (Q / 4 / NP) + 1
430 LA =  INT ((Q - 4 * ST%) / NP
     )
440  FOR I = 0 TO NP:J = 2 * ST% +
     LA * I
450  GOSUB 1000
460  IF V > 0 AND K > 0 THEN V(NK
     ) = V:K(NK) = K: GOSUB 1500:
     NK = NK + 1
470  NEXT
480  GOTO 2000
490 LO = (Q - 5) ^ (I / (NP + I))

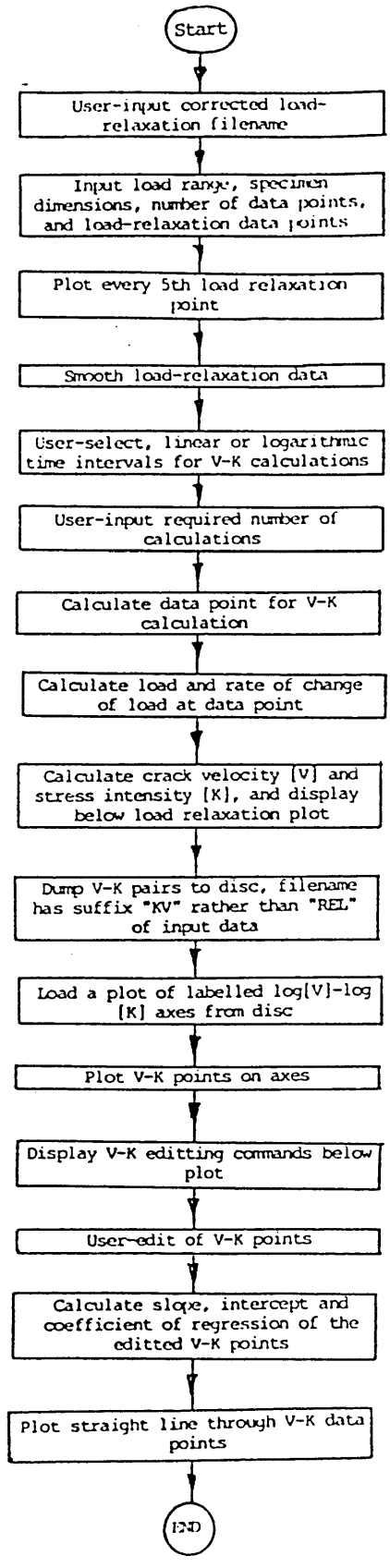
500  FOR I = 0 TO NP:J = 2 + LO ^
     I:ST% = (LO ^ I - LO ^ (I -
     1)) / 4 + 1
510  IF OJ = J THEN 550
520  GOSUB 1000
530  IF V > 0 AND K > 0 THEN V(NK
     ) = V:K(NK) = K: GOSUB 1500:
     NK = NK + 1
540 OJ = J
550  NEXT
560  GOTO 2000
900  FOR L = 1 TO 5:PO = J + (L -
     3) * ST%
910 P1 = L%(PO - 2):P2 = L%(PO -
     1):P3 = L%(PO)P4 = L%(PO + 1
     ):P5 = L%(PO + 2)
920 L(L) = ( - 3 * (P1 + P5) + 12
      * (P2 + P4) + 17 * P3) / 35

930  NEXT : GOTO 1020
1000  IF OL = 2 AND ST% > 3 THEN
      GOTO 900
1010  FOR L = 1 TO 5:L(L) = L%(J +
     (L - 3) * ST%): NEXT
1020 LL = (17 * L(3) + 12 * (L(2)
      + L(4)) - 3 * (L(1) + L(5))
     ) / 35
1030 LL = LL * LR / D
1040 DV = 12 * ST% * D * TI
1050 DL = L(1) - L(5) + 8 * (L(4)
      - L(2)):DL = LR * DL / DV
1060 V =  - NL * LI * DL / (LL *
     LL)
1070 K = LL * WM *  SQR (3 / ((1 -
     MU) * WW * (TT ^ 3) * TN * E
     PY))
1080  RETURN
1500  IF V(NK) <  = 1E - 2 THEN F
     V = 10
1510 VS$ =  STR$ (V(NK)): IF  LEN
     (VS$) <  = FV THEN VP$ = VS$
     : GOTO 1530
1520 VP$ =  LEFT$ (VS$,6): IF FV =
     10 THEN VP$ = VP$ +  RIGHT$
     (VS$,4)
1530  IF K(NK) <  = 1E - 2 THEN F
     K = 10
1540 KS$ =  STR$ (K(NK)): IF  LEN
     (KS$) <  = FK THEN KP$ = KS$
     : GOTO 1560
1550 KP$ =  LEFT$ (KS$,6): IF FK =
     10 THEN KP$ = KP$ +  RIGHT$
     (KS$,4)
1560  HTAB 11: VTAB 21: PRINT NK:
      HTAB 3: PRINT  LEFT$ (VP$ +
     SP$,10): VTAB  PEEK (37): HTAB
     23: PRINT  LEFT$ (KP$ + SP$,
     10)
1570  RETURN
```

```
2000  TEXT
2010 SK =  LOG (6 / 2):SV =  LOG
     (1E4):VM = 1E - 2:MV = 1E -
     6:KM = 600:MK = 200
2020  HOME : VTAB 5: PRINT "ORDER
     ING POINTS"
2030  FOR I = 1 TO NK / 2:KS = K(
     I):K(I) = K(NK + 1 - I):K(NK
      + 1 - I) = KS:VS = V(I):V(I
     ) = V(NK + 1 - I):V(NK + 1 -
     I) = VS: NEXT
2040 SF = 0: FOR I = 1 TO NK - 1:
      IF K(I) > K(I + 1) THEN SF =
     1:KS = K(I + 1):K(I + 1) = K
     (I):K(I) = KS:VS = V(I + 1):
     V(I + 1) = V(I):V(I) = VS
2050  NEXT : IF SF <  > 0 THEN 20
     40
2060  PRINT D$;"BLOADK-V AXES,D1"
     : POKE  - 16304,0: POKE  - 1
     6297,0
2070  FOR I = 1 TO NK
2080 X(I) = 279 * ( LOG (K(I) / M
     K)) / SK:Y(I) = 159 - (159 *
     ( LOG (V(I) / MV)) / SV)
2090  IF X(I) < 0 THEN X(I) = 0
2100  IF X(I) > 279 THEN X(I) = 2
     79
2110  IF Y(I) < 0 THEN Y(I) = 0
2120  IF Y(I) > 159 THEN Y(I) = 1
     59
2130  HPLOT X(I),Y(I)
2140  NEXT
2150  HOME : VTAB 21: PRINT "DO Y
     OU WANT TO EDIT THESE POINTS
     ?  (Y/N)"
2160  IF  PEEK (KB) = 217 THEN  POKE
     KC,0: GOTO 2350
2170  IF  PEEK (KB) = 206 THEN  POKE
     KC,0: GOTO 2190
2180  GOTO 2160
2190  HOME : VTAB 21: PRINT "CALC
     ULATING GRADIENT"
2200  FOR I = 0 TO NK
2210 KK =  LOG (K(I)) ^ 2 + KK:K1
      = K1 +  LOG (K(I)):KV = KV +
      LOG (K(I)) *  LOG (V(I)):V1
      = V1 +  LOG (V(I)):VV =  LOG
     (V(I)) ^ 2 + VV
2220  NEXT
2230 DEM = N * KK - K1 * K1:M = (
     N * KV - K1 * V1) / DEM
2240 CA = (N * KV - K1 * V1) / (N
      * KK - K1 * K1):CB = (KK *
     V1 - K1 * KV) / (N * KK - K1
      * K1)
2250 CR =  SQR ((N * KV - K1 * V1
     ) * (N * KV - K1 * V1) / ((N
      * KK - K1 * K1) * (N * VV -
     V1 * V1)))
2260  HOME : VTAB 21: PRINT "GRAD
     =";CA;" INTCPT=";CB: PRINT "
     COEFF OF REGRESSION = ";CR
2270 P(1,1) = KM:P(2,1) = MK:P(3,
     2) = VM:P(4,2) = MV
2280  FOR I = 1 TO 2:P(I,2) =  EXP
     (CB + CA *  LOG (P(I,1))):P(
     I + 2,1) =  EXP (( LOG (P(I +
     2,2)) - CB) / CA): NEXT
2290  FOR I = 1 TO 4:P1 = P(I,1):
     P2 = P(I,2): IF P1 >  = MK AND
     P1 <  = KM AND P2 >  = MV AND
     P2 <  = VM THEN  GOSUB 6000
2300  NEXT
2310  HPLOT XX(0),YY(0) TO XX(1),
     YY(1)
2320 ZZ = 1:Z$ = ZK$: GOSUB 90
2330  PRINT O$;",D1": PRINT W$: PRINT
     NK: FOR I = 1 TO NK: PRINT K
     (I): PRINT V(I): NEXT : PRINT
     C$
2340  END
2350  HOME : VTAB 21: PRINT "USE
     LEFT-RIGHT ARROW KEYS TO IDE
     NTIFY  POINTS TO BE DELETED
     , AND 'D' TO DELETE"
3010 KO =  PEEK (KB): POKE KC,0
3020  HCOLOR= 0: HPLOT X(PI),Y(PI
     ): FOR T = 1 TO 20: NEXT :
     HCOLOR= 3: HPLOT X(PI),Y(PI)
3030  IF KO <  > 136 AND KO <  >
     149 AND KO <  > 196 THEN 301
     0
3040  IF KO = 136 THEN  HCOLOR= 3
     : HPLOT X(PI),Y(PI):PP =  -
     1
3050  IF KO = 149 THEN  HCOLOR= 3
     : HPLOT X(PI),Y(PI):PP = 1
3060  IF KO = 196 THEN K(PI) =  -
     K(PI): HCOLOR= 0: HPLOT X(PI
     ),Y(PI)
3070 PI = PI + PP
3080  IF PI < 1 THEN PP = 1: FOR
     PI = 0 TO NK: IF K(I) < 0 THEN
      NEXT
3090  IF PI > NK THEN  GOTO 2190
3100  IF K(PI) < 0 THEN 3070
3110  GOTO 3010
6000 XX(PP) = 279 *  LOG (P1 / MK
     ) / SK:YY(PP) = 159 - 159 *
      LOG (P2 / MV) / SV:PP = PP +
     1: IF PP = 2 THEN 2310
6010  RETURN
59990  END
60000 ER =  PEEK (222):LI =  PEEK
     (218) +  PEEK (219) * 256
60010  PRINT B$: POKE 34,0
60020  PRINT C$: PRINT Z$;" IS CL
     OSED": PRINT "TYPE ";ER;" ER
     ROR ON LINE ";LI
```

PROGRAM FLOWCHART:

ALL



APPENDIX 3 - MECHANICAL PROPERTIES OF CALCIUM HYDROXIDE SINGLE CRYSTALS

Calcium hydroxide single crystals prepared [courtesy of Dr J Rhodes and Dr J Smart, University of Sheffield] from three different solutions: pure calcium hydroxide [designated type C1]; calcium hydroxide with colloidal silica [type C2]; and calcium hydroxide plus 0.175 molar ethanoic acid [type C3]. These crystals were of columnar hexagonal shape, with both the height and width of the order of 1-2mm. Attempts were made to measure the strength and elastic modulus of these crystals.

Strength of calcium hydroxide

The small size of the crystals precluded the use of any normal testing apparatus or specimen grips. After a number of less successful methods had been tried, the apparatus shown in figure A3.1 was settled upon. The crystal was glued to small glasss platens, made from cover slip glass. These glass platens were in turn attached to either a steel wire connected to a supporting stand on the upper side, or on the lower side, a small steel hook, onto which a loading beaker was attached. A load was applied to the crystal by filling the attached beaker with water until the crystal fractured, the load at failure being the weight of beaker, hook, glass platen and lower part of the crystal. The fracture surface area was measured on an Omnicon 3000 image analyser. The load, area and tensile strength of the crystals are given in table A3.1. There is obviously a large amount of scatter in the results, which electron microscopy suggested was due to pre-existing flaws in the crystals. A dye penetrant consisting of marker pen ink dissolved in methanol identified some relatively large flaws in the crystals (see table A3.2). However, substitution of the strength and flaw size measurements into the Griffith equation did not result in a consistent value of critcal stress intensity.

The scatter in the results is rather dissapointing, but in view of the small size, which make specimen handling very difficult, and the limitted availability crystals the results are useful as a very rough estimate of the strength and critical stress intensity of calcium hydroxide. The main source of error is that the specimens are unlikely to be loaded in pure tension across the basal plane, which in the highly anisotropic crystals is likely to lead to failure by shear along the basal plane. In future it would be of interest to measure

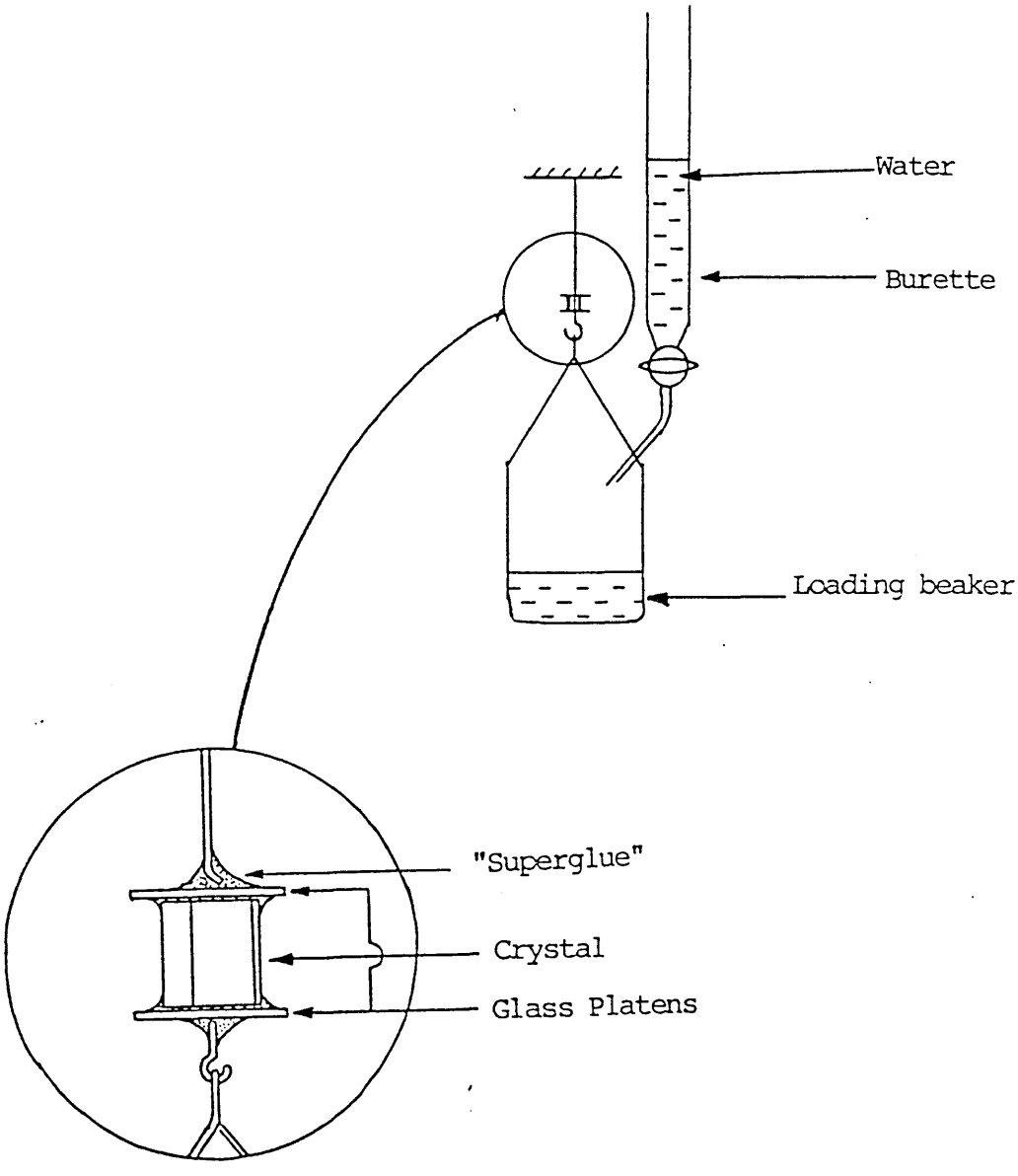


Figure A3.1 Loading arrangement for the measurement of strength of calcium hydroxide single crystals.

the strength parallel to the basal plane, which is expected to be relativley strong.

There appear to be some differences between the crystals produced from different solutions, but with such a small number of results it is by no means certain.

The significance of these results to HCP are that they give a very rough estimate of the expected strength of one of the major components. The behaviour of calcium hydroxide in HCP may be very different from that of single crystals, as calcium hydroxide is present as much smaller crystallites which may be intergrown with other calcium hydroxide crystallites with differently oriented basal planes and other components of HCP.

Table A3.1 Load at failure, cross sectional area and calculated tensile strength of calcium hydroxide crystals.

Specimen type	Fracture load /N	Cross-sectional Area /mm^2	Tensile Strength /MNm^{-2}
C1	0.76	0.92	0.82
	1.74	0.96	1.81
C2	1.16	0.85	1.36
	1.71	0.78	2.19
	2.14	1.54	1.40
	1.81	1.51	1.20
C3	3.89	3.72	1.02
	1.36	2.74	0.49
	0.83	1.62	0.51
	2.45	4.35	0.56
	2.93	2.63	1.11

Table A3.2 Strength, flaw size and calculated critical stress intensity

Specimen type	Tensile Strength /MNm^{-2}	Flaw size /um	Critical Stress Intensity /$MNm^{-3/2}$
C1	0.82	100	0.46
	1.81	63	0.81
C2	1.16	38	0.40
	1.71	42	0.62
C3	0.51	62	0.22
	0.56	79	0.28

APPENDIX 4 - PREDICTION OF SPECIMEN LIFETIME FROM SUBRCITICAL CRACK GROWTH MEASUREMENTS

The predictions of specimen lifetime under a sustained applied load are based on the integration of the of V-K curves, and at present the integrations have assumed Griffith type behaviour. While a tied-crack fracture process may better describe HCP, it is felt that the determination of failure predictions based on tied-crack models are not warranted until a particular fracture criterion can fully describe the behaviour of HCP.

V-K curves

The calculation of failure time [τ] from the slow crack growth parameter [n] and the V-K intercept [log(A)] for an applied load [σ] which results in an initial stress intensity [K_{1i}] is given by the relatively simple equation (Davidge et al, 1973),

$$\tau = \frac{2K_{1i}^{2-n}}{\sigma^2 Y^2 A[n-2]} \qquad \text{.....A4.1}$$

where Y is the crack geometry factor.

No predictions of lifetime were calculated from the values of n and log(A) determined from load-relaxation measurements, because the results were not regarded as worthwile descriptions of the properties of HCP.

The Variation in critical stress intensity with Load rate

The calculation of failure time from the variation in critical stress intensity is a modification of the calculation used by Pletka & Wiederhorn (1982).

The time to failure [τ] can be calculated for a component subjected to a constant applied stress, σ,

$$\tau = BS_i^{n-2}\sigma^{-n} \qquad \text{.....A4.2}$$

where S_i is the intrinsic strength of the material and B is a material constant. S_i is defined in terms of the size, a_i of the critical flaw that causes failure,

$$S_i = K_{1c}/[Y\sqrt{a_i}] \qquad .....A4.3$$

where K_{1c} is the critical stress intensity and Y is the crack geometry constant. The constant B is determined from intercept of a plot of the variation in strength [σ_f] with stressing rate [$\dot{\sigma}$].

$$\ln \sigma_f = \frac{1}{[n+1]} \{\ln [BS_i^{n-2}(n+1)] + \ln [\dot{\sigma}]\} \qquad .....A4.4$$

In the present work the subcritical crack growth parameter was determined from the variation in critical stress intensity [K_{1c}] with crosshead speed [$\dot{x}$]. These variables were converted to strength and stressing rate by suitable conversion factors.

$$\sigma_f = K_{1c}/[Y\sqrt{a}] \qquad .....A4.5 \text{ and}$$
$$\dot{\sigma} = 4.28 \times 10^6 \dot{x}/[Y\sqrt{a}] \qquad .....A4.6$$

The value of crack length, a was 9mm, and K_{1c} was taken as $450 kNm^{-3/2}$ [slightly above the value measured at the highest loading rate], and the value of Y was determined from the equation of Brown & Strawley (1969). [Using the above equation for the intrinsic strength, S_i was determined for these beams as $1.88 MNm^{-2}$]. 4.28×10^6 was an empirical conversion factor, determined from typical failure times, for conversion of crosshead speed to stress intensity rate.

The intercept so determined was equal to 0.530, which gives a value of the material constant B equal to 0.0139.

Using the simple relationship [A4.3] to determine the intrinsic strength [S_i] of beams containing edge notches of length 5, 1, 0.5 and 0.3mm and the value of B equal to 0.0139, the predicted lifetime was calculated for a number of applied loads, and plotted as a function of the flaw free strength of $15 MNm^{-2}$, suggested by the value which was deduced by Higgins & Bailey (1976).

REFERENCES

ALFORD, N. McN.
"A theoretical argument for the existence of high strength cement pastes", Cem. Concr. Res., 11, 605 (1981)

BACHE, H.H., IDORN, G.M., NEPPER-CHRISTENSON, P., NIELSEN, J.
"Morphology of calcium hydroxide in cement paste", Highways Research Board, Special Report 90, 154 (1966)

BALSHIN, M.Y.
"Relation of mechanical properties of powdered metals and their porosity and the ultimate properties of materials", Dokl. Adad. Nauk. SSR, 67, 831 (1949). Abstracted in Chem. Abs., 44, 2425f (1950)

BARENBLATT, G.I.
"The mathematical theory of equilbrium cracks in brittle fracture", Adv. App. Mech., 7, 55 (1962)

BARKER, A.P. BARNES, P.
"Characterisation of calcium hydroxide in set cements using some established and novel techniques", Brit. Ceram. Soc. Proceedings No. 36, "The chemistry and chemically-related properties of cement, Ed. F.P. Glasser", 25 (1984)

BARRICK, J.E. KROKOSKY, E.M.
"The effects of temperature and relative humidity on static strength of hydrated portland cement", J. Testing and Evaluation, 4, 61 (1976)

BASKARAN, S., BHADURI, S.B., HASSELMAN, D.P.H.
"Effect of crystallite size on subcritical crack growth and strain rate sensitivity of cordierite glass-ceramics", J. Am. Ceram. Soc., 68, 112 (1985)

BEAUDOIN, J.J.
"Effect of humidity and porosity on fracture of hardened Portland cement", Cem. Concr. Res., 12, 705 (1982)

BEAUDOIN, J.J.
"Stress corrosion and subcritical crack growth in Portland cement paste", Submitted to Il Cemento (1985a)

BEAUDOIN, J.J.
"Effect of humidity on subcritical crack growth in cement paste", Submitted to Cem. Concr. Res. (1985b)

BENTUR, A., BERGER, R.L., LAWRENCE, F.V., MILESTONE, N.B., MINDESS, S., YOUNG J.F.
"Creep and drying shrinkage of calcium silicate pastes: A hypothesis of irreversible strain", Cem. Concr. Res., 9, 83 (1979)

BERGER, R.L., LAWRENCE, F.V., YOUNG J.F.
"Studies on the hydration of tricalcium silicate pastes. II Strength development and fracture characteristics", Cem. Concr. Res., 3, 497 (1973)

BIRCHALL, J.D., HOWARD, A.J., KENDALL, K.
"Flexural strength and porosity of cements", Nature, 289, 388 (1981)

BIRCHALL, J.D.
"Cements in the context of new materials for an energy expensive future", Phil. Trans. R. Soc. Lond., A310, 31 (1983)

BROWN, J.H.
"Measuring the fracture toughness of cement paste and mortar", Mag. Concr. Res., 24, 185 (1972)

BROWN, J.H.
Private communication

BROWN, W.F. SRAWLEY, J.E.
"Plane strain crack toughness testing of high strength metallic materials", A.S.T.M., Special technical paper 410 (1969)

BTE, G.C.
"Portland cement: Composition, production and properties", Pergamon Press, Oxford (1983)

CARPINTERI, A.
"Static and energetic fracture parameters for rocks and concrete", Mater. Constr., 14, 151 (1981)

DALGLEISH, B.J., PRATT, P.L. MOSS, R.I.
"Preparation techniques and the microscopical examination of Portland cement paste and C_3S", ccr, 10, 665 (1980)

DAVIDGE, R.W., McLAREN, J.R., TAPPIN, G.
"Strength-probability-time [SPT] relationships in ceramics", J. Mat. Sci., 8, 1699 (1973)

DAVIDGE, R.W.
"Strength and toughness an ceramic systems", Phil. Trans. R. Soc. Lond., A310, 113 (1983)

DIAMOND, S.
"Cement paste micostructure - an overview at several levels", in "Hydraulic cement pastes: their structure and properties", Proc. of Cement and Concrete Asscciation conference, Sheffield (1976)

DOUBLE, D.D., HELLAWELL, A., PERRY, S.J.
"The hydration of Portland cement", Proc. R. Soc. Lond., A359, 435 (1978)

DUGDALE, D.S.
"Yielding of steel sheets containing slits", J. Mech. Phys. Solids, 8, 100 (1960)

EDEN, N.B., BAILEY, J.E.
"On the factors affecting the strength of Portland cement", J. Mat. Sci., 19, 150 (1984)

EVANS, A.G.
"A method for evaluating the time-dependant failure characteristics of brittle materials-and its application to polycrystalline alumina", J. Mat. Sci., 7, 1137 (1972)

EVANS, A.G., LINZER, M.
"Failure predictions in structural ceramics using acoustic emission", J. Am. Ceram. Soc., 56, 575 (1973)

EVANS, A.G.
"Slow crack growth in brittle materials under dynamic loading conditions", Int. J. Fract., 10, 251 (1974)

EVANS, A.G., LINZER, M., RUSSELL, L.R.
"Acoustic emission and crack propogation in polycrystalline alumina", Materials Science and Engineering, 15, 253 (1974)

EVANS, A.G., WIEDERHORN, S.M.
"Crack propogation and failure predictions in silicon nitride at elevated temperatures", J. Mat. Sci., 9, 270 (1974)

EVANS, A.G., FABER, K.T.
"Crack-growth resistance of microcracking brittle materials", J. Am. Ceram. Soc., 67, 255 (1984)

FABER, K.T., EVANS, A.G.
"Crack deflection processes-Theory", Acta Metallurgica, 31, 565 (1983)
"Crack deflection processes-Experiment", Acta Metallurgica, 31, 577 (1983)

FELDMAN, R.F., SEREDA, P.J.
"A model for hydrated cement paste as deduced from sorption length changes and mechanical properties", Maters. Constr., 1, 509 (1968)

FELDMAN, R.F., SEREDA, P.J.
"A new model for hydrated cement paste and its practical implications", Eng. J., 53, 53 (1970)

FELDMAN, R.F.
"Mechanisms of creep in hydrated Portland cement", Cem. Concr. Res., 2, 521 (1972)

FELDMAN, R.F., BEAUDOIN, J.J.
"Microstructure and strength of hydrated cement", Cem. Concr. Res., 6, 389 (1976)

FREIMAN, S.W., McKINNEY, K.R., SMITH, H.L.
"Slow crack growth in polycrystalline ceramics", In "Fracture mechanics of ceramics, Ed R.C. Brandt, D.P.H. Hasselman, F.F. Lange", 659, Plenum Press, New York (1974)

FULLER, E.R.
"An evaluation of double torsion testing-Analysis", A.S.T.M., STP 678 (1979)

GARD, J.A., MOHAN, K., TAYLOR, H.F.W., CLIFF, G.
"Analytical electron microscopy of cement pastes: I Tricalcium silicate pastes", jacs, 63, 336 (1980)

GJORV, O.E., SORENSEN, S.I., ARNESEN, A.
"Notch sensitivity and fracture toughness of concrete", Cem. Concr. Res., 7, 333 (1977)

GRANJU, J.L. MASO, J.C.
"Hardened Portland cement pastes, modelisation of the microstructure and evolution laws of mechanical properties I-Basic results", Cem. Concr. Res., 14, 249 (1984)

GRIFFITH, A.A.
"The phenomena of rupture and flow in solids", Phil. Trans. R. Soc. Lond., A221, 163 (1920)

GRUDEMO, A.
"Strength-structure relationhips of cement pastes - I Methods and basic data for studying phase composition and microstructure", CBI Forskning, 6, 1 (1977)

GRUDEMO, A.
"Microcracks, fracture mechanisms and strength of the cement paste matrix", Cem. Concr. Res., 9, 19 (1979)

HIGGINS & BAILEY (1976) - re crack growth, see end of references.

HIGGINS, D.D., BAILEY, J.E.
"Fracture measurements on cement paste", J. Mat. Sci., 11, 1995 (1976)

HILLEMEIR, B., HILSDORF, H.K.
"Fracture mechanics studies on concrete compounds", Cem. Concr. Res., 7, 523 (1977)

HILLERBORG, A.
"Theoretical analysis of the double torsion test",Cem. Concr. Res., 13, 69 (1983)

HJORTH, L.
"Development and application of high-density cement-based materials", Phil. Trans. R. Soc. Lond., A310, 167 (1983)

HSU, T.T., SLATE, F.O., STURMAN, G.M., WINTER, G.
"Microcracking of plain concrete and the shape of the stress strain curve", Proc. A.C.I., 60, 209 (1963)

HUBNER, H., JILLEK, W.
"Sub-critical crack extension and crack resistance in polycrystalline alumina", J. Mat. Sci., 12, 117 (1977)

JENNINGS, H.M., PRATT, P.L. "On the hydration of Portland cement", Proc. Brit. Ceram. Soc., 28, 179 (1979)

JENNINGS, H.M., PRATT, P.L.
"On the reactions leading to calcium silicate hydrate, calcium hydroxide and ettringite during the hydration of cement", Proc. 7th Int. Cong. Chem. Cem., II-141, Paris (1980)

KNEHANS, R., STEINBRECH, R.
"Memory effect of crack resistance during slow crack growth in notched Al_2O_3 bend specimens", J. Mat. Sci. Letters, 1, 327 (1982)

KROKOSKY,E.M.
"Static fatigue in hydrated Portland cement", Mater. Constr., 6, 447 (1973)

LACHOWSKI, E.E., MOHAN, K., TAYLOR, H.F.W., MOORE, A.E.
"Analytical electron microscopy of cement pastes: II Pastes of Portland cements and clinkers", J. Am. Ceram. Soc., 63, 447 (1980)

LAWN, B.R., WILSHAW, T.R.
"Fracture of brittle solids", Cambridge University Press, (1975)

LEA, F.M.
"The chemistry of cement and concrete", Arnold, London (1970)

MARCHESE, B. "SEM topography of twin fracture surfaces of alite pastes 3 years old", Cem. Concr. Res., 7, 9 (1977)

MENDIRATTA, M.G., PETROVIC, J.J.
"Slow crack growth from controlled surface flaws in Si_3N_4", J. Am. Ceram. Soc., 61, 226 (1978)

MINDESS, S., NADEAU, J.S., HAY, J.M.
"Effects of different curing conditions on slow crack growth in cement paste", Cem. Concr. Res., 4, 953 (1974)

MINDESS, S., NADEAU, J.S.
"Efffect of loading rate on the flexural strength of cement and mortar", Ceramic Bulletin, 56, 429 (1977)

MINDESS, S.
"Effect of loading rate on fracture toughness of hardened cement paste", Private comunication.

MINDESS, S.
"The application of fracture mechanics to cement and concrete: A historical review", in, "Fracture mechanics of concrete, Ed. F.H. Wittman", Elsevier, Holland (1983)

MINDESS, S.
"The effect of specimen size on the fracture energy of concrete", Cem. Concr. Res., 14, 431 (1984)

MOAVENZADEH, F., KUGUEL, R. "Fracture of concrete", J. Materials, 4, 497 (1969)

MOORE, A.E.
"Structure andcomposition of compounds in some fully hydrated cement pastes", Proc. 7th Int. Cong. on the Chemistry of Cement, VI-97, Paris (1980)

NADEAU, J.S.
"Subcritical crack growth in vitreous carbon at room temperature", J. Am. Ceram. Soc., 57, 303 (1974)

NADEAU, J.S., MINDESS, S., HAY, J.M.
"Slow crack growth in cement paste", J. Am. Ceram. Soc., 57, 51 (1974)

NAUS, D.J., BATSON, G.B., LOTT, J.L.
"Fracture mechanics of concrete", in "Fracture mechanics of ceramics, Vol 2, Ed. D.J. Brandt et al", 469, Plenum Press, New York (1974)

PARROTT, L.J.
"Novel methods of processing cement gel to examine and control microstructure and properties", Phil. Trans. R. Soc. Lond., A310, 155 (1983)

PARROTT, L.J.
"Stoichiometry of the main reactions in Portland cement", Draft report of RILEM committee 68MMH on the "Hydration of Portland cement" (1985)

PATEL, H.H.
Private communication

PLETKA, B.J., WIEDERHORN, S.M.
"Subcritical crack growth in glass ceramics", in "Fracture mechanics of ceramics, Vol 4, Ed. D.J. Brandt et al", 745, Plenum Press, New York (1976)

PLETKA, B.J., FULLER, E.R., KOEPKE, B.G.
"An evaluation of double torsion testing-Experimental", A.S.T.M., STP 678, 19 (1979)

PLETKA, B.J., WIEDERHORN, S.M.
"A comparison of failure predictions by strength and fracture mechanics techniques", J. Mat. Sci., 17, 1247 (1982)

PRATT, P.L., GHOSE, A.
"Electron microscope studies of Portland cement microstructure during setting and hardening", Phil. Trans. R. Soc. Lond., A310, 93 (1983)

REINHARDT, H.W.
"Crack softening zone in plain concrete under static loading", Cem. Concr. Res., 15, 42 (1985)

RODGERS, S.A., SINCLAIR, W., GROVES, G.W., BROOKE, S.A., DOUBLE, D.D.
"Reactions in the setting of high strength cement pastes", Mat. Res. Soc. Symp. Proc., 42, 45 (1985)

ROY, D.M., GOUDA, G.R.
"High strength generation in cement paste", Cem. Concr. Res., 3, 807 (1973)

RYSKEWITCH E.
"Compression strength of porous sintered alumina and zirconia", J. Am. Ceram. Soc., 36, 65 (1953)

SAGAR DWIVEDI, V., PRATT, P.L.
"Strength, fracture and deformation behaviour of Portland cement paste", Proc. 6th Int. Conf. on Fracture, New Delhi, India (1984)

SCHILLER, K.K.
"Strength of porous materials", Cem. Concr. Res., 1, 419 (1971)

SCRIVENER, K.L.
Ph.D. Thesis, University of London (1984)

SCRIVENER, K.L., PRATT, P.L.
"Backscattered electron images of polished cement sections in the scanning electron microscope", Proc. 6th Int. Conf. on Cement Microscopy, Albuquerque, USA (1984)

SCRIVENER, K.L., BALDIE, K.D., HALSE, G., PRATT, P.L.
"Characterisation of microstructure as a systematic approach to high strength cements", Mat. Res. Soc. Symp. Proc., 42, 39 (1985)

SEREDA, P.J., FELDMAN, R.F., RAMACHANDRAN, V.S.
"Structure formation and development in hardened cement paste", Proc. 7th Int. Cong. Chem. Cem., Sub-theme VI-I, Paris (1980)

SHETTY, D.K., VIRKAR, A.V.
"Determination of the useful range of crack lengths in double torsion specimens", J. Am. Ceram. Soc., 61, 93 (1979)

SINCLAIR, W., GROVES, G.W.
"The microstructure of high strength cement pastes", Mat. Res. Soc. Symp. Proc., 42, 31 (1985)

SOROKA, I.
"Portland cement paste and concrete", Macmillan, London (1979)

TABOR, D.
"Principles of Adhesion-Bonding in cement and concrete", Private communication.

TRANTINA, G.G.
"Stress analysis of double-torsion specimens", J. Am. Ceram. Soc., 60, 338 (1977)

WALSH, D., OTOONI, M.A., TAYLOR, M.E., MARCINOWSKI, M.J.
"Study of Portland cement fracture surfaces by scanning electron microscope techniques", J. Mat. Sci., 9, 423 (1974)

WALSH, P.F.
Discussion of "Measuring the fracture toughness of cement paste and mortar" by J.H. Brown [see above] Mag. Concr. Res., 25, 220 (1973)

WALSH, P.F.
"Crack initiaition in plain concrete", Mag. Concr. Res., 28, 220 (1976)

WECHARATANA, M., SHAH, S.P.
"Double torsion tests for studying slow crack growth in Portland cement mortar", Cem. Concr. Res., 10, 833 (1984)

WEATHERBURN, C.E.
"Mathematical Statistics", Cambridge University Press (1957)

WEAST, R.C.
"Handbook of Chemistry and Physics", B-77, CRC Press, Cleveland, Ohio (1974)

WIEDERHORN, S.M.
"Influence of water vapour on crack propogation in soda-lime glass", J. Am. Ceram. Soc., 50, (1967)

WIEDERHORN, S.M., JOHNSON, H.
"Effect of electrolyte pH on crack propogation in glass", J. Am. Ceram. Soc., 56, 192 (1973)

WIEDERHORN, S.M., JOHNSON, H., DINNESS, A., HEUER, A.H.
"Fracture of glass in vacuum", J. Am. Ceram. Soc., 57, 336 (1974)

WITTMAN, F.H., ZAITSEV, J.U.
Mechanical properties of materials, Vol. 4, 84, The Society of Materials Science, Japan (1972)

YUDENFREUND, M., HANNA, K., SKALNY, J., ODLER, I., BRUNAUER, S.
"Hardened cement pastes of low porosity - V. Compressive strength", Cem. Concr. Res., 2, 731 (1972)

HIGGINS, D.D., BAILEY, J.E., Proc. Cement and Concrete Association conference , Sheffield, 283 (1976). Re crack growth.